Solitons in the Higgs phase: the moduli matrix approach

2006 J. Phys. A: Math. Gen. 39 R315

(http://iopscience.iop.org/0305-4470/39/26/R01)

INSTITUTE OF PHYSICS PUBLISHING JOURNAL OF PHYSICS A: MATHEMATICAL AND GENERAL

J. Phys. A: Math. Gen. **39** (2006) R315–R392 doi:10.1088/0305-4470/39/26/R01

TOPICAL REVIEW

Solitons in the Higgs phase: the moduli matrix approach

Minoru Eto, Youichi Isozumi, Muneto Nitta, Keisuke Ohashi and Norisuke Sakai

Department of Physics, Tokyo Institute of Technology, Tokyo 152-8551, Japan

E-mail: meto@th.phys.titech.ac.jp, isozumi@th.phys.titech.ac.jp, nitta@th.phys.titech.ac.jp, keisuke@th.phys.titech.ac.jp and nsakai@th.phys.titech.ac.jp

Received 2 March 2006
Published 14 June 2006
Online at stacks.iop.org/JPhysA/39/R315

Abstract
We review our recent work on solitons in the Higgs phase. We use $U(N_{\rm C})$ gauge theory with $N_{\rm F}$ Higgs scalar fields in the fundamental representation, which can be extended to possess eight supercharges. We propose the moduli matrix as a fundamental tool to exhaust all BPS solutions, and to characterize all possible moduli parameters. Moduli spaces of domain walls (kinks) and vortices, which are the only elementary solitons in the Higgs phase, are found in terms of the moduli matrix. Stable monopoles and instantons can exist in the Higgs phase if they are attached by vortices to form composite solitons. The moduli spaces of these composite solitons are also worked out in terms of the moduli matrix. Webs of walls can also be formed with characteristic difference between Abelian and non-Abelian gauge theories. Instanton–vortex systems, monopole–vortex–wall systems, and webs of walls in Abelian gauge theories are found to admit negative energy objects with the instanton charge (called intersectons), the monopole charge (called boojums) and the Hitchin charge, respectively. We characterize the total moduli space of these elementary as well as composite solitons. In particular the total moduli space of walls is given by the complex Grassmann manifold $SU(N_{\rm F})/[SU(N_{\rm C}) \times SU(N_{\rm F} - N_{\rm C}) \times U(1)]$ and is decomposed into various topological sectors corresponding to boundary condition specified by particular vacua. The moduli space of k vortices is also completely determined and is reformulated as the half ADHM construction. Effective Lagrangians are constructed on walls and vortices in a compact form. We also present several new results on interactions of various solitons, such as monopoles, vortices and walls. Review parts contain our works on domain walls (Isozumi Y *et al* 2004 *Phys. Rev. Lett.* **93** 161601 (*Preprint* hep-th/0404198), Isozumi Y *et al* 2004 *Phys. Rev.* D **70** 125014 (*Preprint* hep-th/0405194), Eto M *et al* 2005 *Phys. Rev.* D **71** 125006 (*Preprint* hep-th/0412024), Eto M *et al* 2005 *Phys. Rev.* D **71** 105009 (*Preprint* hep-th/0503033), Sakai N and Yang Y

2005 *Comm. Math. Phys.* (in press) (*Preprint* hep-th/0505136)), vortices (Eto M *et al* 2005 *Phys. Rev. Lett.* **96** 161601 (*Preprint* hep-th/0511088), Eto M *et al* 2006 *Phys. Rev.* D **73** 085008 (*Preprint* hep-th/0601181)), domain wall webs (Eto M *et al* 2005 *Phys. Rev.* D **72** 085004 (*Preprint* hep-th/0506135), Eto M *et al* 2006 *Phys. Lett.* B **632** 384 (*Preprint* hep-th/0508241), Eto M *et al* 2005 *AIP Conf. Proc.* **805** 354 (*Preprint* hep-th/0509127)), monopole–vortex–wall systems (Isozumi Y *et al* 2005 *Phys. Rev.* D **71** 065018 (*Preprint* hep-th/0405129), Sakai N and Tong D 2005 *J. High Energy Phys.* JHEP03(2005)019 (*Preprint* hep-th/0501207)), instanton–vortex systems (Eto M *et al* 2005 *Phys. Rev.* D **72** 025011 (*Preprint* hep-th/0412048)), effective Lagrangian on walls and vortices (Eto M *et al* 2006 *Phys. Rev.* D (in press) (*Preprint* hep-th/0602289)), classification of BPS equations (Eto M *et al* 2005 *Preprint* hep-th/0506257) and Skyrmions (Eto M *et al* 2005 *Phys. Rev. Lett.* **95** 252003 (*Preprint* hep-th/0508130)).

PACS numbers: 11.15.−q, 05.45.Yv, 11.10.Lm, 11.25.−w

(Some figures in this article are in colour only in the electronic version)

1. Introduction

Topological solitons play very important roles in broad area of physics [18–22]. They appear various situations in condensed matter physics, cosmology, nuclear physics and high energy physics including string theory. In field theory it is useful to classify solitons by co-dimensions on which solitons depend. Kinks (domain walls), vortices, monopoles and instantons are well-known typical solitons with co-dimensions one, two, three and four, respectively[1]. They carry topological charges classified by certain homotopy groups according to their co-dimensions. If the spatial dimension of spacetime is larger than the co-dimensions, solitons are extended objects having world volume and are sometimes called 'branes'. D-branes are solitons in string theory whereas topological solitons in higher dimensional field theory are models of branes. D-branes and field theory solitons are closely related or sometimes are identified in various situations. Recently the *brane-world scenario* [23–25] are also realized on topological solitons in field theory or D-branes in string theory.

When solitons/branes saturate a lower energy bound, called the Bogomol'nyi bound, they are the most stable among solitons with the same topological charge, and are called *Bogomol'nyi–Prasad–Sommerfield (BPS)* solitons [26]. BPS solitons can be naturally realized in supersymmetric (SUSY) field theories and preserve some fraction of the original SUSY [27]. From the discussion of SUSY representation, they are non-perturbatively stable and therefore play crucial roles in non-perturbative study of SUSY gauge theories and string theory [28].

Since there exists no force between BPS solitons the most general solutions of solitons contain parameters corresponding to positions of solitons. Combined with parameters in the internal space, they are called the *moduli parameters*. A space parametrized by the moduli parameters is no longer a flat space but a curved space called the *moduli space*, possibly containing singularities. The moduli space is the most important tool to study BPS solitons. When solitons can be regarded as particles, say for instantons in $d = 4 + 1$, monopoles in $d = 3 + 1$, vortices in $d = 2 + 1$, kinks in $d = 1 + 1$ and so on, geodesics in their moduli space describe classical scattering of solitons [29]. In quantum theory, for instance, the instanton

[1] In this review, we keep terminology of 'instantons' for Yang–Mills instantons in four Euclidean space. They become particles in $4 + 1$ dimensions.

calculus is reduced to the integration over the instanton moduli space [30]. The same discussion should hold for a 'monopole calculus' in $d = 2+1$, a 'vortex calculus' in $d = 1+1$ and so on. On the other hand, when solitons have world volume, for instance vortex-string in $d = 3+1$, moduli are promoted to massless moduli fields in the effective field theory on the world volume of solitons. Therefore moduli space is crucial to consider the brane-world scenario, solitons in higher dimensions or string theory. The moduli fields describe local deformations along the world volume of solitons. This fact is useful when we consider composite solitons made of solitons with different co-dimensions. Namely, composite solitons may sometimes be regarded as solitons in the effective field theory of the other (host) solitons [31]. For instance a D/fundamental string ending on a D-brane can be realized as a soliton called the BIon [32] in the Dirac–Born–Infeld theory on the D-brane.

Construction of solutions and the moduli spaces of instantons and monopoles were established long time ago and are well known as the ADHM [33, 34] and the Nahm [34, 35] constructions, respectively. Instantons and monopoles are naturally realized as $1/2$ BPS solitons in SUSY gauge theory with 16 supercharges. The effective theories on them are nonlinear sigma models with eight supercharges, whose target spaces must be hyper-Kähler [36–46], and therefore the moduli spaces of instantons and monopoles are hyper-Kähler.

Vacua outside monopoles and instantons are in the Coulomb phase and in the unbroken phase of the gauge symmetry, respectively. Contrary to this fact, vacua outside kinks or vortices are in the Higgs phase where gauge symmetry is completely broken. These solitons can be constructed as $1/2$ BPS solitons in SUSY gauge theory with eight supercharges, where the so-called Fayet–Iliopoulos (FI) term [47] should be contained in the Lagrangian to realize the Higgs vacua. The moduli space of kinks and vortices are Kähler [37] because they preserve four supercharges. Kinks (domain walls) in SUSY $U(1)$ gauge theory with eight supercharges were firstly found in [48] in the strong gauge coupling (sigma model) limit and have been developed recently [4, 5, 49–63]. Domain walls in non-Abelian gauge theory have been firstly discussed in [1, 2, 64] and have been further studied [3, 14, 16, 65]. In particular their moduli space has been determined to be complex Grassmann manifold [3]. On the other hand, vortices were found earlier by Abrikosov, Nielsen and Olesen [66] in $U(1)$ gauge theory coupled with one complex Higgs field, and are now referred as the ANO vortices. Their moduli space was constructed [67–70]. When the number of Higgs fields is large enough vortices are called semi-local vortices [71], and their moduli space contains size moduli similarly to lumps [72–74] or sigma model instantons [75]. Study of vortices in non-Abelian gauge theory, called *non-Abelian vortices*, was initiated in [76, 77] and has been extensively discussed [76–89][2]. Especially their moduli space has been determined in the framework of field theory [6] as well as string theory [76].

One aim of this review is to give a comprehensive understanding of the moduli spaces of $1/2$ BPS kinks and vortices. The other aim is to study the moduli spaces of various $1/4$ BPS composite solitons as discussed below[3].

Domain walls can make a junction as a $1/4$ BPS state [94] and these wall junctions in SUSY theories with four supercharges were further studied in [95–98] (see [8] for more complete references). Domain wall junction in SUSY $U(1)$ gauge theory with eight supercharges was constructed [99] by embedding an exact solution in [95–97]. Finally in [8, 9] the full solutions of domain wall junction, called *domain wall webs*, have been constructed in SUSY non-Abelian gauge theory with eight supercharges. The Hitchin charge is found to be localized around junction points which is always negative in Abelian gauge theory [8] and can be either

[2] Another type of non-Abelian vortices were discussed earlier [90].

[3] Composite solitons were also studied in non-supersymmetric field theories [91–93].

negative or positive in non-Abelian gauge theory [9]. This configuration shares the many properties with the (p, q) 5-brane webs [100].

As noted above, monopoles and instantons do not live in the Higgs phase. Question is what happens if monopoles or instantons are put into the Higgs phase. This situation can be realized by considering SUSY gauge theory with the FI term. In the Higgs phase, magnetic flux from a monopole is squeezed by the Meissner effect into a vortex, and the configuration becomes a confined monopole with vortices attached [101–108]. This configuration is interesting because it gives a dual picture of colour confinement [104]. The confined monopole can be regarded as a kink in the effective field theory on a vortex [103]. In SUSY theory the configuration preserves a quarter of eight supercharges and is a $1/4$ BPS state [105]. Moreover it was found [109] in the strong gauge coupling limit that vortices can end on a domain wall to form a $1/4$ BPS state, like strings ending on a D-brane. This configuration was further studied in gauge theory without taking the strong coupling limit [110]. Finally it was found [11] that all monopoles, vortices and domain walls can coexist as a $1/4$ BPS state. Full solutions constructed in [11] resemble with the Hanany–Witten-type brane configuration [111]. The negative monopole charge (energy) has also been found [11] in $U(1)$ gauge theory and has been later called *boojum* [12, 112].

$1/4$ BPS composite configurations made of instantons and vortices have also been found as solutions of self-dual Yang–Mills equation coupled with Higgs fields (the SDYM-Higgs equation) in $d = 5, 6$ SUSY gauge theory with eight supercharges [13, 106]. Monopoles in the Higgs phase can be obtained by putting a periodic array of these instantons along one space direction inside the vortex world volume [13], while the BPS equation of monopoles is obtained by the Scherk–Schwarz dimensional reduction [113] of the SDYM-Higgs equation. All other BPS equations introduced above can be obtained from the SDYM-Higgs equation by the Scherk–Schwarz and/or ordinary dimensional reductions. The negative instanton charge (energy) has also been found [13] at intersection of vortices in Abelian gauge theory, and is called *intersecton*.

Surprisingly enough this SDYM-Higgs equation was independently found by mathematicians [114–116] earlier than physicists [13, 106]. Moreover they consider it in a more general setting, namely with a Kähler manifold in any dimension as a base space where solitons live and with a general target manifold of scalar fields, unlike ordinary Higgs fields in linear representation. They call their equation simply as a *vortex equation*. If we take a base space as $\mathbf{C}^2$ and a target space as a vector space, the vortex equation reduces to our SDYM-Higgs equation. Whereas if we take a base space as $\mathbf{C}$, the vortex equation reduces to the BPS equation of vortices [117]. Some integration over the moduli space of the vortex equation defines a new topological invariant called the Hamiltonian Gromov–Witten invariant [116, 118] which generalizes the Gromov–Witten invariant and the Donaldson invariant. Therefore studying the moduli space of the SDYM-Higgs equation is very important in mathematics as well as physics.

In this review, we focus on the solitons in the Higgs phase; domain walls, vortices and composite solitons of monopoles/instantons. We solve the half (the hypermultiplet part) of BPS equations by introducing the *moduli matrix*. The rest (the vector multiplet part) of BPS equations is difficult to solve in general. When the number of Higgs fields is larger than the number of colours, they can be solved analytically in the strong gauge coupling limit in which the gauge theories reduce to nonlinear sigma models with hyper-Kähler target spaces. In general cases, we assume that the vector multiplet part of BPS equations produces no additional moduli parameters. This assumption was rigorously proved in certain situations, for instance in the case of the ANO vortices [67] and in the case of compact Kähler base spaces [115, 116], and is now called the Hitchin–Kobayashi correspondence in the mathematical literature.

In the cases of odd co-dimensions it is a rather difficult problem but it was proved for domain walls in $U(1)$ gauge theory [5] and the index theorem [12, 52] supports it for the case of domain walls in non-Abelian gauge theory. Therefore this assumption is correct for the most cases, and we consider that all moduli parameters in the BPS equations are contained in the moduli matrix. We concretely discuss the correspondence between the moduli parameters in the moduli matrix and actual soliton configurations in various cases: (1) domain walls [1, 2], (2) vortices [6, 7], (3) domain wall junctions or webs [8, 9], (4) composites of monopoles (boojums), vortices and walls [11], (5) composites of instantons and vortices [13]. We will see that composite solitons in non-Abelian gauge theory have much more variety than those in Abelian gauge theory. One interesting property which all systems commonly share is the presence of a negative/positive charge localized around junction points of composite solitons. The junction charge is always negative in Abelian gauge theory while it can be either negative or positive in non-Abelian gauge theory.

This review contains many new results. We extend analysis of non-Abelian vortices in [6] to semi-local non-Abelian vortices which contain non-normalizable zero modes. Relation to Kähler quotient construction [76] of the vortex moduli space is completely clarified. The half ADHM construction of vortices is found. We construct effective Lagrangian on non-Abelian (semi-local) vortices in a compact form, which generalizes the Abelian cases [67–70]. Relation between moduli parameters in $1/2$ BPS states in massless theory and $1/4$ BPS states in massive theory is found; for instance orientational moduli of a non-Abelian vortex are translated to position moduli of a monopole. We give a complete answer to the question addressed in [12, 119] whether a confined monopole attached by a vortex ending on a domain wall can pass through that domain wall by changing moduli or not. Namely we find that a monopole can pass through a domain wall if and only if positions of vortices attached to the wall from both sides coincide. If they do not coincide, no monopole exists as a BPS state, suggesting repulsive force between a monopole and a boojum on a junction point of the vortex and the wall.

This review is organized as follows. In section 2 we present the model and investigate its vacua. In section 2.1 we give the Lagrangian of $U(N_{\rm C})$ gauge theory with $N_{\rm F}$ Higgs fields in the fundamental representation in spacetime dimensions $d = 1+1, \ldots, 5+1$. In section 2.2 we analyse the vacuum structure of our model with the massless or massive Higgs fields. In section 2.3 we discuss the strong gauge coupling limit of the model with large number of Higgs fields ($N_{\rm F} > N_{\rm C}$), in which the model reduces to a nonlinear sigma model whose target space is a hyper-Kähler manifold. In section 3 we discuss $1/2$ BPS solitons in the Higgs phase, namely domain walls in section 3.1 and vortices in section 3.2. In section 3.3 we construct the effective action on these solitons. In section 4 we discuss $1/4$ BPS composite solitons. First in section 4.1 we present sets of $1/4$ BPS equations which we consider in this review. In section 4.2 we work out solutions of domain wall webs, or junction made of domain walls. In section 4.3 we work out composite states of monopoles (boojums), vortices and domain walls. In section 4.4 we work out composite states of instantons and (intersecting) vortices. In section 4.5 we interpret some of these $1/4$ BPS composite solitons as $1/2$ BPS solitons on host $1/2$ BPS solitons. Finally section 5 is devoted to a discussion.

2. Model and vacua

2.1. $U(N_{\rm C})$ gauge theory with $N_{\rm F}$ flavours

We are mostly interested in $U(N_{\rm C})$ gauge theory in $(d-1)+1$ dimensions with a number of adjoint scalar fields Σ_p and $N_{\rm F}$ flavours of scalar fields in the fundamental representation as an $N_C \times N_F$ matrix H

$$\mathcal{L} = \mathcal{L}_{\rm kin} - V, \tag{2.1}$$

$$\mathcal{L}_{\rm kin} = {\rm Tr}\left(-\frac{1}{2g^2}F_{\mu\nu}F^{\mu\nu} + \frac{1}{g^2}\mathcal{D}_\mu\Sigma_p\mathcal{D}^\mu\Sigma_p + \mathcal{D}^\mu H(\mathcal{D}_\mu H)^\dagger\right), \tag{2.2}$$

where the covariant derivatives and field strengths are defined as $\mathcal{D}_\mu\Sigma_p = \partial_\mu\Sigma_p + {\rm i}[W_\mu, \Sigma_p]$, $\mathcal{D}_\mu H = (\partial_\mu + {\rm i}W_\mu)H$, $F_{\mu\nu} = -{\rm i}[\mathcal{D}_\mu, \mathcal{D}_\nu]$. Our convention for the metric is $\eta_{\mu\nu} = {\rm diag}(+, -, \ldots, -)$. The scalar potential V is given in terms of diagonal mass matrices M_p and a real parameter c as

$$V = {\rm Tr}\left[\frac{g^2}{4}(c\mathbf{1} - HH^\dagger)^2 + (\Sigma_p H - HM_p)(\Sigma_p H - HM_p)^\dagger\right]. \tag{2.3}$$

This Lagrangian is obtained as the bosonic part of the Lagrangian with eight supercharges by ignoring one of the scalars in the fundamental representation: $H^1 \equiv H$, $H^2 = 0$. Although the gauge couplings for $U(1)$ and $SU(N_C)$ are independent, we have chosen these to be identical to obtain simple solutions classically. The real positive parameter c is called the Fayet–Iliopoulos (FI) parameter, which can appear in supersymmetric $U(1)$ gauge theories [47]. Since we are interested in the Higgs phase, it is crucial to have this parameter c. We use a matrix notation for these component fields, such as $W_\mu = W_\mu^I T_I$, where $T_I\left(I = 0, 1, 2, \ldots, N_C^2 - 1\right)$ are matrix generators of the gauge group G in the fundamental representation satisfying ${\rm Tr}(T_I T_J) = \frac{1}{2}\delta_{IJ}$, $[T_I, T_J] = if_{IJ}{}^K T_K$ with T^0 as the $U(1)$ generator. In order to embed this Lagrangian into a supersymmetric gauge theory with eight supercharges, spacetime dimensions are restricted as $d \leqslant 6$ and the number of adjoint scalars and mass matrices are given by $6 - d$ ($p = 1, \ldots, 6 - d$), since these theories can be obtained by dimensional reductions with possible twisted boundary conditions (the Scherk–Schwarz dimensional reduction [113]) as described below.

Let us note that a common mass $M_p = m_p\mathbf{1}$ for all flavours can be absorbed into a shift of the adjoint scalar field Σ_p, and has no physical significance. In this review, we assume either massless hypermultiplets, or fully non-degenerate mass parameters $m_{pA} \neq m_{pB}$, for $A \neq B$ unless stated otherwise. Then the flavour symmetry $SU(N_F)$ for the massless case reduces in the massive case to

$$G_F = U(1)_F^{N_F - 1}, \tag{2.4}$$

where $U(1)_F$ corresponding to common phase is gauged by $U(1)_G$ local gauge symmetry.

Let us discuss supersymmetric extension of the Lagrangian given by equations (2.1)–(2.3). (Those who are unfamiliar with supersymmetry can skip the rest of this subsection and can go to section 2.2.) Gauge theories with eight supercharges are most conveniently constructed first in 5+1 dimensions and theories in lower dimensions follow from dimensional reductions. The gamma matrices satisfy $\{\Gamma^M, \Gamma^N\} = 2\eta^{MN}$, and the totally antisymmetric product of the gamma matrices $\Gamma^M, \ldots, \Gamma^N$ are denoted by $\Gamma^{M\cdots N}$. The charge conjugation matrix C is defined by $C^{-1}\Gamma_M C = \Gamma_M^T$ and satisfy $C^T = -C$. The building blocks for gauge theories with eight supercharges are vector multiplets and hypermultiplets. The vector multiplet in 5+1 dimensions consists of a gauge field W_M^I ($M = 0, 1, 2, 3, 4, 5$) for generators of gauge group I, an $SU(2)_R$ triplet of real auxiliary fields Y_a^I, and an $SU(2)_R$ doublet of gauginos λ^{iI} ($i = 1, 2$) which are an $SU(2)$-Majorana Weyl spinor, namely $\Gamma_7\lambda^i = \lambda^i$ and $\lambda^i = C\varepsilon^{ij}(\bar\lambda_j)^T$. Here Γ_7 is defined by $\Gamma_7 = \Gamma^{012345}$ and C is the charge conjugation matrix in 5+1 dimensions. All these fields are in the adjoint representation of G.

We have hypermultiplets as matter fields, consisting of an $SU(2)_R$ doublet of complex scalar fields H^{irA} and Dirac field ψ^{rA} (hyperino) whose chirality is $\Gamma_7\psi^{rA} = -\psi^{rA}$. Colour (flavour) indices are denoted as $r, s, \ldots$ $(A, B, \ldots)$. The hypermultiplet in $5 + 1$ dimensions does not allow (finite numbers of) auxiliary fields and superalgebra closes only on-shell, although the vector multiplet has auxiliary fields.

We shall consider a model with minimal kinetic terms for vector and hypermultiplets. In $5 + 1$ dimensions, the model allows only two types of parameters, gauge couplings g_I and a triplet of the Fayet–Iliopoulos (FI) parameters ζ_a with $a = 1, 2, 3$. There exist the triplets of the FI parameters as many as $U(1)$ factors of gauge group in general. To distinguish different gauge couplings for different factor groups, we retained suffix I for g_I. The bosonic part of the Lagrangian is given by

$$\mathcal{L}_6 = -\frac{1}{4g_I^2} F^I_{MN} F^{IMN} + (\mathcal{D}_M H^{irA})^* \mathcal{D}^M H^{irA} + \mathcal{L}_{\text{aux}}, \tag{2.5}$$

$$\mathcal{L}_{\text{aux}} = \frac{1}{2g_I^2}\left(Y_a^I\right)^2 - \zeta_a Y_a^0 + (H^{irA})^* (\sigma^a)^i{}_j (Y_a)^r{}_s H^{jsA}. \tag{2.6}$$

The equation of motion for auxiliary fields Y_a^I gives

$$Y_a^I = \frac{1}{g_I^2}\left[\zeta_a \delta_0^I - (H^{irA})^* (\sigma_a)^i{}_j (T_I)^r{}_s H^{jsA}\right]. \tag{2.7}$$

The supersymmetry transformation for the spinor fields in $5 + 1$ dimensions are given in terms of an $SU(2)$-Majorana Weyl spinor parameter ε^i satisfying $\varepsilon^i = C\epsilon^{ij}(\bar{\varepsilon}_j)^{\mathrm{T}}$, $\Gamma_7 \varepsilon^i = +\varepsilon^i$

$$\delta_\varepsilon \lambda^i = \tfrac{1}{2}\Gamma^{MN} F_{MN} \varepsilon^i + Y_a (\mathrm{i}\sigma_a)^i{}_j \varepsilon^j, \qquad \delta_\varepsilon \psi^{rA} = -\sqrt{2}\mathrm{i}\Gamma^M \mathcal{D}_M H^{irA} \epsilon_{ij} \varepsilon^j. \tag{2.8}$$

We can obtain the $((d - 1) + 1)$-dimensional $(d < 6)$ supersymmetric gauge theory with eight supercharges, by performing the Scherk–Schwarz (SS) [113] and/or the trivial dimensional reductions $(6 - d)$-times from the $(5 + 1)$-dimensional theory (2.6), after compactifying the pth $(p = 5, 4, \ldots, d)$ direction to S^1 with radius R_p. The twisted boundary condition for the SS dimensional reduction along the x^p-direction is given by

$$H^{iA}(x^\mu, x^p + 2\pi R_p) = H^{iA}(x^\mu, x^p)\, \mathrm{e}^{\mathrm{i}\alpha_{pA}}, \qquad (|\alpha_{pA}| \ll 2\pi), \tag{2.9}$$

where μ is the spacetime index in $(d - 1) + 1$ dimensions. We have used the flavour symmetry (2.4) commuting with supersymmetry for this twisting and so supersymmetry is preserved, unlike twisting by symmetry not commuting with supersymmetry often used in the context in which case supersymmetry is broken. If we consider the effective Lagrangian at sufficiently low energies, we can discard an infinite tower of the Kaluza–Klein modes and retain only the lightest mass field as a function of the $((d - 1) + 1)$-dimensional spacetime coordinates

$$W_\mu(x^\mu, x^p) \to W_\mu(x^\mu), \qquad W_p(x^\mu, x^p) \to -\Sigma_p(x^\mu), \tag{2.10}$$

$$H^{iA}(x^\mu, x^p) \to \frac{1}{\prod_p \sqrt{2\pi R_p}} H^{iA}(x^\mu) \exp\left(\mathrm{i}\sum_p m_{pA} x^p\right), \qquad m_{pA} \equiv \frac{\alpha_{pA}}{2\pi R_p}. \tag{2.11}$$

Integrating the $(5 + 1)$-dimensional Lagrangian in equation (2.6) over the x^p-coordinates and introducing the auxiliary fields F_i^{rA} for hypermultiplets, we obtain the $((d-1)+1)$-dimensional effective Lagrangian

$$\begin{aligned}\mathcal{L}_d = &-\frac{1}{4g_I^2} F^I_{\mu\nu} F^{I\mu\nu} + \frac{1}{2g_I^2}\mathcal{D}_\mu \Sigma_p^I \mathcal{D}^\mu \Sigma_p^I + (\mathcal{D}_\mu H^{irA})^* \mathcal{D}^\mu H^{irA} \\ &- (H^{irA})^* [(\Sigma_p - m_{pA})^2]^r{}_s H^{isA} + \mathcal{L}_{\text{aux}},\end{aligned} \tag{2.12}$$

$$\mathcal{L}_{\rm aux} = \frac{1}{2g_I^2}\left(Y_a^I\right)^2 - \zeta_a Y_a^0 + (H^{irA})^*(\sigma^a)^i{}_j(Y_a)^r{}_s H^{jsA} + \left(F_i^{rA}\right)^* F_i^{rA}, \qquad (2.13)$$

where we have redefined the gauge couplings and the FI parameters in $(d-1)+1$ dimensions from $5+1$ dimensions as $g_I^2 \to \left(\prod_p 2\pi R_p\right) g_I^2$, $\zeta_a \to \zeta_a/\left(\prod_p 2\pi R_p\right)$. We obtain $(6-d)$ adjoint real scalar fields Σ_p and $(6-d)$ real mass parameters for hypermultiplets in $(d-1)+1$ dimensions. The $SU(2)_R$ symmetry allows us to choose the FI parameters to lie in the third direction without loss of generality $\zeta_a = (0, 0, c\sqrt{N_{\rm C}/2})$, $c > 0$, although we cannot reduce all the FI parameters to the third direction if there are more FI parameters. Since the equations of motion for auxiliary fields are given by (2.7) and $F_i^{rA} = 0$, we obtain the on-shell version of the bosonic part of the Lagrangian with the scalar potential V as given in equation (2.2). However, we ignored in equation (2.2) one of the hypermultiplet scalars $H^2 = 0$, since H^2 vanishes for almost all soliton solutions as we see in the following sections.

2.2. Vacua

SUSY vacuum is equivalent to the vanishing vacuum energy, which requires both contributions from vector and hypermultiplets to V in equation (2.2) to vanish. The SUSY condition $Y_a = 0$ for vector multiplets can be rewritten as

$$H^1 H^{1\dagger} - H^2 H^{2\dagger} = c\mathbf{1}_{N_{\rm C}}, \qquad H^2 H^{1\dagger} = 0. \qquad (2.14)$$

This condition implies that some of hypermultiplets have to be non-vanishing. Since the non-vanishing hypermultiplets in the fundamental representation breaks gauge symmetry, we call these vacua as Higgs branch of vacua.

In the case of massless theory, the vanishing contribution from the hypermultiplet gives for each index A

$$(\Sigma_p)^r{}_s H^{isA} = 0, \qquad (2.15)$$

which requires $\Sigma_p = 0$ for all p. Therefore we find that the Higgs branches for the massless hypermultiplets are hyper-Kähler quotient [38, 39] given by $\mathcal{M}_{\rm vac} = \{H^{irA} | Y_a^I = 0\}/G$, where G denotes the gauge group. In our specific case of $U(N_{\rm C})$ gauge group with $N_{\rm F}(>N_{\rm C})$ massless hypermultiplets in the fundamental representation, the moduli space is given by the cotangent bundle over the complex Grassmann manifold [38]

$$\mathcal{M}_{\rm vac}^{M_p=0} \simeq T^* G_{N_{\rm F},N_{\rm C}} \simeq T^*\left[\frac{SU(N_{\rm F})}{SU(N_{\rm C}) \times SU(N_{\rm F}-N_{\rm C}) \times U(1)}\right]. \qquad (2.16)$$

The real dimension of the Higgs branch is $4N_{\rm C}(N_{\rm F}-N_{\rm C})$.

In the massive theory, the vanishing contribution to vacuum energy from hypermultiplets gives

$$(\Sigma_p - m_{pA}\mathbf{1})^r{}_s H^{isA} = 0, \qquad (2.17)$$

for each index A. This is satisfied by choosing the adjoint scalar Σ_p to be diagonal matrices whose rth elements are specified by the the non-degenerate mass m_{pA_r} for the hypermultiplet with non-vanishing r colour and A_r flavour

$$H^{1rA} = \sqrt{c}\,\delta^{A_r}{}_A, \qquad H^{2rA} = 0, \qquad \Sigma_p = {\rm diag}\left(m_{pA_1}, m_{pA_2}, \ldots, m_{pA_{N_{\rm C}}}\right). \qquad (2.18)$$

Therefore we find that the Higgs branch of vacua of the massless case is lifted by masses except for fixed points of the tri-holomorphic $U(1)$ Killing vectors [40] induced by the $U(1)$ actions in equation (2.9) or (2.4), when we introduce masses in lower dimensions by the SS dimensional reductions. Introducing non-degenerate masses, only $N_{\rm F}!/[N_{\rm C}! \times (N_{\rm F}-N_{\rm C})!]$ discrete points out of the massless moduli space $T^*G_{N_F,N_C}$ remain as vacua [41]. These discrete vacua are often called colour–flavour locking vacua. In the particular case of $N_F = N_C$, we have the unique vacuum up to gauge transformations. Throughout this review the vacuum given by equation (2.18) is labelled by

$$\langle A_1, A_2, \ldots, A_{N_C}\rangle \tag{2.19}$$

or briefly by $\langle\{A_r\}\rangle$. This kind of labels may also be used for defining an $N_C \times N_C$ minor matrix $H^{\langle\{A_r\}\rangle}$ from the $N_C \times N_F$ matrix H as $(H^{\langle\{A_r\}\rangle})^{qs} = H^{qA_s}$.

2.3. Infinite gauge coupling and nonlinear sigma models

SUSY gauge theories reduce to nonlinear sigma models in the strong gauge coupling limit $g^2 \to \infty$. With eight supercharges, they become hyper-Kähler (HK) nonlinear sigma models [36, 37, 40] on the Higgs branch [42, 43] of gauge theories as their target spaces. This construction of HK manifold is called an HK quotient [38, 39]. If hypermultiplets are massless, the HK nonlinear sigma models receive no potentials. If hypermultiplets have masses, the models are called massive HK nonlinear sigma models which possess potentials as the square of tri-holomorphic Killing vectors on the target manifold [40]. Most vacua are lifted with this potential leaving some discrete points as vacua, which are characterized by fixed points of the Killing vector. In our case of $U(N_C)$ gauge theory with N_F hypermultiplets in the fundamental representation, the model reduces to the massive hyper-Kähler nonlinear sigma model on $T^*G_{N_F,N_C}$ in equation (2.16). With our choice of the FI parameters, H^1 parametrizes the base manifold G_{N_F,N_C}, whereas H^2 its cotangent space. Thus we obtain the Kähler nonlinear sigma model on the Grassmann manifold G_{N_F,N_C} if we set $H^2 = 0$ [44].

Let us give the concrete Lagrangian of the nonlinear sigma models. Since the gauge kinetic terms for W_μ and Σ_p (and their superpartners) disappear in the limit of infinite coupling, we obtain the Lagrangian

$$\mathcal{L}^{g\to\infty} = \mathrm{Tr}[(\mathcal{D}_\mu H^i)^\dagger \mathcal{D}^\mu H^i] + \mathrm{Tr}[(H^{i\dagger}\Sigma_p - M_p H^{i\dagger})(\Sigma_p H^i - H^i M_p)]. \tag{2.20}$$

The auxiliary fields Y^a serve as Lagrange multiplier fields to give constraints (2.14) as their equations of motion. Equation (2.20) gives equations of motion for W_μ and Σ_p as auxiliary fields expressible in terms of hypermultiplets

$$W_\mu^I = \mathrm{i}(A^{-1})^{IJ}\mathrm{Tr}[(H^i\partial_\mu H^{i\dagger} - \partial_\mu H^i H^{i\dagger})T_J], \tag{2.21}$$

$$\Sigma_p^I = 2(A^{-1})^{IJ}\mathrm{Tr}(H^{i\dagger}T_J H^i M_p), \tag{2.22}$$

where $(A^{-1})^{IJ}$ is an inverse matrix of A_{IJ} defined by $A_{IJ} = \mathrm{Tr}(H^{i\dagger}\{T_I, T_J\}H^i)$. As a result the Lagrangian (2.20) with the constraints (2.14) gives the nonlinear sigma model, after eliminating W_μ, Σ_p. This is the HK nonlinear sigma model [38, 41] on the cotangent bundle over the complex Grassmann manifold in equation (2.16). The isometry of the metric, which is the symmetry of the kinetic term, is $SU(N_F)$, although it is broken to its maximal Abelian subgroup $U(1)^{N_F-1}$ by the potential. In the massless limit $M_p = 0$, the potential V vanishes and the whole manifold becomes vacua, the Higgs branch of our gauge theory. Turning on the hypermultiplet masses, we obtain the potential allowing only discrete points as SUSY vacua [41], which are fixed points of the invariant subgroup $U(1)^{N_F-1}$ of the potential. The number of vacua is $N_F!/[N_C!(N_F - N_C)!]$, which is the same as the case of the finite gauge coupling.

In the case of $N_C = 1$ the target space reduces to the cotangent bundle over the compact projective space $\mathbf{C}P^{N_F-1}$, $T^*\mathbf{C}P^{N_F-1} = T^*[SU(N_F)/SU(N_F-1)\times U(1)]$ [45]. This is a toric HK (or hypertoric) manifold and the massive model has discrete N_F vacua [50]. If $N_F = 2$ the target space $T^*\mathbf{C}P^1$ is the simplest HK manifold, the Eguchi–Hanson space [46].

From the target manifold (2.16) one can easily see that there exists a duality between theories with the same number of flavours and two different gauge groups in the case of the infinite gauge coupling [41, 42]:

$$U(N_{\mathrm{C}}) \leftrightarrow U(N_{\mathrm{F}} - N_{\mathrm{C}}). \tag{2.23}$$

This duality holds for the entire Lagrangian of the nonlinear sigma models.

3. 1/2 BPS solitons

3.1. Walls

3.1.1. BPS equations for domain walls. Domain walls are static BPS solitons of co-dimension one interpolating between different discrete vacua like equation (2.18). In order to obtain domain wall solutions we require that all fields should depend on one spatial coordinate, say $y \equiv x^2$. We also set $H^2 = 0$ and define $H \equiv H^1$. We have shown in appendix B in [2] that the condition $H^2 = 0$ is deduced in our model (but it is not always the case in general models [4]). The Bogomol'nyi completion of the energy density for domain walls can be performed as

$$\begin{aligned}\mathcal{E} = \frac{1}{g^2}\mathrm{Tr}\left(\mathcal{D}_y\Sigma - \frac{g^2}{2}(c\mathbf{1}_{N_{\mathrm{C}}} - HH^\dagger)\right)^2 + \mathrm{Tr}[(\mathcal{D}_yH + \Sigma H - HM)(\mathcal{D}_yH + \Sigma H - HM)^\dagger]\\ + c\partial_y\mathrm{Tr}\,\Sigma - \partial_y\{\mathrm{Tr}[(\Sigma H - HM)H^\dagger]\}.\end{aligned} \tag{3.1}$$

This energy bound is saturated when the BPS equations for domain walls are satisfied

$$D_yH = -\Sigma H + HM, \qquad D_y\Sigma = \frac{g^2}{2}(c\mathbf{1}_{N_{\mathrm{C}}} - HH^\dagger), \tag{3.2}$$

and the energy per unit volume (tension) of domain walls interpolating between the vacuum $\langle\{A_r\}\rangle$ at $y \to +\infty$ and the vacuum $\langle\{B_r\}\rangle$ at $y \to -\infty$ is obtained as

$$T_{\mathrm{w}} = \int_{-\infty}^{+\infty}\mathrm{d}y\,\mathcal{E} = c[\mathrm{Tr}\Sigma]_{-\infty}^{+\infty} = c\left(\sum_{k=1}^{N_{\mathrm{C}}} m_{A_k} - \sum_{k=1}^{N_{\mathrm{C}}} m_{B_k}\right). \tag{3.3}$$

The tension T_{w} depends only on boundary conditions at spatial infinities $y \to \pm\infty$ and is a topological charge.

There exists one dimensionless parameter $g\sqrt{c}/|\Delta m|$ in our system. Depending on whether the gauge coupling constant is weak ($g\sqrt{c} \ll |\Delta m|$) or strong ($|\Delta m| \ll g\sqrt{c}$), domain walls have different internal structure. Let us review an internal structure of $U(1)$ gauge theory [110]. Walls have a three-layer structure shown in figure 1(*a*) in weak gauge coupling. The outer two thin layers have the same width of order $L_{\mathrm{o}} = 1/g\sqrt{c}$ and the internal fat layer has a width of order $L_{\mathrm{i}} = |\Delta m|/g^2c(\gg L_{\mathrm{o}})$. The wall in $U(1)$ gauge theory with $N_{\mathrm{F}} = 2$ interpolating between the vacuum $\langle 1\rangle(H = \sqrt{c}(1, 0), \Sigma = m_1)$ at $y \to -\infty$ and the vacuum $\langle 2\rangle(H = \sqrt{c}(0, 1), \Sigma = m_2)$ at $y \to +\infty$ is shown in figure 1(*a*). The first (second) flavour component of the Higgs field exponentially decreases in the left (right) outer layer so that the entire $U(1)$ gauge symmetry is restored in the inner core.

In the strong gauge coupling ($g\sqrt{c} \gg |\Delta m|$) the internal structure becomes simpler for both Abelian and non-Abelian cases. The middle layer disappears and two outer layers of the Higgs phase grow with the total width being of order $1/|\Delta m|$.

An internal structure becomes important at finite or weak gauge coupling, for instance when we discuss domain wall junction [8, 9] in section 4.2 or Skyrmion as instantons inside domain walls [16].

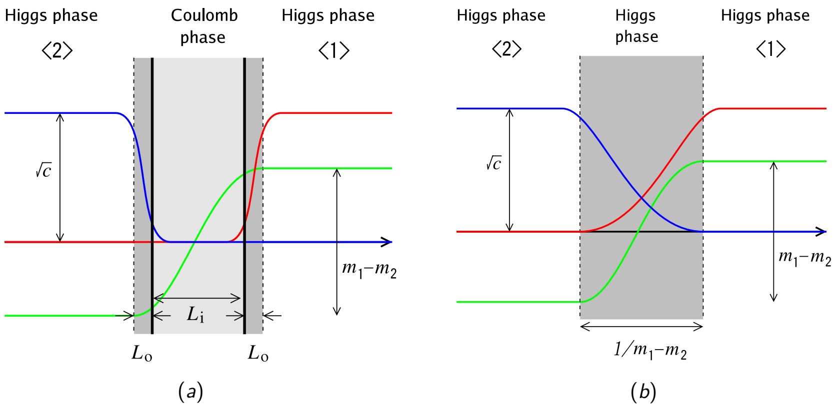

Figure 1. Internal structures of the domain walls: (*a*) a three-layer structure if $g\sqrt{c} \ll |\Delta m|$, (*b*) a single-layer structure if $g\sqrt{c} \gg |\Delta m|$.

3.1.2. Wall solutions and their moduli space. Let us solve the BPS equations (3.2). Defining an N by N invertible matrix $S(y) \in GL(N_C, \mathbf{C})$ by the 'Wilson line'

$$S(y) \equiv \mathbf{P}\exp\left(\int \mathrm{d}y(\Sigma + \mathrm{i}W_y)\right) \tag{3.4}$$

with $\mathbf{P}$ denoting the path ordering, we obtain the relation

$$\Sigma + \mathrm{i}W_y = S^{-1}(y)\partial_y S(y). \tag{3.5}$$

Using S the first equation in (3.2) can be solved as

$$H = S^{-1}(y)H_0\,\mathrm{e}^{My}. \tag{3.6}$$

Defining a $U(N_C)$ gauge invariant

$$\Omega \equiv SS^\dagger, \tag{3.7}$$

the second equation in (3.2) can be rewritten as

$$\partial_y(\Omega^{-1}\partial_y\Omega) = g^2\big(c - \Omega^{-1}H_0\,\mathrm{e}^{2My}H_0{}^\dagger\big). \tag{3.8}$$

We call this the master equation for domain walls. This equation is difficult to solve analytically in general[4]. However it can be solved immediately as

$$\Omega_{g\to\infty} \equiv \Omega_0 = c^{-1}H_0\,\mathrm{e}^{2My}H_0{}^\dagger \tag{3.9}$$

in the strong gauge coupling limit $g^2 \to \infty$, in which the model reduces to the HK nonlinear sigma model. Some exact solutions are also known for particular finite gauge coupling with restricted moduli parameters [61]. Existence and uniqueness of solutions of (3.8) were proved for the $U(1)$ gauge group [5]. One can expect from the index theorem [12] that it holds for the $U(N_C)$ gauge group.

Therefore we conclude that all moduli parameters in wall solutions are contained in the moduli matrix H_0. However one should note that two sets (S, H_0) and $(S', H_0{}')$ related by *the V-transformation*

$$S' = VS, \qquad H_0{}' = VH_0, \qquad V \in GL(N_C, \mathbf{C}) \tag{3.10}$$

give the same physical quantities W_y and Σ, where the quantity Ω transforms as

$$\Omega' = V\Omega V^\dagger \tag{3.11}$$

and equation (3.8) is covariant. Thus we need to identify these two as $(S, H_0) \sim (S', H_0')$, which we call *the V-equivalence relation*. The moduli space of the *BPS equations* (3.2) is

[4] Non-integrability of this equation has been addressed recently in [120] by using the Painlevé test.

found to be the complex Grassmann manifold

$$\mathcal{M}_{\text{wall}}^{\text{total}} \simeq \{H_0 | H_0 \sim V H_0,\ V \in GL(N_{\mathrm{C}}, \mathbf{C})\}$$
$$\simeq G_{N_{\mathrm{F}},N_{\mathrm{C}}} \simeq \frac{SU(N_{\mathrm{F}})}{SU(N_{\mathrm{C}}) \times SU(N_{\mathrm{F}} - N_{\mathrm{C}}) \times U(1)}, \tag{3.12}$$

with dimension $\dim \mathcal{M}_{\text{wall}}^{\text{total}} = 2N_{\mathrm{C}}(N_{\mathrm{F}} - N_{\mathrm{C}})$. We did not put any boundary conditions at $y \to \pm\infty$ to get the moduli space (3.12). Therefore it contains configurations with all possible boundary conditions, and can be decomposed into the sum of topological sectors

$$\mathcal{M}_{\text{wall}}^{\text{total}} = \sum_{\text{BPS}} \mathcal{M}^{\langle A_1,\ldots,A_{N_{\mathrm{C}}}\rangle \leftarrow \langle B_1,\ldots,B_{N_{\mathrm{C}}}\rangle}. \tag{3.13}$$

Here each topological sector $\mathcal{M}^{\langle A_1,\ldots,A_{N_{\mathrm{C}}}\rangle \leftarrow \langle B_1,\ldots,B_{N_{\mathrm{C}}}\rangle}$ is specified by the boundary conditions, $\langle A_1, \ldots, A_{N_{\mathrm{C}}}\rangle$ at $y \to +\infty$ and $\langle B_1, \ldots, B_{N_{\mathrm{C}}}\rangle$ at $y \to -\infty$. It is interesting to observe that this space also contains vacuum sectors, $B_r = A_r$ for all r, as isolated points because these states of course satisfy the BPS equations (3.2). More explicit decomposition will be explained in the next subsection. We often call $\mathcal{M}_{\text{wall}}^{\text{total}}$ the *total moduli space* for domain walls. One has to note that we cannot define the usual Manton's metric on the total moduli space because it is made by gluing different topological sectors. The Manton's metric is defined in each topological sector.

We have seen that the total moduli space of domain walls is the complex Grassmann manifold (3.12). On the other hand, the moduli space of *vacua* for the corresponding model with massless hypermultiplet is the cotangent bundle over the complex Grassmann manifold (2.16). This is not just a coincidence. It has been shown in [4] that the moduli space of domain walls in a massive theory is a special Lagrangian submanifold the moduli space of vacua in the corresponding massless theory.

For any given moduli matrix H_0 the V-equivalence relation (3.10) can be uniquely fixed to obtain the following matrix, called *the standard form*:

$$H_0 = \begin{array}{c} \begin{array}{ccccccccccc} A_1 & & A_2 & & A_{N_{\mathrm{C}}} & \leftarrow & B_1 & & B_{N_{\mathrm{C}}} & & B_2 \end{array} \\ \left(\begin{array}{cccccccccccc} 1 & * & & \cdots & & * & \mathrm{e}^{v_1} & & & & & \mathbf{O} \\ & & 1 & * & & & \cdots & & & * & \mathrm{e}^{v_2} & \\ & & & & & & \vdots & & & & & \\ \mathbf{O} & & & & 1 & * & \cdots & * & \mathrm{e}^{v_{N_{\mathrm{C}}}} & & & \end{array}\right) \end{array}, \tag{3.14}$$

where A_r is ordered as $A_r < A_{r+1}$ but B_r is not. Here in the rth row the left-most nonzero (r, A_r)-elements are fixed to be one, the right-most nonzero (r, B_r)-elements are denoted by $\mathrm{e}^{v_r}(\in \mathbf{C}^* \equiv \mathbf{C} - \{0\} \simeq \mathbf{R} \times S^1)$. Some elements between them must vanish to fix V-transformation (3.10), but some of them denoted by $*(\in \mathbf{C})$ are complex parameters which can vanish. (See appendix B of [2] for how to fix V-transformation completely.) Substituting the standard form (3.14) into solution (3.6) one finds that configuration interpolates between $\langle A_1, \ldots, A_{N_{\mathrm{C}}}\rangle$ at $y \to +\infty$ and $\langle B_1, \ldots, B_{N_{\mathrm{C}}}\rangle$ at $y \to -\infty$. In order to obtain the topological sector $\mathcal{M}^{\langle A_1,\ldots,A_{N_{\mathrm{C}}}\rangle \leftarrow \langle B_1,\ldots,B_{N_{\mathrm{C}}}\rangle}$ we have to gather matrices in the standard form (3.14) with all possible ordering of B_r. We can show that the generic region of the topological sector $\mathcal{M}^{\langle A_1,\ldots,A_{N_{\mathrm{C}}}\rangle \leftarrow \langle B_1,\ldots,B_{N_{\mathrm{C}}}\rangle}$ is covered by the moduli parameters in the moduli matrix with ordered $B_r(< B_{r+1})$. Therefore its complex dimension is calculated to be

$$\dim_{\mathbf{C}} \mathcal{M}^{\langle\{A_r\}\rangle \leftarrow \langle\{B_r\}\rangle} = \sum_{r=1}^{N_{\mathrm{C}}} (B_r - A_r). \tag{3.15}$$

The maximal number of domain walls is realized in the maximal topological sector $\mathcal{M}^{\langle 1,2,\ldots,N_{\mathrm{C}}\rangle \leftarrow \langle N_{\mathrm{F}}-N_{\mathrm{C}}+1,\ldots,N_{\mathrm{F}}-1,N_{\mathrm{F}}\rangle}$ with complex dimension $N_{\mathrm{C}}(N_{\mathrm{F}} - N_{\mathrm{C}})$.

When a moduli matrix contains only one modulus, like

$$H_0 = \begin{pmatrix} 1 & 0 & 0 & 0 & 0 & 0 \\ 0 & 1 & 0 & 0 & \mathrm{e}^r & 0 \\ 0 & 0 & 1 & 0 & 0 & 0 \end{pmatrix}, \tag{3.16}$$

we call the configuration generated by this matrix as a *single wall*. In particular, we call a single wall generated by a moduli matrix (3.16) with no zeros between 1 and e^r as an *elementary wall*. Whereas a single wall with some zeros between 1 and e^r is called a *composite wall*, because it can be broken into a set of elementary walls with a moduli deformation.

3.1.3. Properties. In order to clarify the meaning of the moduli parameters we explain how to estimate the positions of domain walls from the moduli matrix H_0 according to appendix A of [2]. We also show explicit decomposition (3.13) of the total moduli space (3.12) by using simple examples in this subsection.

Using Ω in (3.7) the energy density $\mathcal{E}$ of domain wall, the integrand in equation (3.3), can be rewritten as

$$\mathcal{E} = c\partial_y \operatorname{Tr} \Sigma + \frac{1}{g^2}\left(\partial_y^4 \text{ term}\right) = c\partial_y^2(\log\det\Omega) + \frac{1}{g^2}\left(\partial_y^4 \text{ term}\right). \tag{3.17}$$

The ∂_y^4 term can be neglected when we discuss wall positions. Apart from the core of domain wall, Ω approaches to $\Omega_0 = c^{-1} H_0\, \mathrm{e}^{2My} H_0^\dagger$ in equation (3.9). There the energy density (3.17) can be expressed by the moduli matrix as

$$\begin{aligned} \mathcal{E} &\approx c\partial_y^2 \log\det\left(\frac{1}{c} H_0\, \mathrm{e}^{2My} H_0^\dagger\right) \\ &= c\partial_y^2 \log \sum_{\langle\{A_r\}\rangle} \left[|\tau^{\langle\{A_r\}\rangle}|^2 \exp\left(2\sum_{r=1}^{N_\mathrm{C}} m_{A_r} y\right)\right]. \end{aligned} \tag{3.18}$$

Here the sum is taken over all possible vacua $\langle\{A_r\}\rangle = \langle A_1, A_2, \ldots, A_{N_\mathrm{C}}\rangle$ and $\tau^{\langle\{A_r\}\rangle}$ is defined by

$$\tau^{\langle\{A_r\}\rangle} \equiv \exp(a^{\langle\{A_r\}\rangle} + \mathrm{i}b^{\langle\{A_r\}\rangle}) \equiv \det H_0^{\langle\{A_r\}\rangle} \tag{3.19}$$

with $(H_0^{\langle\{A_r\}\rangle})^{st} = H_0^{sA_t}$ an N_C by N_C minor matrix of H_0. It is useful to define a *weight* of a vacuum $\langle\{A_r\}\rangle$ as $\mathrm{e}^{2\mathcal{W}^{\langle\{A_r\}\rangle}}$ with

$$\mathcal{W}^{\langle\{A_r\}\rangle}(y) \equiv \sum_{r=1}^{N_\mathrm{C}} m_{A_r} y + a^{\langle\{A_r\}\rangle}, \tag{3.20}$$

and an *average magnitude* of the vacua by

$$\exp 2\langle\mathcal{W}\rangle \equiv \sum_{\langle\{A_r\}\rangle} \exp 2\mathcal{W}^{\langle\{A_r\}\rangle}. \tag{3.21}$$

Then the energy density can be rewritten as

$$\mathcal{E} \approx c\partial_y^2\langle\mathcal{W}\rangle = \frac{c}{2}\partial_y^2 \log \sum_{\langle\{A_r\}\rangle} \exp 2\mathcal{W}^{\langle\{A_r\}\rangle}. \tag{3.22}$$

This approximation is valid away from the core of domain walls but not good near their core. This expression holds exactly in the whole region at the strong gauge coupling limit.

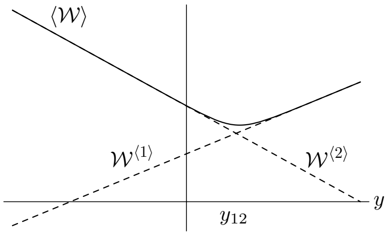

Figure 2. Comparison of the profile of $\langle\mathcal{W}\rangle$, $\mathcal{W}^{\langle 1\rangle}$, $\mathcal{W}^{\langle 2\rangle}$ as functions of y. Linear functions $\mathcal{W}^{\langle A\rangle}$ are good approximations in their respective dominant regions.

It may be useful to order τ's according to the sum of masses of hypermultiplets corresponding to the labels of flavours, like

$$\{\ldots,\tau^{\langle\{A_r\}\rangle},\ldots,\tau^{\langle\{B_r\}\rangle},\ldots\},\qquad \text{so that}\qquad \sum_{r=1}^{N_{\mathrm{C}}} m_{A_r} > \sum_{r=1}^{N_{\mathrm{C}}} m_{B_r}. \tag{3.23}$$

When only one τ is nonzero with the rests vanishing as

$$\{0,\ldots,0,\tau^{\langle\{A_r\}\rangle},0,\ldots,0\}, \tag{3.24}$$

only one weight $\mathrm{e}^{2\mathcal{W}^{\langle\{A_r\}\rangle}}$ survives and the logarithm $\log\det\Omega$ inside the y-derivative in equation (3.22) becomes linear with respect to y. Therefore the energy (3.22) vanishes and the configuration is in a SUSY vacuum. Next let us consider general situation. In a region of y such that one $\mathcal{W}^{\langle\{A_r\}\rangle}$ is larger than the rests, $\exp\mathcal{W}^{\langle\{A_r\}\rangle}$ is dominant in the logarithm in equation (3.22). Therefore the logarithm $\log\det\Omega$ inside differentiations in equation (3.22) is almost linear with respect to y, the energy (3.22) vanishes and configuration is close to a SUSY vacuum in that region of y. The energy does not vanish only when two or more $\mathcal{W}^{\langle\{A_r\}\rangle}$'s are comparable. If two $\mathcal{W}^{\langle\{A_r\}\rangle}$'s are comparable and are larger than the rests, there exists a domain wall. This is a key observation throughout this review.

We now discuss the $U(1)$ gauge theory in detail. There exist N vacua, $\langle A\rangle$ with $A=1,\ldots,N$. The moduli matrix and weight are

$$H_0=\sqrt{c}(\tau^{\langle 1\rangle},\tau^{\langle 2\rangle},\ldots,\tau^{\langle N_{\mathrm{F}}\rangle}), \tag{3.25}$$

$$\exp(2\mathcal{W}^{\langle A\rangle}(y))=\exp 2(m_A y+a^{\langle A\rangle}), \tag{3.26}$$

respectively, with $\tau^{\langle A\rangle}\in\mathbf{C}$ and $a^{\langle A\rangle}=\mathrm{Re}(\log\tau^{\langle A\rangle})$. Here $\tau^{\langle A\rangle}$ are regarded as the homogeneous coordinates of the total moduli space $\mathbf{C}P^{N_{\mathrm{F}}-1}$. Any single wall is generated by a moduli matrix (3.26) with only two non-vanishing τ's. If these two are a nearest pair, an elementary wall is generated.

Example 1 (single wall)**.** We now restrict ourselves to the simplest case, $N_{\mathrm{F}}=2$. This model contains two vacua $\langle 1\rangle$ and $\langle 2\rangle$ allowing one domain wall connecting them. The weights of these vacua are $\mathrm{e}^{2\mathcal{W}^{\langle 1\rangle}}$ and $\mathrm{e}^{2\mathcal{W}^{\langle 2\rangle}}$, respectively. When one weight $\mathrm{e}^{2\mathcal{W}^{\langle A\rangle}}$ is larger than the other, configuration approaches to the vacuum $\langle A\rangle$ as seen in figure 2. Energy density is concentrated around the region where both the weights are comparable. Therefore the wall position is determined by equating them,

$$y=-\frac{a^{\langle 1\rangle}-a^{\langle 2\rangle}}{m_1-m_2}=-\frac{\log|\tau^{\langle 1\rangle}/\tau^{\langle 2\rangle}|}{m_1-m_2}. \tag{3.27}$$

We also have the $U(1)$ modulus in the phase of $\tau^{\langle 1\rangle}/\tau^{\langle 2\rangle}$ which does not affect the shape of the wall. This is a Nambu–Goldstone mode coming from the flavour $U(1)$ symmetry

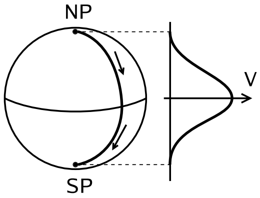

Figure 3. $\mathbf{C}P^1$ and the potential V. The base space of $T^*\mathbf{C}P^1$, $\mathbf{C}P^1 \simeq S^2$, is displayed. This model contains two discrete vacua denoted by N and S. The potential V is also displayed on the right of the $\mathbf{C}P^1$. It admits a single wall solution connecting these two vacua expressed by a curve. The $U(1)$ isometry around the axis connecting N and S is spontaneously broken by the wall configuration.

spontaneously broken by the wall configuration. The moduli space of single wall is a cylinder $\mathcal{M}^{k=1} \simeq \mathbf{R} \times S^1 \simeq \mathbf{C}^* \equiv \mathbf{C} - \{0\}$. This is non-compact. In the limit of $a^{\langle 1\rangle} \to -\infty$ or $a^{\langle 2\rangle} \to -\infty$ the configuration becomes a vacuum. These limits naturally define how to add two points, which correspond to the two vacuum states, to $\mathcal{M}^{k=1}$. We thus obtain the total moduli space as a compact space:

$$\mathbf{C}P^1 \simeq S^2 = \mathcal{M}^{k=1} + \text{two points} = \mathbf{R} \times S^1 + \text{two points}. \tag{3.28}$$

This is an explicit illustration of the decomposition (3.13) of the total moduli space.

In the strong gauge coupling limit, the model reduces to a nonlinear sigma model on $T^*\mathbf{C}P^1$, the Eguchi–Hanson space, allowing a single domain wall [48, 54, 55]. In figure 3 we display the base space $\mathbf{C}P^1$ of the target space, the potential V on it, two vacua N and S, and a curve in the target space mapped from a domain wall solution connecting these vacua.

Example 2 (double wall (appendix A of [2]). Let us switch to the second simplest case, $N_{\mathrm{F}} = 3$. This model contains three vacua $\langle 1\rangle$, $\langle 2\rangle$ and $\langle 3\rangle$ whose weights are $\mathrm{e}^{2\mathcal{W}^{\langle 1\rangle}}$, $\mathrm{e}^{2\mathcal{W}^{\langle 2\rangle}}$ and $\mathrm{e}^{2\mathcal{W}^{\langle 3\rangle}}$, respectively. This model admits three single walls generated by the moduli matrices

$$H_0 = \sqrt{c}(\tau^{\langle 1\rangle}, \tau^{\langle 2\rangle}, 0), \qquad \sqrt{c}(0, \tau^{\langle 2\rangle}, \tau^{\langle 3\rangle}), \qquad \sqrt{c}(\tau^{\langle 1\rangle}, 0, \tau^{\langle 3\rangle}). \tag{3.29}$$

We now show that the first two are elementary wall while the last is not elementary but a composite of the first two, as defined below equation (3.16). Let us consider the full moduli matrix $H_0 = \sqrt{c}(\tau^{\langle 1\rangle}, \tau^{\langle 2\rangle}, \tau^{\langle 3\rangle})$. By equating two of the three weights we have three solutions of y:

$$y_{12} = -\frac{a^{\langle 1\rangle} - a^{\langle 2\rangle}}{m_1 - m_2}, \qquad y_{23} = -\frac{a^{\langle 2\rangle} - a^{\langle 3\rangle}}{m_2 - m_3}, \qquad y_{13} = -\frac{a^{\langle 1\rangle} - a^{\langle 3\rangle}}{m_1 - m_3}. \tag{3.30}$$

Not all of these correspond to wall positions. To see this we draw the three linear functions $\mathcal{W}^{\langle A\rangle}$ and $\langle \mathcal{W}\rangle = 1/2 \log(\mathrm{e}^{2\mathcal{W}^{\langle 1\rangle}(y)} + \mathrm{e}^{2\mathcal{W}^{\langle 2\rangle}(y)} + \mathrm{e}^{2\mathcal{W}^{\langle 3\rangle}(y)})$ in figure 4 according to cases (a) $y_{23} < y_{12}$ and (b) $y_{12} < y_{23}$. We observe that there exist two domain walls in case (a) $y_{23} < y_{12}$ but only one wall in case (b) $y_{12} < y_{23}$. By taking a limit $a^{\langle 1\rangle} \to -\infty$ ($\mathrm{e}^{2\mathcal{W}^{\langle 1\rangle}} \to 0$) or $a^{\langle 3\rangle} \to -\infty$ ($\mathrm{e}^{2\mathcal{W}^{\langle 3\rangle}} \to 0$), we obtain a configuration of a single wall located at y_{23} or y_{12}, respectively. They are configurations of elementary walls generated by the first two moduli matrices in equation (3.29). The configuration (a) in figure 4 is the case that these two walls approach each other with finite distance. If these two walls get close further we obtain the configuration (b) in figure. This looks almost a single wall. In the limit $a^{\langle 2\rangle} \to -\infty$ ($\mathrm{e}^{2\mathcal{W}^{\langle 2\rangle}} \to 0$), the configuration really becomes a single wall generated by the last moduli matrix of (3.29). Therefore the last one generates a composite wall made of two elementary walls compressed. This is a common feature when Abelian domain walls interact.

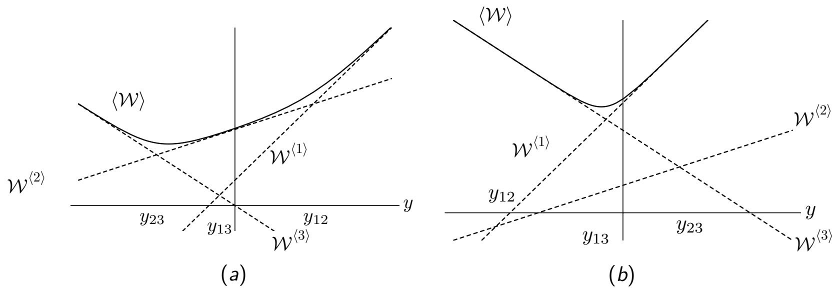

Figure 4. Comparison of the profile of $\langle\mathcal{W}\rangle$, $\mathcal{W}^{\langle 1\rangle}$, $\mathcal{W}^{\langle 2\rangle}$ as functions of y. $\langle\mathcal{W}\rangle$ connects smoothly dominant linear functions $\mathcal{W}^{\langle A\rangle}$ in respective regions: (*a*) $y_{23} < y_{12}$ and (*b*) $y_{23} > y_{12}$.

The moduli space of the double wall is $\mathcal{M}^{k=2} \simeq \mathbf{C}^* \times \mathbf{C}$ with $\mathbf{C}^*$ denoting the overall position and phase and $\mathbf{C}$ denoting relative ones. This is non-compact. In the two limits $a^{\langle 1\rangle} \to -\infty$ and $a^{\langle 3\rangle} \to -\infty$ which we took above, the configuration reach two single-wall sectors $\mathcal{M}^{k=1}_{(1)}$ and $\mathcal{M}^{k=1}_{(2)}$ both of which are isomorphic to $\mathbf{C}^*$. These limits naturally define gluing the two single-wall sectors to the double wall sector $\mathcal{M}^{k=2}$. Finally the three vacuum sectors are added to it, resulting the total moduli space $\mathbf{C}P^2$:

$$\mathbf{C}P^2 = \mathcal{M}^{k=2} + \mathcal{M}^{k=1}_{(1)} + \mathcal{M}^{k=1}_{(2)} + \text{three points}. \tag{3.31}$$

This is another explicit illustration of the decomposition (3.13) of the total moduli space.

Note that the function $\log\sum_{\langle A\rangle} \mathrm{e}^{2\mathcal{W}^{\langle A\rangle}}$ in equation (3.22) can be approximated by piecewise linear function obtained by the largest weight $\mathcal{W}^{\langle A\rangle}$ in each region of y, as seen in (4). This is known as tropical geometry in the mathematical literature.

The $U(1)$ gauge theory ($N_\mathrm{C} = 1$) with N_F flavours admits the N_F vacua and the $N_\mathrm{F} - 1$ walls which are ordered.

$$\mathbf{C}P^{N_\mathrm{F}-1} = \sum_{k=1}^{N_\mathrm{F}-1} \sum_{i_k} \mathcal{M}^k_{(i_k)}. \tag{3.32}$$

We now make a comment on symmetry properties of domain walls. In the Abelian case with N_F, the number of walls are $N_\mathrm{F} - 1$. Each wall carries approximate Nambu–Goldstone modes for translational invariance if they are well separated. Only the overall translation is an exact Nambu–Goldstone mode. They carry Nambu–Goldstone modes for spontaneously broken $U(1)^{N_\mathrm{F}-1}$ flavour symmetry.

Next let us turn our attention to non-Abelian gauge theory ($N_\mathrm{C} > 1$). We have defined single walls, elementary walls and composite walls below equation (3.16). However these definitions are not covariant under the V-transformation (3.10). They can be defined covariantly as follows. To this end we first should note that τ's defined in equation (3.19) are the so-called Plücker coordinates of the complex Grassmann manifold. These coordinates $\{\tau^{\langle\{A_r\}\rangle}\}$ are not independent but satisfy the so-called Plücker relations

$$\sum_{k=0}^{N_\mathrm{C}} (-1)^k \tau^{\langle A_1\cdots A_{N_\mathrm{C}-1} B_k\rangle} \tau^{\langle B_0\cdots \underline{B_k}\cdots B_{N_\mathrm{C}}\rangle} = 0 \tag{3.33}$$

where the bar under B_k denotes removing B_k from $\langle B_0 \cdots B_k \cdots B_{N_\mathrm{C}}\rangle$. Among these equations, only ${}_{N_\mathrm{F}}C_{N_\mathrm{C}} - 1 - N_\mathrm{C}(N_\mathrm{F} - N_\mathrm{C})$ equations give independent constraints with reducing the number of independent coordinates to the complex dimension $N_\mathrm{C}(N_\mathrm{F} - N_\mathrm{C})$ of the Grassmann manifold.

Using the Plücker coordinates, single walls are defined to be configurations generated by two non-vanishing τ's with the rests vanishing. These are configurations interpolating between two vacua $\langle \underline{\cdots} A\rangle$ and $\langle \underline{\cdots} B\rangle$ $(A \neq B)$, where underlined dots denote the same set of labels. We can show that the Plücker relations (3.33) do not forbid these configurations. If the labels are different by one the configurations are said to be elementary walls, whereas if they are different by more than one the configurations are said to be composite walls. On the other hand, the Plücker relations (3.33) forbid configurations to interpolate between two vacua whose labels have two or more different integers, such as $\langle \underline{\cdots} 123\rangle$ and $\langle \underline{\cdots} 456\rangle$.

Example. Let us consider the simplest model of $N_{\rm F} = 4$ and $N_{\rm C} = 2$ with one nontrivial Plücker relation. This model contains the six vacua, $\langle 12\rangle$, $\langle 13\rangle$, $\langle 14\rangle$, $\langle 23\rangle$, $\langle 24\rangle$ and $\langle 34\rangle$. The Plücker relation (3.33) becomes

$$\tau^{\langle 12\rangle}\tau^{\langle 34\rangle} - \tau^{\langle 13\rangle}\tau^{\langle 24\rangle} + \tau^{\langle 14\rangle}\tau^{\langle 23\rangle} = 0. \tag{3.34}$$

This allows, for example, $\tau^{\langle 12\rangle}$ and $\tau^{\langle 13\rangle}$ to be non-vanishing with the rests vanishing. So we have a single wall connecting $\langle 12\rangle$ and $\langle 13\rangle$. However, when all τ's except for $\tau^{\langle 12\rangle}$ and $\tau^{\langle 34\rangle}$ vanish, the Plücker relation (3.34) reduces to $\tau^{\langle 12\rangle}\tau^{\langle 34\rangle} = 0$, which requires one of them also to vanish. We thus see that there exits no domain wall interpolating between two vacua $\langle 12\rangle$ and $\langle 34\rangle$.

Configurations of the single domain walls can also be estimated by comparing weights of the two vacua as those in the Abelian gauge theory: The domain wall interpolating $\langle \underline{\cdots} A\rangle$ and $\langle \underline{\cdots} B\rangle$ is given by $\mathcal{W}^{\langle \underline{\cdots} A\rangle} = \mathcal{W}^{\langle \underline{\cdots} B\rangle}$. Then we again obtain the same transition as equation (3.27)

$$y = -\frac{a^{\langle \underline{\cdots} A\rangle} - a^{\langle \underline{\cdots} B\rangle}}{m_A - m_B}. \tag{3.35}$$

Of course the Plücker relations (3.34) can forbid a set of three or more than three τ's to be non-vanishing with the rests vanishing. In other words, if it is allowed by the Plücker relations (3.34), that configuration can be realized.

We make several comments on characteristic properties of domain walls in non-Abelian gauge theory.

Unlike the case of $U(1)$ gauge theory, all of moduli are not (approximate) Nambu–Goldstone (NG) modes. There exist $N_{\rm C}(N_{\rm F} - N_{\rm C})$ walls. They carry approximate NG modes for translational symmetry with the overall being an exact NG mode, if they are well separated. Only $N_{\rm F} - 1$ phases are NG modes for spontaneously broken $U(1)^{N_{\rm F}-1}$ flavour symmetry. However the rests $N_{\rm C}(N_{\rm F} - N_{\rm C}) - N_{\rm F} + 1$ are not related with any symmetry, but are required by unbroken SUSY. These additional modes are called quasi-NG modes in the context of spontaneously broken global symmetry with keeping SUSY [44, 121].

It may be worth pointing out that a gauge field W_y in co-dimensional direction can exist in wall configurations in non-Abelian gauge theory, unlike the Abelian cases where it can be eliminated by a gauge transformation. See [2] in detail.

In the strong coupling limit exact duality relation holds, $N_{\rm C} \leftrightarrow N_{\rm F} - N_{\rm C}$ in equation (2.23). This relation can be promoted to wall solutions as shown in appendix D in [2]. Although this duality is not exact for finite coupling there still exists a one-to-one dual map by the relation

$$H_0 \tilde{H}_0^\dagger = 0 \tag{3.36}$$

among the moduli matrix H_0 in the original theory and the $(N_{\rm F} - N_{\rm C}) \times N_{\rm F}$ moduli matrix $\tilde{H}_0$ of the dual theory. This relation determines $\tilde{H}_0$ uniquely from H_0 up to the V-equivalence (3.10).

3.1.4. D-brane configuration. We found the ordering rules of non-Abelian domain walls in [2]. In this subsection we show that these rules can be obtained easily from D-brane configuration in string theory [3]. This configuration was obtained by generalizing that for the $U(1)$ gauge theory considered in [49]. We restrict dimensionality to $d = 3+1$ in this subsection, but we can consider from dimension $d = 1+1$ to $d = 4+1$ by taking T-duality. We realize our theory with gauge group $U(N_{\mathrm{C}})$ on N_{C} D3-branes with the background of N_{F} D7-branes;

$$\begin{array}{ll} N_{\mathrm{C}}\mathrm{D3}: & 0123 \\ N_{\mathrm{F}}\mathrm{D7}: & 01234567 \\ \mathbf{C}^2/\mathbf{Z}_2\mathrm{ALE}: & \quad\;\; 4567. \end{array} \tag{3.37}$$

A string connecting D3-branes provides the gauge multiplets whereas a string connecting D3-branes and D7-branes provides the hypermultiplets in the fundamental representation. In order to get rid of adjoint hypermultiplet we have divided four spatial directions of their world volume by $\mathbf{Z}_2$ to form the orbifold $\mathbf{C}^2/\mathbf{Z}_2$. The orbifold singularity is blown up to the Eguchi–Hanson space by S^2 with the area

$$A = c g_s l_s^4 = \frac{c}{\tau_3} \tag{3.38}$$

with g_s the string coupling, $l_s = \sqrt{\alpha'}$ the string length and $\tau_3 = 1/g_s l_s^4$ the D3-brane tension. Our D3-branes are fractional D3-branes that is, D5-branes wrapping around S^2. The gauge coupling constant g of the gauge theory realized on the D3-brane is

$$\frac{1}{g^2} = \frac{b}{g_s} \tag{3.39}$$

with b the B-field flux integrated over the S^2, $b \sim AB_{ij}$. The positions of the D7-branes in the x^8-direction gives the masses for the fundamental hypermultiplets whereas the positions of the D3-branes in the x^8-direction is determined by the VEV of Σ (when Σ can be diagonalized $\Sigma = \mathrm{diag}\,\Sigma_{rr}$):

$$x^8|_{A\text{-thD7}} = l_s^2 m_A, \qquad x^8|_{r\text{-thD3}} = l_s^2 \Sigma_{rr}(x^1). \tag{3.40}$$

Any D3-brane must lie in a D7-brane as vacuum states, but at most one D3-brane can lie in each D7-brane because of the s-rule [120]. Therefore the vacuum $\langle A_1, \ldots, A_{N_{\mathrm{C}}}\rangle$ is realized with A_r denoting positions of D3-branes, and the number of vacua is ${}_{N_{\mathrm{F}}}C_{N_{\mathrm{C}}}$ with reproducing field theory.

As domain wall states, Σ depends on one coordinate $y \equiv x^1$. All D3-branes lie in a set of N_{C} out of N_{F} D7-branes in the limit $y \to +\infty$, giving $\langle A_1, \ldots, A_{N_{\mathrm{C}}}\rangle$, but lie in another set of D7-branes in the opposite limit $y \to -\infty$, giving another vacuum $\langle B_1, \ldots, B_{N_{\mathrm{C}}}\rangle$. The N_{C} D3-branes exhibit kinks somewhere in the y-coordinate as illustrated in figure 5. Here we labelled B_r such that the A_rth brane at $y \to +\infty$ goes to the B_rth brane at $y \to -\infty$. If we separate adjacent walls far enough the configuration between these walls approaches a vacuum as illustrated on the right of figure 5. These configurations clarify dynamics of domain walls easily. In non-Abelian gauge theory two domain walls can penetrate each other if they are made of separated D3-branes like figure 6(*a*) but they cannot if they are made of adjacent D3-branes like figure 6(*b*). In the latter case, reconnection of D3-branes occur in the limit that two walls are compressed.

Taking a T-duality along the x^4-direction in configuration (3.37), the ALE geometry is mapped to two NS5-branes separated in the x^4-direction. The configuration becomes the

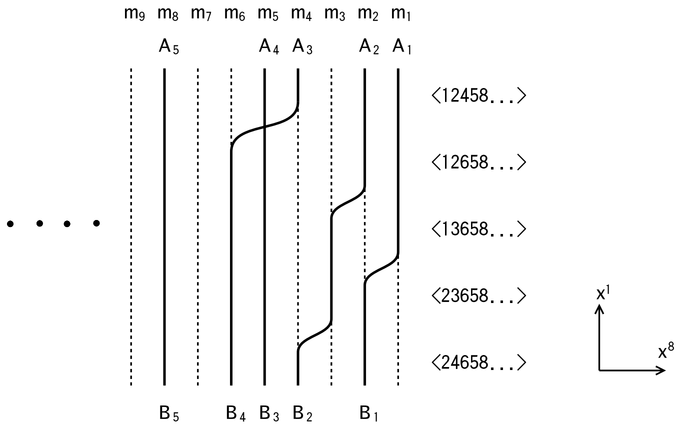

Figure 5. Multiple non-Abelian walls as kinky D-branes.

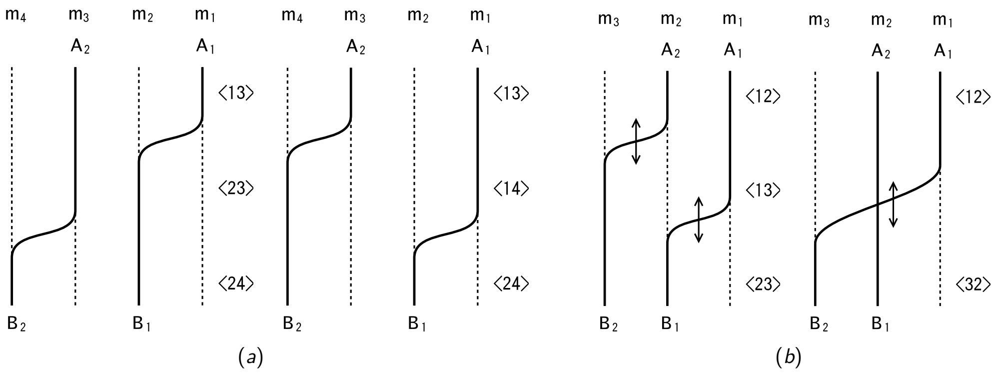

Figure 6. (*a*) Penetrable walls in $N_{\mathrm{F}} = 4$ and $N_{\mathrm{C}} = 2$ and (*b*) impenetrable walls $N_{\mathrm{F}} = 3$ and $N_{\mathrm{C}} = 2$.

Hanany–Witten-type brane configuration [111]

$$\begin{array}{lll} N_{\mathrm{C}}\mathrm{D4}: & 01234 & \\ N_{\mathrm{F}}\mathrm{D6}: & 0123\ \ 567 & \\ 2\mathrm{NS5}: & 0123\qquad\quad 89. & \end{array} \tag{3.41}$$

The relations between the positions of branes and physical quantities in field theory on D4-branes are summarized as

$$\begin{aligned} & x^8|_{r\text{-thD4}} = l_s^2 \Sigma_{rr}(x^1), \\ & x^8|_{A\text{-thD6}} = l_s^2 m_A, \\ & \Delta x^4|_{\mathrm{NS5}} = \frac{g_s l_s}{g^2}, \qquad (\Delta x^5, \Delta x^6, \Delta x^7)|_{\mathrm{NS5}} = g_s l_s^3 (0, 0, c). \end{aligned} \tag{3.42}$$

D-brane configurations of domain walls are obtained completely parallel to the configuration before taking the T-duality. However this configuration has some merits. First the strong gauge coupling limit corresponds to zero separation $\Delta x^4 = 0$ of two NS5-brane along x^4. In that limit, the duality (2.23) becomes exact [3] due to the Hanany–Witten effect [111].

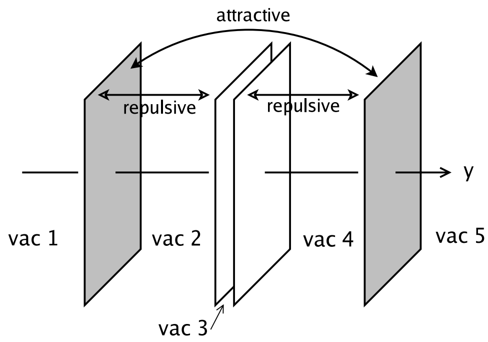

Figure 7. Interactions between four domain walls in the T^*F_n sigma model.

By using this configuration in the strong gauge coupling limit, it has been shown in [63] that the domain wall moduli space has half properties of the monopole moduli space and that the former can be described by the half Nahm construction.

If we put D7(D6)-branes separated along the x^9-direction in configurations before (after) taking T-duality, complex masses of hypermultiplets appear. We can consider configuration with Σ and one more scalar depending on x^2 as well as x^1 as a 1/4 BPS state [10]. That is a domain wall junction discussed in section 4.2.

3.1.5. More general models. We have considered non-degenerate masses of hypermultiplets so far. If we consider (partially) degenerate masses more interesting physics appear [64]. Non-Abelian $U(n)$ flavour symmetry arises in the original theory instead of $U(1)^{N_F-1}$ in equation (2.4), and some of them are broken and associated Nambu–Goldstone bosons can be localized on a wall unlike only $U(1)$ localization in the case of non-degenerate masses. Nonlinear sigma model on $U(N)$ (called the chiral Lagrangian) appears on domain walls in the model with $N_F = 2N_C \equiv 2N$ with masses $m_A = m$ for $A = 1, \ldots, N$ and $m_A = -m$ for $A = N+1, \ldots, 2N$. Including four derivative term, the Skyrme model appears on domain walls in that model [16].

It has been shown in [4] that the moduli space of domain walls is always the union of special Lagrangian submanifolds of the moduli space of vacua of the corresponding massless theory. As an example, domain walls and their moduli space have been considered in the linear sigma model giving the cotangent bundle over the Hirzebruch surface F_n. Interestingly, as special Lagrangian submanifolds, this model contains a weighted projective space $W\mathbf{C}P^2_{1,1,n}$ in addition to F_n. The moduli space of the domain walls has been shown to be the union of these special Lagrangian submanifolds, both of which is connected along a lower dimensional submanifold. Interesting consequence of this model is as follows. This model admits four domain walls which are ordered. The inner two walls are always compressed to form a single wall in the presence of outer two walls, and the position of that single wall is locked between the outer two walls. However if we take away outer two walls to infinities, the compressed walls can be broken into two walls. These phenomena can be regarded as an evidence for the attractive/repulsive force exists between some pairs of domain walls as in figure 7.

3.2. Vortices

In this section, we consider vortices as 1/2 BPS states. There exist various types of vortices. First we consider the ANO vortices embedded into non-Abelian gauge theory with $N_F = N_C$, which are usually called non-Abelian vortices. We determine their moduli space completely by using the moduli matrix [6]. Then we find a complete relationship between our moduli space and the moduli space constructed by the Kähler quotient, which was given in [76] by using a D-brane configuration in string theory. Proving this equivalence has been initiated in [6] and is completed in this review as a new result. Next we extend these results to the case of semi-local vortices [71], which exist in the theory with the large number of Higgs fields ($N_F > N_C$). This part is also new.

3.2.1. Vortex solutions and their moduli space. We consider the case of massless hypermultiplets which gives only continuously degenerated and connected vacua. The case of hypermultiplets with non-degenerate masses will be investigated in section 4.3. In the following we simply set $H^2 = 0$ and $H \equiv H^1$ because of boundary conditions and BPS equations. Although the adjoint scalars Σ_p $(p = 1, \ldots, 6 - d)$ appear in $d = 3, 4, 5$ from higher dimensional components of the gauge field, they trivially vanish in the vacua and also in vortex solutions. Therefore we can consistently set $\Sigma_p = 0$. In the theory with $N_F = N_C$ in any dimension, the vacuum is unique and is in the so-called colour–flavour locking phase, $H^1 = \sqrt{c}\mathbf{1}_{N_C}$ and $H^2 = 0$, where symmetry of the Lagrangian is spontaneously broken down to $SU(N_C)_{G+F}$. This symmetry will be further broken in the presence of vortices, and therefore it acts as an isometry on the moduli space.

The Bogomol'nyi completion of energy density for vortices in the x^1–x^2 plane can be obtained as

$$\mathcal{E} = \mathrm{Tr}\left[\frac{1}{g^2}\left(B_3 + \frac{g^2}{2}(c\mathbf{1}_N - HH^\dagger)\right)^2 + (\mathcal{D}_1 H + \mathrm{i}\mathcal{D}_2 H)(\mathcal{D}_1 H + \mathrm{i}\mathcal{D}_2 H)^\dagger\right] + \mathrm{Tr}[-cB_3 + 2\mathrm{i}\partial_{[1} H\mathcal{D}_{2]}H^\dagger] \tag{3.43}$$

with a magnetic field $B_3 \equiv F_{12}$. This leads to the vortex equations

$$0 = \mathcal{D}_1 H + \mathrm{i}\mathcal{D}_2 H, \tag{3.44}$$

$$0 = B_3 + \frac{g^2}{2}(c\mathbf{1}_N - HH^\dagger), \tag{3.45}$$

and their tension

$$T = -c\int \mathrm{d}^2x\, \mathrm{Tr}\, B_3 = 2\pi ck, \tag{3.46}$$

with $k\,(\in \mathbf{Z})$ measuring the winding number of the $U(1)$ part of broken $U(N_C)$ gauge symmetry. The integer k is called the vorticity or the vortex number.

Let us first consider the simplest example of the model with $N_C = N_F = 1$ in order to extract fundamental properties of vortices. Vortices in this model are called Abrikosov–Nielsen–Olesen (ANO) vortices [66]. A profile function of the ANO vortex has been established numerically very well, although no analytic solution is known. We illustrate numerical solutions of the profile function with the vortex number $k = 1, \ldots, 5$ in figure 8. One can see that the Higgs field vanishes at the centre of the ANO vortex, and the winding to the Higges vacuum is resolved smoothly. Then the magnetic flux emerges there, whose intensity is given by $B_3 = -g^2c/2$ due to the vortex equation (3.45). Therefore a characteristic size of ANO vortex can be estimated to be of order $1/(g\sqrt{c})$ by taking the total flux 2π into account.

In the non-Abelian case with $N_F = N_C \equiv N \geqslant 2$, a solution for single vortex can be constructed by embedding such ANO vortex solution $(B_{3\star}, H_\star)$ in the Abelian case into those

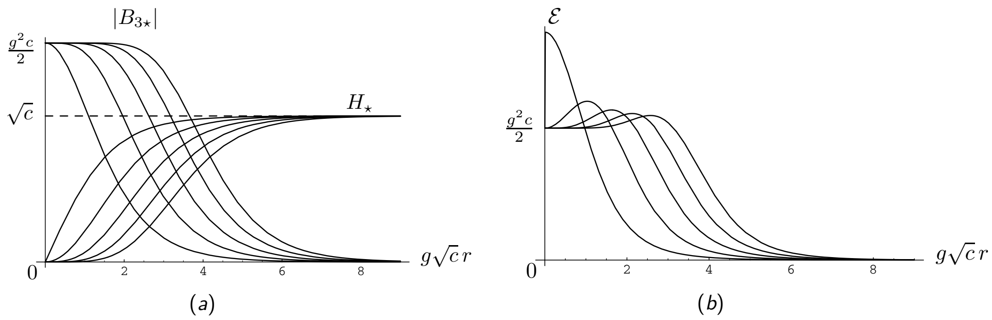

Figure 8. Distributions of numerical vortex solutions with vorticity $k = 1, \ldots, 5$ as functions of the radius r. The magnetic flux is centred at $r = 0$, whereas the Higgs field vanishes at $r = 0$ and approaches to the vacuum value $\sqrt{c}$ at $r \to \infty$. Energy density has a dip at $r = 0$ except for the case of unit ($k = 1$) vorticity. (*a*) Magnetic flux and Higgs field, and (*b*) energy.

in the non-Abelian case, like

$$B_3 = U\ \mathrm{diag}(B_{3\star}, 0, \ldots, 0)U^{-1}, \qquad H = U\ \mathrm{diag}(H_\star, \sqrt{c}, \ldots, \sqrt{c})U^{-1}. \tag{3.47}$$

Here U takes a value in a coset space, the projective space $SU(N)/[SU(N-1) \times U(1)] \simeq \mathbf{C}P^{N-1}$, arising from the fact that the $SU(N)_{\mathrm{G+F}}$ symmetry is spontaneously broken by the existence of the vortex. It parametrizes the orientation of the non-Abelian vortex in the internal space, whose moduli are called *orientational moduli*. Note that at the centre of the ANO vortex $x^{1,2} = x_0^{1,2}$, the rank of the $N \times N$ matrix H reduces to $N - 1$, $(\det(H(x_0^{1,2})) = 0)$, implying the existence of an N-column vector $\vec{\phi}$ satisfying

$$H\left(x_0^{1,2}\right)\vec{\phi} = 0. \tag{3.48}$$

Components of this vector are precisely the homogeneous coordinates of the orientational moduli $\mathbf{C}P^{N-1}$. Its components are actually given by $\vec{\phi} = U(1, 0, \ldots)^{\mathrm{T}}$. Roughly speaking, the moduli space of multiple non-Abelian vortices is parametrized by a set of the position moduli and the orientational moduli, both of which are attached to each vortex as we will see later.

We now turn back to general cases with arbitrary N_{C} and N_{F} ($>N_{\mathrm{C}}$). The vortex equation (3.44) can be solved by use of the method similar to that in the case of domain walls. Defining a complex coordinate $z \equiv x^1 + \mathrm{i}x^2$, the first of the vortex equations (3.44) can be solved as [6]

$$H = S^{-1}H_0(z), \qquad W_1 + \mathrm{i}W_2 = -\mathrm{i}2S^{-1}\bar{\partial}_z S. \tag{3.49}$$

Here $S = S(z, \bar{z}) \in GL(N_{\mathrm{C}}, \mathbf{C})$ is defined in the second of equations (3.49), and $H_0(z)$ is an arbitrary N_{C} by N_{F} matrix whose components are holomorphic with respect to z. We call H_0 the *moduli matrix* of vortices. With a gauge invariant quantity

$$\Omega(z, \bar{z}) \equiv S(z, \bar{z})S^\dagger(z, \bar{z}) \tag{3.50}$$

the second vortex equations (3.45) can be rewritten as

$$\partial_z(\Omega^{-1}\bar{\partial}_z\Omega) = \frac{g^2}{4}(c\mathbf{1}_{N_{\mathrm{C}}} - \Omega^{-1}H_0H_0^\dagger). \tag{3.51}$$

We call this the *master equation* for vortices[5]. This equation is expected to give no additional moduli parameters. It was proved for the ANO vortices ($N_F = N_C = 1$) [67] and is consistent with the index theorem [76] in general N_C and N_F as seen below.

Therefore we assume that the moduli matrix H_0 describes thoroughly the moduli space of vortices. We should, however, note that there exists a redundancy in solution (3.49): physical quantities H and $W_{1,2}$ are invariant under the following V-transformations

$$H_0(z) \to H_0'(z) = V(z)H_0(z), \qquad S(z,\bar{z}) \to S'(z,\bar{z}) = V(z)S(z,\bar{z}), \tag{3.52}$$

with $V(z) \in GL(N_C, \mathbf{C})$ for ${}^\forall z \in \mathbf{C}$, whose elements are holomorphic with respect to z. Incorporating all possible boundary conditions, we find that the total moduli space of vortices $\mathcal{M}^{\text{total}}_{N_C,N_F}$ is given by

$$\mathcal{M}^{\text{total}}_{N_C,N_F} = \frac{\{H_0(z)|H_0(z) \in M_{N_C,N_F}\}}{\{V(z)|V(z) \in M_{N_C,N_C}, \det V(z) \neq 0\}} \tag{3.53}$$

where $M_{N,N'}$ denotes a set of holomorphic $N \times N'$ matrices. This is of course an infinite-dimensional space which may not be defined well in general.

The original definition of the total moduli space is the space of solutions of two BPS equations in (3.44) and (3.45) divided by the $U(N_C)$ local gauge equivalence denoted as $G(x)$: {equations(3.44) and (3.45)}$/G(x)$. On the other hand, we have solved the first vortex equation (3.44), but have to assume the existence and the uniqueness of the solution of the master equation (3.51), in order to arrive at the total moduli space (3.53). Let us note that the first vortex equation (3.44) is invariant under the complex extension $G^{\mathbf{C}} = U(N_C)^{\mathbf{C}} = GL(N_C, \mathbf{C})$ of the local gauge group $G = U(N_C)$. Our procedure to obtain the total moduli space $\mathcal{M}^{\text{total}}_{N_C,N_F}$ in equation (3.53) implies that it can be rewritten as {equation(3.44)}$/G^{\mathbf{C}}(x)$. Therefore the uniqueness and existence of solution of the master equation (3.51) is equivalent to the isomorphism between these spaces {equations (3.44) and (3.45)}$/G(x) \simeq$ {equation (3.44)}$/G^{\mathbf{C}}(x)$. This isomorphism is rigorously proven at least if we compactify the base space (co-dimensions of vortices) $\mathbf{C}$ to $\mathbf{C}P^1$. This is called the Hitchin–Kobayashi correspondence [115–117].[6] We will establish the finite-dimensional version of this equivalence (for each topological sector) directly in another method using moduli matrix in section 3.2.3.

We require that the total energy of configurations must be finite in order to obtain physically meaningful vortex configurations. This implies that any point at infinity S^1_∞ must belong to the same gauge equivalence class of vacua. Therefore elements of the moduli matrix H_0 must be polynomial functions of z. (If exponential factors exist they become dominant at the boundary S^1_∞ and the configuration fails to converge to the same gauge equivalence class there.) Furthermore the topological sector of the moduli space of vortices should be determined under a fixed boundary condition with a given vorticity k.

The energy density (3.43) of BPS states can be rewritten in terms of the gauge invariant matrix Ω in equation (3.50) as

$$\begin{aligned}\mathcal{E}|_{\text{BPS}} &= \text{Tr}[-cB_3 + 2\mathrm{i}\partial_{[1} H\mathcal{D}_{2]}H^\dagger]|_{\text{BPS}} \\ &= 2c\bar{\partial}_z\partial_z\left(1 - \frac{4}{g^2 c}\bar{\partial}_z\partial_z\right)\log\det\Omega.\end{aligned} \tag{3.54}$$

[5] The master equation reduces to the so-called Taubes equation [67] in the case of ANO vortices ($N_C = N_F = 1$) by rewriting $c\Omega(z,\bar{z}) = |H_0|^2\,\mathrm{e}^{-\xi(z,\bar{z})}$ with $H_0 = \prod_i (z - z_i)$. Note that $\log\Omega$ is regular everywhere while ξ is singular at vortex positions. Non-integrability of the master equation has been shown in [120].

[6] Actually it is proved for arbitrary gauge group G with arbitrary matter contents and arbitrary *compact* base space. It may be interesting to note that this isomorphism is an infinite-dimensional version of the Kähler quotient.

The last four-derivative term above does not contribute to the tension if a configuration approaches to a vacuum on the boundary. Equation (3.51) implies asymptotic behaviour at infinity $z \to \infty$ becomes $\Omega \to \frac{1}{c} H_0 H_0^\dagger$. The condition of vorticity k requires

$$T = 2\pi c k = -\frac{c}{2}\mathrm{i}\oint \mathrm{d}z\, \partial_z \log\det(H_0 H_0^\dagger) + \mathrm{c.c.} \tag{3.55}$$

The total moduli space is decomposed into topological sectors $\mathcal{M}_{N_{\mathrm{F}},N_{\mathrm{C}},k}$ with vorticity k.

3.2.2. The case with $N_{\mathrm{F}} = N_{\mathrm{C}}$: the non-Abelian ANO vortices. Let us consider the case with $N_{\mathrm{C}} = N_{\mathrm{F}} \equiv N$. In this case, the vacuum, given by $H = \sqrt{c}\mathbf{1}_N$, is unique and no flat direction exists. The tension formula (3.55) with $N_{\mathrm{F}} = N_{\mathrm{C}}$ implies that the vorticity k can be rewritten as

$$k = \frac{1}{2\pi}\,\mathrm{Im}\oint \mathrm{d}z\, \partial \log(\det H_0). \tag{3.56}$$

We thus obtain the boundary condition on S^1_∞ for H_0 as

$$\det(H_0) \sim z^k \qquad \text{for} \quad z \to \infty, \tag{3.57}$$

that is, $\det H_0(z)$ has k zeros. We denote positions of zeros by $z = z_i$ $(i = 1, \ldots, k)$. These can be recognized as the positions of vortices:

$$P(z) \equiv \det H_0(z) = \prod_{i=1}^{k}(z - z_i), \tag{3.58}$$

and the orientation moduli $\vec{\phi}_i$ of the ith vortex are determined by

$$H_0(z_i)\vec{\phi}_i = 0 \quad \leftrightarrow \quad H(z = z_i, \bar{z} = \bar{z}_i)\vec{\phi}_i = 0. \tag{3.59}$$

The moduli space $\mathcal{M}_{N,k}$ for k-vortices in $U(N)$ gauge theory can be formally expressed as a quotient

$$\mathcal{M}_{N,k} = \frac{\{H_0(z) | H_0(z) \in M_N, \deg(\det(H_0(z))) = k\}}{\{V(z) | V(z) \in M_N, \det V(z) = 1\}} \tag{3.60}$$

where M_N denotes a set of $N \times N$ matrices of polynomial function of z, and 'deg' denotes a degree of polynomials. The condition $\det V(z) = 1$ holds because we have fixed $P(z)$ as a monic polynomial (coefficient of highest power is unity) as in equation (3.58) by using the V-transformation (3.52). This is a finite-dimensional subspace of the total moduli space (3.53).

The V-transformation (3.52) allows us to reduce degrees of polynomials in H_0 by applying the division algorithm. After fixing the V-transformation completely, any moduli matrix H_0 can be uniquely transformed to a triangular matrix, which we call the *standard form* of vortices:

$$H_0 = \begin{pmatrix} P_1(z) & R_{2,1}(z) & R_{3,1}(z) & \cdots & R_{N,1}(z) \\ 0 & P_2(z) & R_{3,2}(z) & \cdots & R_{N,2}(z) \\ \vdots & & \ddots & & \vdots \\ & & & & R_{N,N-1}(z) \\ 0 & \cdots & & 0 & P_N(z) \end{pmatrix}. \tag{3.61}$$

Here $P_r(z)$ are monic polynomials defined by $P_r(z) = \prod_{i=1}^{k_r}(z - z_{r,i})$ with $z_{r,i} \in \mathbf{C}$, and $R_{r,m}(z) \in \mathrm{Pol}(z; k_r)$ where $\mathrm{Pol}(z; n)$ denotes a set of polynomial functions of order less than n. We would like to emphasize that the standard form (3.61) has *one-to-one correspondence* to a point in the moduli space $\mathcal{M}_{N,k}$. Since $\tau(z) = \prod_{r=1}^{N} P_r(z) \sim z^k$ asymptotically for

$z \to \infty$, we obtain the vortex number $k = \sum_{r=1}^{N} k_r$ from equation (3.55). The positions of the k-vortices are the zeros of $P_r(z)$. Collecting all matrices with given k in the standard form (3.61) we obtain the whole moduli space $\mathcal{M}_{N,k}$ for k-vortices, as in the case of domain walls. Its generic points are parametrized by the matrix with $k_N = k$ and $k_r = 0$ for $r \neq N$, given by

$$H_0(z) = \begin{pmatrix} \mathbf{1}_{N-1} & -\vec{R}(z) \\ 0 & P(z) \end{pmatrix} \tag{3.62}$$

where $(\vec{R}(z))^r = R_r(z) \in \mathrm{Pol}(z; k)$ constitutes an $N-1$ vector and $P(z) = \prod_{i=1}^{k}(z - z_i)$. This moduli matrix contains the maximal number of the moduli parameters in $\mathcal{M}_{N,k}$. Thus the dimension of the moduli space is $\dim(\mathcal{M}_{N,k}) = 2kN$. This coincides with the index theorem shown in [76] implying the uniqueness and existence of a solution of the master equation (3.51).

The standard form (3.61) has the merit of covering the entire moduli space only once without any overlap. To clarify the global structure of the moduli space, however, it may be more useful to parametrize the moduli space with overlapping patches. We can parametrize the moduli space by a set of ${}_{k+N-1}C_k$ patches defined by

$$(H_0)^r{}_s = z^{k_s}\delta^r{}_s - T^r{}_s(z), \qquad T^r{}_s(z) = \sum_{n=1}^{k_s}(T_n)^r{}_s z^{n-1} \in \mathrm{Pol}(z; k_s). \tag{3.63}$$

Coefficients $(T_n)^r{}_s$ of monomials in $T^r{}_s(z)$ are moduli parameters as coordinates in a patch. We denote this patch by $\mathcal{U}^{(k_1,k_2,\ldots,k_N)}$:

$$\mathcal{U}^{(k_1,k_2,\ldots,k_N)} = \{(T_{n_s})^r{}_s\}, \qquad n_s = 1, \ldots, k_s, \qquad r = 1, \ldots, N_{\mathrm{C}}. \tag{3.64}$$

We can show that each patch fixes the V-transformation (3.52) completely including any discrete subgroup, and therefore that the isomorphism $\mathcal{U}^{(k_1,k_2,\ldots,k_N)} \simeq \mathbf{C}^{kN}$ holds. The transition functions between these patches are given by the V-transformation (3.52), completely defining the moduli space as a *smooth* manifold,

$$\mathcal{M}_{N,k} \simeq \bigcup \mathcal{U}^{(k_1,k_2,\ldots,k_N)}. \tag{3.65}$$

To see this explicitly we show an example of single vortex ($k = 1$). In this case there exist N patches defined in N H_0's given by

$$H_0(z) \sim \begin{pmatrix} 1 & & 0 & -b_1^{(N)} \\ & \ddots & & \vdots \\ 0 & & 1 & -b_{N-1}^{(N)} \\ 0 & \cdots & 0 & z - z_0 \end{pmatrix} \sim \begin{pmatrix} 1 & & -b_1^{(N-1)} & 0 \\ & \ddots & \vdots & \\ 0 & & z - z_0 & 0 \\ 0 & \cdots & -b_N^{(N-1)} & 1 \end{pmatrix} \sim \cdots$$
$$\sim \begin{pmatrix} z - z_0 & 0 & \cdots & 0 \\ -b_2^{(1)} & 1 & & 0 \\ \vdots & & \ddots & \\ -b_N^{(1)} & 0 & & 1 \end{pmatrix}, \tag{3.66}$$

and transition functions between them are summarized by

$$\vec{\phi} \sim \begin{pmatrix} b_1^{(N)} \\ \vdots \\ \vdots \\ b_{N-1}^{(N)} \\ 1 \end{pmatrix} = b_{N-1}^{(N)} \begin{pmatrix} b_1^{(N-1)} \\ \vdots \\ b_{N-2}^{(N-1)} \\ 1 \\ b_N^{(N-1)} \end{pmatrix} = \cdots = b_1^{(N)} \begin{pmatrix} 1 \\ b_2^{(1)} \\ \vdots \\ b_{N-1}^{(1)} \\ b_N^{(1)} \end{pmatrix}. \tag{3.67}$$

These b's are the standard coordinates for $\mathbf{C}P^{N-1}$, and we identify components of the vector $\vec{\phi}$ as the orientational moduli satisfying equation (3.59). We thus confirm $\mathcal{M}_{N,k=1} \simeq \mathbf{C}\times\mathbf{C}P^{N-1}$ recovering the result [77] obtained by a symmetry argument. To see the procedure more explicitly, we show, in the case of $N = 2$, that the V-transformation connects sets of coordinates in two patches as

$$\begin{pmatrix} z-z_0 & 0 \\ -b' & 1 \end{pmatrix} \sim \begin{pmatrix} 0 & -b \\ 1/b & z-z_0 \end{pmatrix} \begin{pmatrix} z-z_0 & 0 \\ -1/b & 1 \end{pmatrix} = \begin{pmatrix} 1 & -b \\ 0 & z-z_0 \end{pmatrix}, \tag{3.68}$$

where we obtain a transition function $b' = 1/b$.

The next example is the case of $N = 2$ and $k = 2$ which is more interesting and cannot be obtained by symmetry argument only. The moduli space $\mathcal{M}_{N=2,k=2}$ is parametrized by the three patches $\mathcal{U}^{(0,2)}, \mathcal{U}^{(1,1)}, \mathcal{U}^{(2,0)}$ defined in H_0's given by

$$H_0 = \begin{pmatrix} 1 & -az-b \\ 0 & z^2-\alpha z-\beta \end{pmatrix}, \qquad \begin{pmatrix} z-\phi & -\varphi \\ -\tilde{\varphi} & z-\tilde{\phi} \end{pmatrix}, \qquad \begin{pmatrix} z^2-\alpha z-\beta & 0 \\ -a'z-b' & 1 \end{pmatrix}, \tag{3.69}$$

respectively. We find that the transition functions between $\mathcal{U}^{(0,2)}$ and $\mathcal{U}^{(1,1)}$ are given by

$$a = \frac{1}{\tilde{\varphi}}, \qquad b = -\frac{\tilde{\phi}}{\tilde{\varphi}}, \qquad \alpha = \phi + \tilde{\phi}, \qquad \beta = \varphi\tilde{\varphi} - \phi\tilde{\phi} \tag{3.70}$$

and that those between $\mathcal{U}^{(0,2)}$ and $\mathcal{U}^{(2,0)}$ are given by

$$a = \frac{a'}{a'2\beta - a'b'\alpha - b'2}, \qquad b = -\frac{b' + a'\alpha}{a'2\beta - a'b'\alpha - b'2} \tag{3.71}$$

with common parameters α, β. Positions of two vortices z_1, z_2 are given by solving an equation $P(z_i) = 0$. We find that orientations of the vortices satisfying equation (3.59) are expressed by four kinds of forms

$$\vec{\phi}_i \sim \begin{pmatrix} az_i + b \\ 1 \end{pmatrix} \sim \begin{pmatrix} z_i - \tilde{\phi} \\ \tilde{\varphi} \end{pmatrix} \sim \begin{pmatrix} \varphi \\ z_i - \phi \end{pmatrix} \sim \begin{pmatrix} 1 \\ a'z_i + b' \end{pmatrix} \tag{3.72}$$

with the equivalence relation $\vec{\phi} \sim \vec{\phi}' = \lambda\vec{\phi}$, $(\lambda \in \mathbf{C}^*)$ of $\mathbf{C}P^{N-1}$. The above equivalence relations between the various forms for orientation are consistent with the transition functions (3.70) and (3.71), since the orientations are, by definition, independent of the patches which we take.

We now see properties of the three patches $\mathcal{U}^{(0,2)}, \mathcal{U}^{(1,1)}$ and $\mathcal{U}^{(2,0)}$. If we set $a = 0$ ($a' = 0$) in $\mathcal{U}^{(0,2)}$ ($\mathcal{U}^{(2,0)}$), the orientations of two vortices are parallel

$$\vec{\phi}_1 \sim \vec{\phi}_2 \sim (b, 1)^{\mathrm{T}} (\sim (1, b')^{\mathrm{T}}). \tag{3.73}$$

This is in contrast to the patch $\mathcal{U}^{(1,1)}$ where parallel vortices are impossible, as long as the two vortices are separated. Configurations for parallel multiple vortices can be realized by embedding the configuration for multiple ANO vortices in the Abelian gauge theory in the same way as equation (3.47). In contrast we can take the orientations of two vortices opposite each other in the patch $\mathcal{U}^{(1,1)}$, like

$$\vec{\phi}_1 = (1, 0)^{\mathrm{T}}, \qquad \vec{\phi}_2 = (0, 1)^{\mathrm{T}} \tag{3.74}$$

by setting $\phi = z_1, \tilde{\phi} = z_2$ and $\varphi = \tilde{\varphi} = 0$. In this case, the moduli matrix $H_0(z)$, Ω as a solution of equation (3.51) and physical fields B_3, H are all diagonal, and thus we find that this case is realized by embedding two sets of single ANO vortices in the Abelian case into two different diagonal components of the moduli matrices of this non-Abelian case. The moduli space for non-Abelian vortices described by patches (3.69) are far larger than subspaces which can be described by embedding the Abelian cases. Such subspaces can be interpolated with

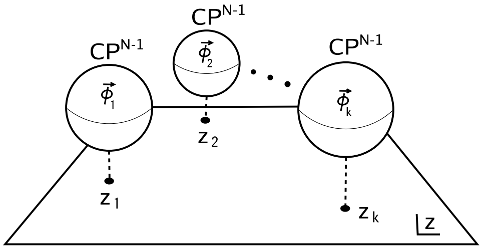

Figure 9. The moduli space for separated vortices.

continuous moduli in the whole moduli space. Actually, as long as the vortices are separated $z_1 \neq z_2$, the positions $z_1, z_2 \in \mathbf{C}$ and the orientations $\vec{\phi}_1, \vec{\phi}_2 \in \mathbf{C}P^1$ are independent of each others and can parametrize the moduli space, as we discuss later.

In generic cases with arbitrary N and k, we can find that orientational moduli $\vec{\phi}_i \in \mathbf{C}P^{N-1}$ are attached to each vortex at $z = z_i \in \mathbf{C}$ as an independent moduli parameters. Thus the asymptotic form (open set) of the moduli space for separated vortices are found to be

$$\mathcal{M}_{N,k} \leftarrow (\mathbf{C} \times \mathbf{C}P^{N-1})^k / \mathcal{S}_k \tag{3.75}$$

with $\mathcal{S}_k$ permutation group exchanging the positions of the vortices[7]. Here '$\leftarrow$' denotes a map resolving the singularities on the right hand side. We sketch the structure of separated vortices in figure 9. Equation (3.75) can be easily expected from physical intuition; for instance the $k = 2$ case was found in [84]. The most important thing is how orbifold singularities of the right-hand side in (3.75) are resolved by coincident vortices [6]. In the $N = 1$ case, $\mathcal{M}_{N=1,k} \simeq \mathbf{C}^k/\mathcal{S}_k \simeq \mathbf{C}^k$ holds instead of (3.75) [67], and the problem of singularity does not occur.

3.2.3. Equivalence to the Kähler quotient. In this subsection we rewrite our moduli space of vortices in the form of Kähler quotient which was originally found in [76] by using a D-brane configuration. This form is close to the ADHM construction of instantons and so we may call it the *half ADHM construction*.

First of all, let us consider a vector whose N components are elements of Pol$(z; k)$ satisfying an equation

$$H_0(z)\vec{\phi}(z) = \vec{J}(z)P(z) = 0 \qquad \mod P(z) \tag{3.76}$$

where $P(z) \equiv \det(H_0(z))$ and $\vec{J}(z)$ is a certain holomorphic polynomial obtained, that is, the equation requires that the l.h.s. can be divided by the polynomial $P(z)$. We can show there exist k linearly-independent solutions $\{\vec{\phi}_i(z)\}$, $(i = 1, \ldots, k)$ for $\vec{\phi}(z)$ with given $H_0(z)$. We obtain the $N \times k$ matrices $\mathbf{\Phi}(z)$ and $\mathbf{J}(z)$, defined by

$$\mathbf{\Phi}(z) = (\vec{\phi}_1(z), \vec{\phi}_2(z), \ldots, \vec{\phi}_k(z)), \qquad \mathbf{J}(z) = (\vec{J}_1(z), \vec{J}_2(z), \ldots, \vec{J}_k(z)), \tag{3.77}$$

with satisfying

$$H_0(z)\mathbf{\Phi}(z) = \mathbf{J}(z)P(z). \tag{3.78}$$

Let us consider a product $z\mathbf{\Phi}(z)$. Since components of this product are not elements of Pol(z, k) but Pol$(z, k + 1)$ generally, this matrix leads to an $N \times k$ *constant* matrix $\mathbf{\Psi}$ as a

[7] Interestingly this is a 'half' of the open set of the moduli space of k separated $U(N)$ instantons on non-commutative $\mathbf{R}^4$, $(\mathbf{C}^2 \times T^*\mathbf{C}P^{N-1})^k/\mathcal{S}_k$. The singularity of the latter is resolved in terms of the Hilbert scheme at least for $N = 1$ [123]. Also it was pointed out in [76] that the moduli space of vortices is a special Lagrangian submanifold of the moduli space of non-commutative instantons.

quotient of division by the polynomial $P(z)$. Moreover a remainder of this division can be written as $\mathbf{\Phi}(z)$ multiplied by a certain $k \times k$ *constant* matrix $\mathbf{Z}$ since each column vector of the remainder is also a solution of equation (3.76). Therefore we find that the product determines the matrices $\mathbf{Z}$ and $\mathbf{\Psi}$ uniquely as

$$z\mathbf{\Phi}(z) = \mathbf{\Phi}(z)\mathbf{Z} + \mathbf{\Psi} P(z). \tag{3.79}$$

Note that when we extract the matrix $\mathbf{\Phi}(z)$ from the moduli matrix H_0, there exists a redundancy due to a rearrangement of $\vec{\phi}_i(z)$ which leads to an equivalence relation $\mathbf{\Phi}(z) \simeq \mathbf{\Phi}'(z) = \mathbf{\Phi}(z)U^{-1}$ with $U \in GL(k, \mathbf{C})$. This fact implies that we should also consider an equivalence relation for the matrices $\mathbf{Z}$, Ψ as

$$(\mathbf{Z}, \mathbf{\Psi}) \simeq (\mathbf{Z}', \mathbf{\Psi}') = (U\mathbf{Z}U^{-1}, \mathbf{\Psi}U^{-1}), \tag{3.80}$$

where a $GL(k, \mathbf{C})$ action on $\mathbf{\Phi}(z)$ and $\{\mathbf{Z}, \Psi\}$ is free: if $\mathbf{\Phi}(z)X = 0$ then $X = 0$. Since the action is free, the quotient space is smooth. This is precisely the complexified transformation appearing in the Kähler quotient construction. On the other hand the Kähler quotient construction of the moduli space in [76] is given by k by k matrix Z and N by k matrix ψ. The concrete correspondence is obtained by fixing the imaginary part of the complexified transformation as

$$\{\mathbf{Z}, \mathbf{\Psi}\}//GL(k, \mathbf{C}) \simeq \{(Z, \psi)|[Z^\dagger, Z] + \psi^\dagger\psi \propto \mathbf{1}_k\}/U(k) \equiv \mathcal{M}^{\mathrm{HT}}. \tag{3.81}$$

Therefore, the above procedure defines the mapping from our moduli space $\mathcal{M}_{N,k}$ (3.60) into the Kähler quotient (3.81).[8] This is a topological sector version of the Hitchin–Kobayahsi correspondence as informed below equation (3.53).

By combining equations (3.78) and (3.79), we derive a direct relation between the moduli matrix $H_0(z)$ and the matrices $\{\mathbf{Z}, \Psi\}$ as

$$\nabla^\dagger L = 0, \qquad \text{with} \qquad L^\dagger \equiv (H_0(z), \mathbf{J}(z)), \qquad \nabla \equiv \begin{pmatrix} -\mathbf{\Psi} \\ z - \mathbf{Z} \end{pmatrix}. \tag{3.82}$$

By use of this equation, we can concretely relate coefficients (coordinates) $(T_m)^r{}_s$ in a patch $\mathcal{U}^{k_1,\ldots,k_{N_\mathrm{C}}}$ of H_0 (3.63) with the matrices $\{\mathbf{Z}, \Psi\}$ as

$$\begin{aligned} (\mathbf{\Psi})^r{}_{(s,m)} &= \begin{cases} \delta^r_s \delta^1_m & \text{for } k_r > 0 \\ (T_m)^r{}_s & \text{for } k_r = 0, \end{cases} \\ (\mathbf{Z})^{(r,n)}{}_{(s,m)} &= \begin{cases} \delta^{n+1}_m \delta^r_s & \text{for } 1 \leqslant n < k_r \\ (T_m)^r{}_s & \text{for } n = k_r, \end{cases} \end{aligned} \tag{3.83}$$

where the label (s, m) runs from $(s, 1)$ to (s, k_s) with $1 \leqslant s \leqslant N_\mathrm{C}$, and the equation

$$\det(z - \mathbf{Z}) = \det(H_0(z)) = P(z) \tag{3.84}$$

holds. To show this relation, we need $\mathbf{J}(z)$ in the patch $\mathcal{U}^{k_1,\ldots,k_{N_\mathrm{C}}}$ as

$$(\mathbf{J}(z))^r{}_{(s,m)} = \left.\frac{H_0^{rs}(z)}{z^m}\right|_{\mathrm{reg}} = z^{k_s - m}\delta^r_s - \sum_{l=m+1}^{k_s} (T_l)^r{}_s z^{l-m-1} \tag{3.85}$$

where 'reg' implies to remove terms with negative power of z. By substituting equations (3.63), (3.83) and (3.85), we can confirm equation (3.82).

Using the whole set of H_0's in equation (3.63), we obtain the set of $(\mathbf{Z}, \mathbf{\Psi})$'s in equation (3.83). On the other hand, the $GL(k, \mathbf{C})$ action (3.80) in the Kähler quotient

[8] The choice of the D-term condition $[Z^\dagger, Z] + \psi^\dagger\psi \propto \mathbf{1}_k$ is not unique. There exist many candidates of it but all of them give topologically isomorphic manifolds [79].

(3.81) can be fixed to the form (3.83). Namely the Kähler quotient (3.81) is also covered by ${}_{N+k-1}C_k$ patches given by (3.83) where $(T_m)^r{}_s$ are coordinates of the patches. Combining this result with the argument (3.76)–(3.81), we finally find that the moduli space of vortices given by our moduli matrix is completely equivalent to that defined by the Kähler quotient:

$$\mathcal{M}_{N,k} \simeq \{\mathbf{Z}, \mathbf{\Psi}\}//GL(k, \mathbf{C}). \tag{3.86}$$

Thus this result confirms the result in [76] from the field theoretical point of view, while they used a method of D-brane construction.

Let us examine the relation with simple examples. For the separated vortices $z_i \neq z_j$, we find $\vec{\phi}_i(z) = \vec{\phi}_i \prod_{j\neq i}(z - z_j)$ with orientations $\vec{\phi}_i$ satisfying equations (3.59) gives $\mathbf{\Psi}$ for the orientational moduli and the diagonal matrix $\mathbf{Z}$ whose elements correspond to the positions of the vortices

$$\mathbf{Z} = \mathrm{diag}(z_1, z_2, \ldots, z_k), \qquad \mathbf{\Psi} = (\vec{\phi}_1, \cdots, \vec{\phi}_k), \tag{3.87}$$

although the matrix $\mathbf{Z}$ is not always diagonalizable by $GL(k, \mathbf{C})$ if there are coincident vortices.

In what follows we illustrate the correspondence in the case of $(N, k) = (2, 2)$. The moduli data in the patches (3.69) can be summarized by two matrices $\mathbf{Z}$ and $\mathbf{\Psi}$ as follows:

$$\begin{pmatrix} \mathbf{\Psi} \\ \mathbf{Z} \end{pmatrix} = \begin{pmatrix} b & a \\ 1 & 0 \\ 0 & 1 \\ \beta & \alpha \end{pmatrix}, \begin{pmatrix} 1 & 0 \\ 0 & 1 \\ \phi & \varphi \\ \tilde{\varphi} & \tilde{\phi} \end{pmatrix}, \begin{pmatrix} 1 & 0 \\ b' & a' \\ 0 & 1 \\ \beta & \alpha \end{pmatrix}. \tag{3.88}$$

The transition functions (3.70) and (3.71) between these three patches can be expressed by the complexified gauge transformation between moduli data as $(\mathbf{Z}', \mathbf{\Psi}') = (U\mathbf{Z}U^{-1}, \mathbf{\Psi}U^{-1})$ with appropriate $U \in GL(2, \mathbf{C})$.

3.2.4. The cases of $N_{\mathrm{F}} > N_{\mathrm{C}}$: non-Abelian semi-local vortices. In the cases with $N_{\mathrm{F}} > N_{\mathrm{C}}$, there appear additional moduli for vortices, typically, moduli for sizes of vortices due to additional Higgs fields. A vortex possessing such size moduli is called a semi-local vortex and its size is limited below by the size of ANO vortex. We also have non-normalizable moduli.

As in the last subsection, we take elements of the moduli matrix $H_0(z)$ as polynomials with respect to z. This is because we are interested in configurations with boundary conditions such that any point of the boundary belongs to the same vacuum. The tension of k vortices in this case is given by

$$T = 2\pi ck = \frac{c}{2}\oint \mathrm{d}z\,\mathrm{d}\bar{z}\,\partial\bar{\partial}\log\big(\det H_0 H_0^\dagger\big) = \frac{c}{2}\oint \mathrm{d}z\,\mathrm{d}\bar{z}\,\partial\bar{\partial}\log\left(\sum_{\langle\{A_r\}\rangle}|\tau^{\langle\{A_r\}\rangle}|^2\right), \tag{3.89}$$

where τ is defined similarly to equation (3.19) for the case of domain walls:

$$\tau^{\langle\{A_r\}\rangle}(z) \equiv \det H_0^{\langle\{A_r\}\rangle}(z). \tag{3.90}$$

Equation (3.89) requires that the maximal degree of a set of polynomials $\{\tau^{\langle\{A_r\}\rangle}\}$ is k.

We now discuss moduli parameters of a single vortex in the Abelian case with $N_{\mathrm{C}} = 1$ and general N_{F}. The condition $k = 1$ implies

$$H_0(z) = \big(a_1 z + b_1, a_2 z + b_2, \ldots, a_{N_{\mathrm{F}}} z + b_{N_{\mathrm{F}}}\big), \qquad a_A, b_A \in \mathbf{C} \tag{3.91}$$

where $\{a_A\}$ are homogeneous coordinates of $\mathbf{C}P^{N_{\mathrm{F}}-1}$. Some of these parameters are not normalizable moduli of the vortex but are non-normalizable moduli which should be interpreted as moduli of vacua on the boundary, as shown in the following. In a region sufficiently far from the origin ($z \neq 0$, $|b_A/z| \ll |a_A|$), the moduli matrix behaves as

$$H_0(z) \overset{z\neq 0}{\simeq} \left(a_1 + \frac{b_1}{z}, \ldots, a_{N_{\rm F}} + \frac{b_{N_{\rm F}}}{z}\right) \overset{z\to\infty}{\to} (a_1, a_2, \ldots, a_{N_{\rm F}}) \tag{3.92}$$

where we have used a V-transformation $V(z) = z^{-1}$ which is non-singular and is allowed in regions with $z \neq 0$. We thus have found that a_A parametrize the moduli space $\mathbf{C}P^{N_{\rm F}-1}$ of the Higgs vacua at the boundary, as $H^A|_{\rm boundary} = \sqrt{c}a_A/\sqrt{|a|^2}$. Therefore the set $\{a_A\}$ should be fixed as a boundary condition. Without loss of generality we can choose the boundary condition as $H'|_{\rm boundary} = \sqrt{c}(1, 0, \ldots, 0) = H|_{\rm boundary}U$ with the flavour symmetry $U \in SU(N_{\rm F})$. Under this boundary condition the moduli matrix should be taken as

$$H_0' = (z - z_0, b_2', b_3', \ldots, b_{N_{\rm F}-1}') \simeq H_0U. \tag{3.93}$$

Here the parameter $z_0 = -(b \cdot a^\dagger)/|a|^2$ describes the position of the semi-local vortex, and it also has a size modulus $b' \equiv \sqrt{\sum_{A=2}^{N_{\rm F}} |b_A'|^2} = \sqrt{|a|^2|b|^2 - |b \cdot a^\dagger|^2/|a|^2}$. Furthermore, in the cases of $N_{\rm F} \geqslant 3$, the vortex has an internal modulus $\{b_A'/b'\}$ describing non-vanishing Higgs fields at its centre. Note that even when the size modulus of the semi-local vortex is zero, $b' = 0$, it becomes the ANO vortex with the size $1/g\sqrt{c}$.

In general cases for $N_{\rm F}$ and $N_{\rm C}$, the moduli matrix H_0 contains moduli of the vacua on the boundary (restricted to $H^2 = 0$)

$$\mathcal{M}_{\rm boundary} = G_{N_{\rm F},N_{\rm C}} \simeq \frac{SU(N_{\rm F})}{SU(N_{\rm C}) \times SU(N_{\rm F} - N_{\rm C}) \times U(1)}, \tag{3.94}$$

which should be fixed.

Therefore, the moduli space $\mathcal{M}_{N_{\rm C},N_{\rm F},k}$ of k-vortices in $U(N_{\rm C})$ gauge theory coupled to $N_{\rm F}$ hypermultiplets can be formally expressed as the quotient of

$$\mathcal{M}_{N_{\rm C},N_{\rm F},k} = \frac{\{H_0(z)|H_0(z) \in M_{N_{\rm C},N_{\rm F}}, \max\{\deg \tau^{\langle\{A_r\}\rangle}\} = k\}}{\{V(z)|V(z) \in M_{N_{\rm C},N_{\rm C}}, \det V(z) = {\rm const} \neq 0\} \times \mathcal{M}_{\rm boundary}} \tag{3.95}$$

where $M_{N,N'}$ denotes a set of $N \times N'$ matrices of polynomial functions of z. Let us investigate the moduli space for semi-local non-Abelian vortices concretely. Using the flavour symmetry $SU(N_{\rm F})$, we can choose a vacuum on the boundary as $\langle{\rm vac}\rangle = \langle 1, 2, \ldots, N_{\rm C}\rangle$ without loss of generality. Namely we have conditions

$$\det(H^{\langle{\rm vac}\rangle}) = (\sqrt{c})^{N_{\rm C}}, \qquad \det(H^{\langle\{A_r\}\rangle}) = 0 \qquad \text{for} \quad \langle\{A_r\}\rangle \neq \langle{\rm vac}\rangle. \tag{3.96}$$

By use of the relation $\det H^{\langle\{A_r\}\rangle}/\det H^{\langle\{B_r\}\rangle} = \tau^{\langle\{A_r\}\rangle}/\tau^{\langle\{B_r\}\rangle}$ we find that the boundary condition with vorticity k requires

$$\deg \tau^{\langle{\rm vac}\rangle}(z) = k, \qquad \text{and} \qquad \deg \tau^{\langle\{A_r\}\rangle}(z) < k \qquad \text{for} \quad \langle\{A_r\}\rangle \neq \langle{\rm vac}\rangle. \tag{3.97}$$

Due to the Plücker relations (3.33) all of these conditions are not independent, but only the following two conditions turn out to be independent:

$$\begin{aligned} &\deg \tau^{\langle{\rm vac}\rangle}(z) = k, \\ &(\mathbf{F}(z))^r{}_A \equiv \tau^{\langle 1,\ldots,r-1,A,r+1,\ldots,N_{\rm C}\rangle}(z) \in {\rm Pol}(z; k), \end{aligned} \tag{3.98}$$

with $N_{\rm C} < A \leqslant N_{\rm F}$.

Let us decompose the moduli matrix H_0 to an $N_{\rm C} \times N_{\rm C}$ matrix $\mathbf{D}(z)$ and an $N_{\rm C} \times (N_{\rm F} - N_{\rm C})$ matrix $\mathbf{Q}(z)$ as

$$H_0(z) = (\mathbf{D}(z), \mathbf{Q}(z)). \tag{3.99}$$

Then the first and the second conditions in equation (3.98) are regarded as conditions for the matrices $\mathbf{D}(z)$ and $\mathbf{Q}(z)$, respectively. Under these constraints, we can obtain the moduli matrix for the semi-local vortices. For instance, in the case of $k = 1$, the moduli matrix in a patch $\mathcal{U}^{(0,\ldots,0,1)}$ contains an $(N_C - 1)$-component vector $\vec{b}$ as orientational moduli and additional moduli $\{q_A\}$ as in the following:

$$H_0(z) \simeq \begin{pmatrix} \mathbf{1}_{N_C-1} & -\vec{b} & 0 & 0 & \cdots & 0 \\ \mathbf{0} & z - z_0 & q_{N_C+1} & q_{N_C+2} & \cdots & q_{N_F} \end{pmatrix}. \tag{3.100}$$

Since the monic polynomial $P(z) \equiv \tau^{\langle \mathrm{vac} \rangle}(z) = \det \mathbf{D}(z)$ satisfies condition (3.98) similar to equation (3.58), we can use the same strategy as we used in the $N_F = N_C$ case to fix the V-transformation. We thus find that $\mathbf{D}(z)$ consists of kN_C complex moduli parameters corresponding to positions and orientations of k vortices. We also obtain holomorphic $N_C \times k$ matrix $\mathbf{\Phi}(z)$ whose components belong to $\mathrm{Pol}(z; k)$ as a solution of the equation

$$\mathbf{D}(z)\mathbf{\Phi}(z) = \mathbf{J}(z)P(z). \tag{3.101}$$

Next let us consider moduli described by $\mathbf{Q}(z)$. Here we can easily find the identities given by

$$0 = H_0^{r[A_1} H_0^{1A_2} H_0^{2A_3} \cdots H_0^{N_C A_{N_C+1}]} \propto H_0^{r[A_1} \tau^{\langle A_2 \cdots A_{N_C+1}]\rangle} \tag{3.102}$$

where the square bracket means anti-symmetrization with respects to indices A_s, $(s = 1, \ldots, N_C + 1)$. By setting $\{A_s\}$ to $\{1, 2, \ldots, N_C, A\}$ in the above we obtain an identity for the matrices

$$\mathbf{D}(z)\mathbf{F}(z) = \mathbf{Q}(z)P(z). \tag{3.103}$$

By use of this identity, we find condition (3.98) requires that each column of $\mathbf{F}(z)$ should be written by a linear combination of column vectors of $\mathbf{\Phi}(z)$ in equation (3.101), that is, $\mathbf{F}(z)$ should be solved with a constant $k \times (N_F - N_C)$ matrix $\widetilde{\mathbf{\Psi}}$ as, $\mathbf{F}(z) = \mathbf{\Phi}(z)\widetilde{\mathbf{\Psi}}$. Comparing equation (3.101) with equation (3.103) we find that $\mathbf{Q}(z)$ satisfying the condition must be written by

$$\mathbf{Q}(z) = \mathbf{J}(z)\widetilde{\mathbf{\Psi}}, \tag{3.104}$$

and conversely $\mathbf{Q}$ given in the above with an arbitrary $\widetilde{\mathbf{\Psi}}$ realizes the second condition. Therefore, the matrix $\widetilde{\mathbf{\Psi}}$ describes the additional moduli for semi-local vortices entirely. As a result, we find that the dimension of the moduli space of k vortices in the cases with general N_F and N_C is given by

$$\dim \mathcal{M}_{N_C,N_F,k} = 2kN_C + 2k(N_F - N_C) = 2kN_F \tag{3.105}$$

in accord with the result of the index theorem [76].

In this case of semi-local vortices also we can extract the matrices $\mathbf{Z}$, $\mathbf{\Psi}$ from $\mathbf{\Phi}(z)$ in equation (3.101). The $GL(k, \mathbf{C})$ action (3.80) acts also on $\widetilde{\mathbf{\Psi}}$ as

$$(\mathbf{Z}, \mathbf{\Psi}, \widetilde{\mathbf{\Psi}}) \simeq (U\mathbf{Z}U^{-1}, \mathbf{\Psi}U^{-1}, U\widetilde{\mathbf{\Psi}}) \tag{3.106}$$

with $U \in GL(k, \mathbf{C})$. Therefore the moduli space for semi-local non-Abelian vortices in terms of the moduli matrix can be translated to that of the Kähler quotient as

$$\mathcal{M}_{N_C,N_F,k} \simeq \{\mathbf{Z}, \mathbf{\Psi}, \widetilde{\mathbf{\Psi}}\}//GL(k, \mathbf{C}). \tag{3.107}$$

We can fix the imaginary part of the $GL(k, \mathbf{C})$ action as in equation (3.81), to give

$$\mathcal{M}_{N_C,N_F,k} \simeq \{(Z, \psi, \tilde{\psi}) | [Z^\dagger, Z] + \psi^\dagger\psi - \tilde{\psi}\tilde{\psi}^\dagger \propto \mathbf{1}_k\}/U(k), \tag{3.108}$$

with $k \times (N_F - N_C)$ matrix $\tilde{\psi}$. This again recovers the result in [76].

Finally, it may be useful to summarize the relations between the moduli matrix $H_0(z)$ and the matrices for Kähler quotient as

$$\nabla^\dagger L = \widetilde{\nabla}^\dagger L = 0 \tag{3.109}$$

where an $(N_{\rm F}+k)\times N_{\rm C}$ matrix L, an $(N_{\rm F}+k)\times k$ matrix ∇ and an $(N_{\rm F}+k)\times(N_{\rm F}-N_{\rm C})$ matrix $\widetilde{\nabla}$ are defined by

$$L^\dagger \equiv (H_0(z), \mathbf{J}(z)), \qquad \nabla \equiv \begin{pmatrix} -\mathbf{\Psi} \\ 0 \\ z-\mathbf{Z} \end{pmatrix} \qquad \text{and} \qquad \widetilde{\nabla} \equiv \begin{pmatrix} 0 \\ \mathbf{1}_{N_{\rm F}\text{-}N_{\rm C}} \\ -\widetilde{\mathbf{\Psi}} \end{pmatrix}. \tag{3.110}$$

3.2.5. Lumps as semi-local vortices in the strong coupling limit. Nonlinear sigma models admits lumps [72, 73] as co-dimension two solitons, which can be obtained from semi-local vortices ($N_{\rm F} > N_{\rm C}$) in the limit of strong gauge coupling $g^2 \to \infty$ keeping the vortex size finite. Thus lumps also have a size modulus. If we take the limit of vanishing size modulus, the lumps reduce to a singular configuration. This phenomenon reflects the fact that ANO vortices (with size $1/g\sqrt{c}$) become singular in the strong gauge coupling limit.

If we take the strong coupling limit keeping $\log\Omega$ smooth, the master equation (3.51) can be solved algebraically as

$$\Omega|_{g^2\to\infty} = c^{-1} H_0(z) H_0^\dagger(\bar z). \tag{3.111}$$

Namely, we can obtain unique and exact solutions for lumps with given arbitrary H_0. Here we should note that if we take a solution (3.111) with the quantity $H_0(z)H_0(z)^\dagger$ having a vanishing point, $H_0(z_0)H_0(z_0)^\dagger = 0$, the lhs of equation (3.51) leads to a singular profile implying that the strong coupling limit is improper in such a case. Therefore, the moduli matrix H_0 whose rank reduces somewhere in the z-plane, which describes an embedding of ANO vortices, is prohibited for lump solutions. To obtain the moduli space for lumps, subspaces with ANO vortices embedded should be removed from that for the semi-local vortices. We thus find that the total moduli space for lumps $\mathcal{M}^{\rm total}_{N_{\rm C},N_{\rm F}}|_{g^2\to\infty}$ is obtained as a set of holomorphic maps from the z-plane to the Grassmann manifold $G_{N_{\rm F},N_{\rm C}}$, to give

$$\begin{aligned}\mathcal{M}^{\rm total}_{N_{\rm C},N_{\rm F}}\Big|_{g^2\to\infty} &= \frac{\{H_0(z)|H_0(z)\in M_{N_{\rm F},N_{\rm C}}, \operatorname{rank}(H_0(z)) = N_{\rm F}\}}{\{V(z)|V(z)\in M_{N_{\rm C},N_{\rm C}}, \operatorname{rank}(V(z)) = N_{\rm C}\}} \\ &= \{H_0|\mathbf{C}\to G_{N_{\rm F},N_{\rm C}}, \bar\partial_z H_0 = 0\}.\end{aligned} \tag{3.112}$$

Due to the removal of the subspaces, this moduli space has singularities, which are known as small-lump singularities. In other words, the moduli space of semi-local vortices can be obtained by resolving small lump singularities in the lump moduli space by inserting the ANO vortices.

3.2.6. Vortices on cylinder. Interesting relation has been observed between domain walls and vortices [7]. In order to study the relation, it is most useful to consider vortices on a cylinder ($-\infty < x^1 < \infty, x^2 \simeq x^2 + 2\pi R$) with one dimension compactified with the radius R. Vortices can exist when the Higgs scalars are massless. However, domain walls require massive Higgs scalars making the vacua discrete. It is best to introduce the mass for the Higgs scalars by a compactification with a twisted boundary condition, usually referred as a Scherk–Schwarz dimensional reduction. One can obtain solutions of 1/2 BPS equations for vortices on the cylinder as we have described before on a plane. If the vortices are placed on the cylinder and the twisted boundary condition is applied, the moduli matrix should satisfy

$$H_0(z + 2\pi {\rm i} R) = H_0(z)\,{\rm e}^{2\pi {\rm i} MR}, \tag{3.113}$$

where the twisting phase ${\rm e}^{2\pi {\rm i}MR}$ is related to the mass matrix M for the hypermultiplets. In order to make the periodicity in x^2 explicit, one can use periodic variable u instead of z as

$$H_0(z) = \hat H_0(u)\,{\rm e}^{Mz}, \qquad \text{with} \qquad u = \exp\frac{z}{R}. \tag{3.114}$$

The V-equivalence relation becomes in this case

$$\hat{H}_0(u) \simeq \hat{H}'_0(u) = V(u)\hat{H}_0(u) \tag{3.115}$$

with $V(u) \in GL(N_{\rm C}, \mathbf{C})$ for $u \in \mathbf{C} - \{0\}$. By keeping all the Kaluza–Klein modes, we have found a duality between vortices and domain walls [7].

On the other hand, we should retain only the lowest mode, if we restrict ourselves to phenomena at energies low compared to the Kaluza–Klein mass scales $1/R$. Then we should take a particular form of moduli matrix given by the constant $\hat{H}_0$

$$H_0(z) = \hat{H}_0\,{\rm e}^{Mz}. \tag{3.116}$$

This constant $\hat{H}_0$ is precisely the moduli matrix for domain walls that we have discussed.

3.3. Effective lagrangians

The low-energy effective Lagrangian on solitons is given by promoting the moduli parameters to fields on the world volume of the soliton and by assuming the weak dependence on the world-volume coordinates of the solitons [29]. In our case, we promote the moduli parameters ϕ^α in the moduli matrix H_0 to fields on the world volume of the soliton, such as walls or vortices

$$H_0(\phi^\alpha) \to H_0(\phi^\alpha(x)), \tag{3.117}$$

where the coordinates on the world volume is denoted as x^m. We introduce 'the slow-movement parameter' λ, which is assumed to be much smaller than the typical mass scale in the problem. Please note that we are using the slow-movement approximation to the case of nontrivial world volume besides the time dependence, although the original proposal was made for the case without the spatial world volume. It is also worth pointing out that we can obtain not only the effective Lagrangian for the quasi-Nambu–Goldstone (QNG) modes, but also for the Nambu–Goldstone (NG) modes, which are required by the spontaneously broken global symmetry. We will present the procedure and results in terms of component fields, although it is extremely useful and straightforward to use the superfield formalism respecting the preserved supersymmetry especially in the case of 1/2 BPS system such as walls or vortices [14], that we are going to describe below.

3.3.1. Effective Lagrangian on walls. In the case of domain walls, all the moduli parameters are contained in the constant moduli matrix H_0 [1, 2]. Since the typical mass scales of the wall are $g\sqrt{c}$ and the characteristic mass difference Δm of hypermultiplets, we assume the slow-movement of moduli fields

$$\lambda \ll \min(\Delta m, g\sqrt{c}). \tag{3.118}$$

The 1/2 BPS background fields of the wall are of the order of $\lambda^0 = \mathcal{O}(1)$, whereas derivatives in terms of the world-volume coordinates and induced fields by the fluctuations ϕ^α are of order λ

$$H^1 \sim \mathcal{O}(1), \qquad \Sigma \sim \mathcal{O}(1), \qquad \partial_m \sim \mathcal{O}(\lambda). \tag{3.119}$$

$$W_m \sim \mathcal{O}(\lambda), \qquad H^2 \sim \mathcal{O}(\lambda), \qquad F_{my}(W) \sim \mathcal{O}(\lambda). \tag{3.120}$$

Decomposing the field equations in powers of λ, we find the BPS equations (3.2) automatically at the order λ^0, whereas we obtain all the induced fields at higher orders. Assuming $H^2 = 0$, we vary the fundamental Lagrangian to obtain the equations of motion (with $H^2 = 0$). The equation of motion for the gauge field fluctuations W_m reads

$$0 = \frac{1}{g^2}\mathcal{D}_y F_{my} + \frac{\mathrm{i}}{g^2}[\Sigma, \mathcal{D}_m\Sigma] + \frac{\mathrm{i}}{2}(H\mathcal{D}_m H^\dagger - \mathcal{D}_m H H^\dagger). \tag{3.121}$$

After a long calculation we obtain the gauge field in terms of the matrix S defined in (3.5) and the variations δ_m with respect to chiral scalar fields and $\delta_m^\dagger$ with respect to anti-chiral scalar fields

$$W_m = \mathrm{i}\big((\delta_m S^\dagger)S^{\dagger-1} - S^{-1}\big(\delta_m^\dagger S\big)\big), \tag{3.122}$$

$$\delta_m \equiv (\partial_m\phi^\alpha)\frac{\partial}{\partial\phi^\alpha}, \qquad \delta_m^\dagger \equiv (\partial_m\phi^{\alpha *})\frac{\partial}{\partial\phi^{\alpha *}}. \tag{3.123}$$

Similarly we obtain other fluctuations induced to order λ

$$\mathcal{D}_m H = S^\dagger\delta_m(\Omega^{-1}H_0)\,\mathrm{e}^{My}, \qquad \mathcal{D}_m\Sigma + \mathrm{i}F_{my} = S^\dagger\delta_m(\Omega^{-1}\partial_y\Omega)S^{\dagger-1}. \tag{3.124}$$

The effective Lagrangian is obtained by substituting equations (3.122) and (3.124) to the fundamental Lagrangian and by integrating over the co-dimension y of the walls

$$\begin{aligned}
\mathcal{L}_{\rm wall} + T_{\rm w} &= \int \mathrm{d}y\,\mathrm{Tr}\left[\mathcal{D}^m H\mathcal{D}_m H^\dagger + \frac{1}{g^2}\big(\mathcal{D}^m\Sigma - \mathrm{i}F^m{}_y\big)(\mathcal{D}_m\Sigma + \mathrm{i}F_{my})\right] \\
&= \int \mathrm{d}y\,\mathrm{Tr}\left[\Omega\delta^m(\Omega^{-1}H_0)\,\mathrm{e}^{2My}\delta_m^\dagger\big(H_0^\dagger\Omega^{-1}\big) + \frac{1}{g^2}\Omega\delta^m(\Omega^{-1}\partial_y\Omega)\Omega^{-1}\delta_m^\dagger(\partial_y\Omega\Omega^{-1})\right] \\
&= \int \mathrm{d}y\,\mathrm{ReTr}\left[c\delta^m\big(\Omega^{-1}\delta_m^\dagger\Omega_0\big) + \frac{\partial_y^2}{2g^2}\big((\delta^m\Omega)\Omega^{-1}\big(\delta_m^\dagger\Omega\big)\Omega^{-1}\big)\right] \\
&= \int \mathrm{d}y\,\delta^m\delta_m^\dagger\left[\left(c - \frac{\partial_y^2}{g^2}\right)\log\det\Omega + \frac{1}{2g^2}\mathrm{Tr}(\Omega^{-1}\partial_y\Omega)^2\right] \\
&\quad - \frac{1}{g^2}\,\mathrm{Re}\,\mathrm{Tr}\big[\Omega^{-1}\Omega'\delta^m\big(\Omega^{-1}\delta_m^\dagger\Omega\big)\big]\Big|_{-\infty}^{\infty} \\
&\equiv \delta^m\delta_m^\dagger K(\phi,\phi^*) = K_{ij}(\phi,\phi^*)\partial^m\phi^i\partial_m\phi^{j*},
\end{aligned} \tag{3.125}$$

where $T_{\rm w}$ is the tension of the (multi-)wall corresponding to the classical action of the background solution. This Kähler metric can be derived from the following Kähler potential for the moduli chiral superfields ϕ, ϕ^* of the preserved four supersymmetry

$$K(\phi,\phi^*) = \int \mathrm{d}y\left[c\log\det\Omega + \frac{1}{2g^2}\mathrm{Tr}(\Omega^{-1}\partial_y\Omega)^2\right]. \tag{3.126}$$

This effective Lagrangian contains both NG as well as QNG moduli fields. Equation (3.126) is manifestly invariant under the local $U(N_{\rm C})$ gauge transformation. Under the V-equivalence transformation of H_0 with an arbitrary $N_{\rm C}\times N_{\rm C}$ matrix of chiral superfield $\Lambda(x,\theta,\bar\theta)$, given by $H_0 \to H_0{}' = \mathrm{e}^{\Lambda}H_0$ with $V = \mathrm{e}^{\Lambda}$, the Kähler potential receives a Kähler transformation from equation (3.11):

$$\log\det\Omega \to \log\det\Omega + \det\Lambda + \det\Lambda^\dagger. \tag{3.127}$$

Since the purely chiral superfield $\log\det\Lambda$ or anti-chiral superfield $\log\det\Lambda^\dagger$ does not contribute to the effective Lagrangian. It is worth pointing out that, if we regard the Ω as dynamical variables, the above Kähler potential serves as a Lagrangian from which the master equation (3.8) for Ω can be derived. This fact can be understood most easily by means of superfield approach which enable us to rewrite the Lagrangian in terms of only

Ω after solving the hypermultiplet part of the equations of motion in the slow-movement approximation [14].

For the infinite gauge coupling limit $g \to \infty$, the effective Lagrangian for (multi) domain walls reduces to

$$\mathcal{L}_{\rm walls}^{g^2\to\infty} = c\int {\rm d}^4\theta \int {\rm d}y \log\det\Omega_0, \qquad \Omega_0 = \frac{1}{c} H_0\, {\rm e}^{2My} H_0{}^\dagger. \tag{3.128}$$

3.3.2. Effective Lagrangian on vortices. In the case of vortices, we have only single mass scale. Therefore small-movement approximation is valid when

$$\lambda \ll g\sqrt{c}. \tag{3.129}$$

The equation of motion for the gauge field fluctuations becomes

$$0 = \frac{1}{g^2}(\mathcal{D}_x F_{mx} + \mathcal{D}_y F_{my}) + \frac{\rm i}{2}(H\mathcal{D}_m H^\dagger - \mathcal{D}_m H H^\dagger). \tag{3.130}$$

The solution W_m is given by the same formula (3.122) as in the wall case. Other fluctuations induced to order λ are similarly given by

$$\mathcal{D}_m H = S^\dagger \delta_m(\Omega^{-1}H_0). \tag{3.131}$$

By substituting these solutions (3.122) and (3.131) to the fundamental Lagrangian and by integrating over the co-dimension x, y of the vortices, the effective Lagrangian on the vortex world volume is obtained in terms of the matrix Ω for vortices

$$\mathcal{L}_{\rm vortex} = \int {\rm d}^2x \Big[\delta_m\delta_m^\dagger c\log\det\Omega + \frac{4}{g^2}\,{\rm Tr}\,\big\{\bar\partial_z(\delta_m\Omega\Omega^{-1})\delta_m^\dagger(\partial_z\Omega\Omega^{-1}) - \bar\partial_z(\partial_z\Omega\Omega^{-1})\delta_m^\dagger(\delta_m\Omega\Omega^{-1})\big\}\Big], \tag{3.132}$$

where $z \equiv x^1 + {\rm i}x^2$ and the variation δ_m and its conjugate $\delta_m^\dagger$ act on complex moduli fields as $\delta_m\Omega = \sum_\alpha \partial_m\phi^\alpha(\delta\Omega/\delta\phi^\alpha)$ and $\delta_m^\dagger\Omega = \sum_\alpha \partial_m\phi^{\alpha*}(\delta\Omega/\delta\phi^{\alpha*})$, respectively. This is a nonlinear sigma model with the Kähler metric which can be obtained from the following Kähler potential

$$K = \int {\rm d}^2x\, {\rm Tr}\left[-2cV + {\rm e}^{2V}\Omega_0 + \frac{16}{g^2}\int_0^1 {\rm d}t \int_0^t {\rm d}s\, \bar\partial V\, {\rm e}^{2sL_V}\partial V\right], \tag{3.133}$$

where $V \equiv -\frac{1}{2}\log\Omega$, $\Omega_0 \equiv c^{-1}H_0H_0^\dagger$ and the operation L_V is defined by

$$L_V \times X = [V, X]. \tag{3.134}$$

This Kähler potential can be derived from the superfield formalism straightforwardly [14] without going through the Kähler metric in equation (3.132). The ANO case is reduced to the results in [68–70].

In the case of a single vortex, the integration in the Lagrangian (3.133) can be performed explicitly to give

$$K_{\text{single vortex}} = \pi c|z_0|^2 + \frac{4\pi}{g^2}\log\left(1 + \sum_{i=1}^{N-1}|b_i|^2\right), \tag{3.135}$$

in accord with the symmetry argument. Here z_0 is the position of the vortex, and b_i are the inhomogeneous coordinates of the $\mathbf{C}P^{N_{\rm F}-1}$ as the orientational moduli.

Let us consider the limit of strong gauge coupling, where the gauge theory with $N_{\rm F} > N_{\rm C}$ reduces to the nonlinear sigma model on the cotangent bundle over the Grassmann manifold $T^*G_{N_{\rm F},N_{\rm C}}$. Then the semi-local vortices of the $N_{\rm F} > N_{\rm C}$ case for finite gauge couplings become sigma-model lumps as explained in section 3.2.5. Since the second term in the effective Lagrangian (3.132) for the vortices vanishes in this limit, the Kähler potential of the effective Lagrangian on the world volume of nonlinear sigma model lumps as

$$K_{\text{lumps}} = c \int \mathrm{d}^2 x \, \log\det \Omega_0, \qquad \Omega_0 = \frac{1}{c} H_0 H_0^\dagger. \tag{3.136}$$

This form of the Kähler potential has been obtained previously [72, 73] in the case of the $\mathbf{C}P^{N_F-1}$ lumps corresponding to the case of the Abelian gauge theory ($N_C = 1$).

4. 1/4 BPS solitons

4.1. 1/4 BPS equations and their solutions

A series of 1/2 BPS equations for solitons in unbroken or Coulomb phases of non-Abelian gauge theories are well known: instantons, monopoles, the Hitchin system which have co-dimensions 4, 3 and 2, respectively [18, 22]. The Hitchin system is known to admit no finite energy solutions but, as we show in the next subsection, we can realize finite energy solutions in a finite region and so call them Hitchin vortices. Monopoles and Hitchin vortices can be obtained by dimensional reductions of instantons.

When these solitons are put into the Higgs phase, vortices and walls in sections 3.1 and 3.2 are attached to these solitons. For instance, magnetic flux coming out of a monopole must be squeezed into vortex tubes by the Meissner effect resulting in two vortices in the opposite direction attached to the monopole. This composite soliton can be regarded as a kink on the world volume of a vortex [103]. Similarly instantons in the Higgs phase can be realized as vortices on a vortex [13], and the Hitchin vortex can be realized at a junction of walls [8, 9]. These composite solitons preserve 1/4 of supersymmetry and can be derived from instantons in the Higgs phase by either simple or Scherk–Schwarz (SS) dimensional reduction.

In this section we systematically derive the 1/4 BPS equations, the Bogomol'nyi energy bound and formal solutions, and describe generic structure of the moduli space of these composite solitons by our moduli matrix approach. The instanton–vortex–vortex (IVV) system, the monopole–vortex–wall (MVW) system and the Hitchin-wall–wall (HWW) system depend on coordinates along directions (co-dimensions) denoted by $\times$, and have the world volume whose spatial part is denoted by '$\bigcirc$' as follows:

IVV ($d = 5, 6$)	1	2	3	4	MVW ($d = 4, 5$)	1	2	3	HWW ($d = 3, 4$)	1	3
Instantons	$\times$	$\times$	$\times$	$\times$	Monopoles	$\times$	$\times$	$\times$	Hitchin vortices	$\times$	$\times$
Vortices	$\times$	$\times$	$\bigcirc$	$\bigcirc$	Vortices	$\times$	$\times$	$\bigcirc$	Walls	$\times$	$\bigcirc$
Vortices	$\bigcirc$	$\bigcirc$	$\times$	$\times$	Walls	$\bigcirc$	$\bigcirc$	$\times$	Walls	$\bigcirc$	$\times$

For the largest dimensions of the fundamental theory for each composite soliton, namely $d = 6, 5, 4$ for IVV, MVW or HWW, respectively, another world-volume direction x^5 is present, but is not written explicitly. Since we are interested in static solutions, we are allowed to choose $W_0 = W_5 = 0$. The topological charges are also obtained by the dimensional reductions and are classified by the sign of their contributions to the energy density as summarized below. It has been recently found that Abelian gauge theories admit negative energy objects with the instanton charge localized at intersection of vortices [13], those with the monopole charge at junctions of vortices and walls [11, 12], and those with the Hitchin charge at junctions of walls [8, 9]. In particular the first two are called *intersections* and *boojums*, respectively.

Dim\charge	Positive	Negative
$d = 5, 6$ instantons	Instantons inside vortices	Intersectons
$d = 4, 5$ monopole	Monopoles attached by vortices	Boojums
$d = 3, 4$ Hitchin	Non-Abelian wall junctions	Abelian wall junctions

4.1.1. Instanton–vortex system. The 1/4 BPS equations can be derived by performing the Bogomol'nyi completion of the energy density as follows [13, 106],

$$\begin{aligned}\mathcal{E} &= \mathrm{Tr}\left[\frac{1}{2g^2}F_{mn}F_{mn} + \mathcal{D}_m H(\mathcal{D}_m H)^\dagger + \frac{1}{g^2}(Y^3)^2\right]\\ &= \mathrm{Tr}\left[\frac{1}{g^2}\{(F_{13}-F_{24})^2 + (F_{14}+F_{23})^2 + (F_{12}+F_{34}+Y^3)^2\} + (\mathcal{D}_1 H + \mathrm{i}\mathcal{D}_2 H)(\mathcal{D}_1 H\right.\\ &\quad\left. + \mathrm{i}\mathcal{D}_2 H)^\dagger + (\mathcal{D}_3 H + \mathrm{i}\mathcal{D}_4 H)(\mathcal{D}_3 H + \mathrm{i}\mathcal{D}_4 H)^\dagger + \frac{1}{2g^2}F_{mn}\tilde{F}_{mn} - c(F_{12}+F_{34}) + \partial_m J_m\right]\\ &\geqslant \mathrm{Tr}\left[\frac{1}{2g^2}F_{mn}\tilde{F}_{mn} - c(F_{12}+F_{34}) + \partial_m J_m\right], \end{aligned} \tag{4.1}$$

where $m, n, k, l = 1, 2, 3, 4$ and $W^0 = W^5 = 0$ is chosen. The above energy density is minimized if the following set of the first-order differential equations is satisfied:

$$F_{13} - F_{24} = 0, \qquad F_{14} + F_{23} = 0, \tag{4.2}$$

$$F_{12} + F_{34} = -Y_3, \tag{4.3}$$

$$\mathcal{D}_1 H + \mathrm{i}\mathcal{D}_2 H = 0, \qquad \mathcal{D}_3 H + \mathrm{i}\mathcal{D}_4 H = 0. \tag{4.4}$$

We call a set of these as the self-dual Yang–Mills–Higgs (SDYM-Higgs) equation. This equation was also obtained by mathematicians [114–116] and is simply called the vortex equation although this contains instantons also. It has been shown recently in [124] that this set of equations can be derived (at least in the case of $U(1)$ gauge group) from the Donaldson–Uhlenbeck–Yau equations on C^3 [125] by dimensional reduction on S^2. It is easy to recognize that these equations are a combination of the 1/2 BPS equations for constituent solitons. They can also be derived from the requirement of preserving the 1/4 of supersymmetry defined by the following set of three projection operators for supertransformation parameters $\varepsilon^i\gamma^{05}\varepsilon^i = -\varepsilon^i$, $\gamma^{12}(\mathrm{i}\sigma_3\varepsilon)^i = -\varepsilon^i$, $\gamma^{34}(\mathrm{i}\sigma_3\varepsilon)^i = -\varepsilon^i$, only two of which are independent. The first projection corresponds to the supersymmetry preserved by instantons with co-dimensions in x^1–x^2–x^3–x^4, the second and the third projections correspond to vortices with co-dimensions x^1–x^2 and x^3–x^4 planes, respectively. The Bogomol'nyi bound T_{IVV} for the energy density of the 1/4 BPS composite solitons can be rewritten as a sum of three topological charges

$$T_{\mathrm{IVV}} = \mathcal{I}_{1234} + \mathcal{V}_{12}v_{34} + \mathcal{V}_{34}v_{12}, \tag{4.5}$$

where we have defined

$$\mathcal{I}_{1234} \equiv \frac{1}{4g^2}\int \mathrm{d}^4x\, \mathrm{Tr}(\epsilon_{mnkl}F_{mn}F_{kl}), \tag{4.6}$$

$$\mathcal{V}_{ij} \equiv -c\int \mathrm{d}x^i\,\mathrm{d}x^j\, F_{ij}. \tag{4.7}$$

Here $\mathcal{I}_{1234}$ is the mass of the instantons and $\mathcal{V}_{ij}$ is that of vortices with co-dimensions in the x^i–x^j plane and $v_{kl} = \int \mathrm{d}x^k\,\mathrm{d}x^l$ is the x^k–x^l world volume of vortices. The world-volume integration has also the x^5 direction in the case of the fundamental theory in $d = 6$.

Let us introduce the complex coordinates

$$z \equiv x^1 + \mathrm{i}x^2, \qquad w \equiv x^3 + \mathrm{i}x^4 \tag{4.8}$$

and the corresponding components for gauge fields

$$\bar{W}_z \equiv \tfrac{1}{2}(W_1 + \mathrm{i}W_2), \qquad \bar{W}_w \equiv \tfrac{1}{2}(W_3 + \mathrm{i}W_4). \tag{4.9}$$

It is crucial to recognize that equation (4.2) are the integrability conditions for the existence of the following solutions of equation (4.4)

$$\bar{W}_z = -\mathrm{i}S^{-1}\bar{\partial}_z S, \qquad \bar{W}_w = -\mathrm{i}S^{-1}\bar{\partial}_w S, \qquad H = S^{-1}H_0(z, w) \tag{4.10}$$

with $S(z, \bar{z}, w, \bar{w}) \in GL(N_{\mathrm{C}}, \mathbf{C})$. The solution is characterized by an $N_{\mathrm{C}} \times N_{\mathrm{F}}$ matrix function $H_0(z, w)$ whose components are holomorphic with respect to both z and w. We call this $H_0(z, w)$ as the moduli matrix for the instanton–vortex–vortex system. By introducing a $U(N_{\mathrm{C}})$ gauge invariant matrix

$$\Omega(z, \bar{z}, w, \bar{w}) \equiv SS^\dagger \tag{4.11}$$

as in the 1/2 BPS cases, we can rewrite the remaining equation (4.3) as [13]

$$4\partial_z(\Omega^{-1}\bar{\partial}_z\Omega) + 4\partial_w(\Omega^{-1}\bar{\partial}_w\Omega) = cg^2(\mathbf{1}_{N_{\mathrm{C}}} - \Omega^{-1}\Omega_0), \qquad c\Omega_0 \equiv H_0H_0^\dagger, \tag{4.12}$$

which we call the master equation for the instanton–vortex–vortex system. When the Higgs fields are decoupled by putting $c = 0$ and $H_0 = 0$, this equation reduces to the so-called Yang's equation [126], in the form of the left-hand side of (4.12) being equal to zero. The existence and uniqueness of a solution of the master equation (4.12) was rigorously proved in [115, 116] in the form of the Hitchin–Kobayashi correspondence, at least when the base manifold is compact Kähler manifold instead of $\mathbf{C}^2$ in our case. We simply expect that this holds for $\mathbf{C}^2$ once the moduli matrix $H_0(z, w)$ is given.

Similarly to the 1/2 BPS cases, two moduli matrices related by the following V-equivalence relation gives identical physics

$$H_0 \sim H_0' = V(z, w)H_0, \qquad S \sim S' = V(z, w)S, \tag{4.13}$$

where $V(z, w) \in GL(N_{\mathrm{C}}, \mathbf{C})$ has components holomorphic with respect to both z and w. Therefore the total moduli space of this system is the quotient divided by $\sim$ defined in the V-equivalence relation (4.13)

$$\mathcal{M}_{\mathrm{IVV}}^{\mathrm{total}} \equiv \{H_0|\mathbf{C}^2 \to M(N_{\mathrm{C}} \times N_{\mathrm{F}}, \mathbf{C}), \bar{\partial}_z H_0 = 0, \bar{\partial}_w H_0 = 0\}/\sim. \tag{4.14}$$

Under the V-equivalence relation, Ω transforms as $\Omega \sim V\Omega V^\dagger$.

4.1.2. Monopole–vortex–wall system. We can obtain 1/4 BPS equations for the monopole–vortex–wall system by performing the SS reduction along the x^4(or x^3) direction in equations (4.2)–(4.4):

$$\mathcal{D}_2\Sigma_4 - F_{31} = 0, \qquad \mathcal{D}_1\Sigma_4 - F_{23} = 0, \tag{4.15}$$

$$\mathcal{D}_3\Sigma_4 - F_{12} - \frac{g^2}{2}(c\mathbf{1}_{N_{\mathrm{C}}} - HH^\dagger) = 0, \tag{4.16}$$

$$\mathcal{D}_1H + \mathrm{i}\mathcal{D}_2H = 0, \qquad \mathcal{D}_3H + \Sigma_4H - HM_4 = 0, \tag{4.17}$$

where the mass parameter M_p is obtained by (SS) twisting the phase in compactifying along the x^p direction. These equations describe composite states of monopoles with co-dimensions in x^1–x^2–x^3, vortices with co-dimensions in the x^1–x^2 plane and walls perpendicular to the x^3 direction. These equations were originally found in [103] without walls and later in [11] with walls. The Bogomol'nyi energy bound of this system is also obtained by the SS reduction of equation (4.5) as

$$E_{\mathrm{MVW}} = \mathcal{M}_{123} + \mathcal{V}_{12} v_3 + \mathcal{W}_{3,4} v_{12}, \tag{4.18}$$

where we have defined

$$\mathcal{M}_{123} \equiv \frac{2}{g^2} \int \mathrm{d}^3 x\, \mathrm{Tr}[\epsilon_{mnk} \partial_k (F_{mn} \Sigma_4)], \tag{4.19}$$

$$\mathcal{W}_{3,4} \equiv c \int \partial_3 (\mathrm{Tr}\, \Sigma_4). \tag{4.20}$$

$\mathcal{M}_{123}$ denotes the mass of the monopoles and $\mathcal{W}_{3,4}$ denotes the mass of walls perpendicular to the x^3 direction with the mass matrix M_4 to specify the tension. $\mathcal{V}_{12}$ is defined in equation (4.7). Here a check over the suffix in $\mathcal{I}_{123\check{4}}$ denotes to omit that reduced direction, and $v_3 = \int \mathrm{d}x^3$ is the x^3 world volume of vortices.

Since equation (4.15) provides the integrability conditions, equations (4.17) are solved by

$$\bar{W}_z = -\mathrm{i} S^{-1} \bar{\partial}_z S, \qquad W_3 - \mathrm{i}\Sigma_4 = -\mathrm{i} S^{-1} \partial_3 S, \qquad H = S^{-1} H_0(z)\, \mathrm{e}^{M_4 x^3}, \tag{4.21}$$

with $S(z, \bar{z}, x^3) \in GL(N_{\mathrm{C}}, \mathbf{C})$ and $H_0(z)$ is the moduli matrix for the monopole–vortex–wall system, which is holomorphic with respect to only z, after the $\mathrm{e}^{M_4 x^3}$ factor is extracted. The V-equivalence relation $\sim$ for this system becomes

$$H_0 \sim H_0' = V(z) H_0, \qquad S \sim S' = V(z) S, \tag{4.22}$$

where $V(z) \in GL(N_{\mathrm{C}}, \mathbf{C})$ has components holomorphic with respect to only z. The total moduli space of this system is the quotient by this V-equivalence relation $\sim$

$$\mathcal{M}_{\mathrm{MVW}}^{\mathrm{total}} \equiv \{H_0 | \mathbf{C} \to M(N_{\mathrm{C}} \times N_{\mathrm{F}}, \mathbf{C}),\, \bar{\partial}_z H_0 = 0\} / \sim . \tag{4.23}$$

In terms of a gauge invariant matrix

$$\Omega(z, \bar{z}, x^3) \equiv S S^\dagger, \tag{4.24}$$

equation (4.16) can be converted to the master equation of this system [11]

$$4\partial_z(\Omega^{-1} \bar{\partial}_z \Omega) + \partial_3(\Omega^{-1} \partial_3 \Omega) = c g^2 (\mathbf{1}_{N_{\mathrm{C}}} - \Omega^{-1} \Omega_0), \qquad c\Omega_0 \equiv H_0\, \mathrm{e}^{2 M_4 x^3} H_0^\dagger. \tag{4.25}$$

4.1.3. Wall webs. A further SS reduction in equations (4.15)–(4.17) along the x^2(or x^1) direction gives another set of 1/4 BPS equations [8, 9]

$$F_{13} - \mathrm{i}[\Sigma_2, \Sigma_4] = 0, \qquad \mathcal{D}_1 \Sigma_4 - \mathcal{D}_3 \Sigma_2 = 0, \tag{4.26}$$

$$\mathcal{D}_1 \Sigma_2 + \mathcal{D}_3 \Sigma_4 = Y_3, \tag{4.27}$$

$$\mathcal{D}_1 H + \Sigma_2 H - H M_2 = 0, \qquad \mathcal{D}_3 H + \Sigma_4 H - H M_4 = 0. \tag{4.28}$$

Note that we do not perform the SS reduction along the x^3 direction. These equations describe composite states of Hitchin vortices with co-dimensions in the x^1–x^3 plane and webs of walls as straight lines in the x^1–x^3 plane. The Bogomol'nyi energy bound of this system is given by

$$T_{\mathrm{HWW}} = \mathcal{H}_{13} + \mathcal{W}_{1,2} v_3 + \mathcal{W}_{3,4} v_1 \tag{4.29}$$

where we have defined

$$\mathcal{H}_{12} \equiv \frac{8}{g^2} \int \mathrm{d}^2x \, \mathrm{Tr}[\partial_{[1}((\mathcal{D}_{3]}\Sigma_4)\Sigma_2)]. \tag{4.30}$$

This is the mass of solitons in the Hitchin system. It is also called Y-charge in the literature, especially in the context of the Abelian gauge theory.

Since equation (4.26) provides the integrability conditions, equations (4.28) are solved by

$$W_1 - \mathrm{i}\Sigma_2 = -\mathrm{i}S^{-1}\partial_1 S, \qquad W_3 - \mathrm{i}\Sigma_4 = -\mathrm{i}S^{-1}\partial_3 S, \qquad H = S^{-1}H_0\,\mathrm{e}^{M_2x^1+M_4x^3}, \tag{4.31}$$

where $S(x^1, x^3) \in GL(N_\mathrm{C}, \mathbf{C})$ and the mere constant complex matrix H_0 is the moduli matrix for the Hitchin-wall–wall system. Because of the V-equivalence relation

$$H_0 \sim H_0' = VH_0, \qquad S \sim S' = VS, \qquad V \in GL(N_\mathrm{C}, \mathbf{C}), \tag{4.32}$$

the total moduli space of this system is the complex Grassmann manifold

$$\mathcal{M}^{\mathrm{total}}_{\mathrm{HWW}} \equiv \{H_0 | H_0 \sim VH_0, \, V \in GL(N_\mathrm{C}, \mathbf{C})\} \simeq G_{N_\mathrm{F}, N_\mathrm{C}}. \tag{4.33}$$

This total moduli space is isomorphic to that of the 1/2 BPS walls. In terms of a gauge invariant matrix

$$\Omega(x^1, x^3) \equiv SS^\dagger, \tag{4.34}$$

equation (4.27) can be recast into the master equation [8, 9]

$$\partial_1(\Omega^{-1}\partial_1\Omega) + \partial_3(\Omega^{-1}\partial_3\Omega) = cg^2(\mathbf{1}_{N_\mathrm{C}} - \Omega^{-1}\Omega_0), \qquad c\Omega_0 \equiv H_0\,\mathrm{e}^{2M_2x^1+2M_4x^3}H_0^\dagger. \tag{4.35}$$

4.1.4. Summary. In the strong gauge coupling limit in theories with $N_\mathrm{F} > N_\mathrm{C}$, the master equations (4.12), (4.25) and (4.35) can be solved algebraically as

$$\Omega_{g^2\to\infty} = \Omega_0. \tag{4.36}$$

We thus obtain exact solutions in all the systems. In this limit the total moduli spaces of 1/4 BPS systems are reduced, as in equation (3.112), to

$$\begin{aligned}
&\mathcal{M}^{\mathrm{total}}_{\mathrm{IVV}}\big|_{g^2\to\infty} \simeq \{H_0|\mathbf{C}^2 \to G_{N_\mathrm{F},N_\mathrm{C}}, \, \bar\partial_z H_0 = \bar\partial_w H_0 = 0\}, \\
&\mathcal{M}^{\mathrm{total}}_{\mathrm{MVW}}\big|_{g^2\to\infty} \simeq \{H_0|\mathbf{C} \to G_{N_\mathrm{F},N_\mathrm{C}}, \, \bar\partial_z H_0 = 0\}, \\
&\mathcal{M}^{\mathrm{total}}_{\mathrm{HVV}}\big|_{g^2\to\infty} \simeq G_{N_\mathrm{F},N_\mathrm{C}}.
\end{aligned} \tag{4.37}$$

The third one is isomorphic to the corresponding one at finite gauge coupling, while the first two develop small lump singularities as the case of semi-local vortices in section 3.2.4. These small lump singularities are resolved in $\mathcal{M}^{\mathrm{total}}_{\mathrm{MVW}}$ at finite gauge coupling by ANO vortices, but it is not the case in $\mathcal{M}^{\mathrm{total}}_{\mathrm{IVV}}$ which still contains small instanton singularities.

We have seen that 1/4 BPS systems and their BPS equations and charges are related by the SS dimensional reduction. Accordingly we obtain the relations among moduli matrices $H_0^{\mathrm{IVV}}(z, w)$ of the instanton–vortex–vortex system, $H_0^{\mathrm{MVW}}(z)$ of the monopole–vortex–wall system, and H_0^{HWW} of the Hitchin-wall–wall system. The construction methods (4.10), (4.21) and (4.31) in addition to the SS reductions reveal the following relations among moduli matrices:

$$H_0^{\mathrm{IVV}}(z, w)\big|_{\mathrm{MVW}} = H_0^{\mathrm{MVW}}(z)\,\mathrm{e}^{M_4 w}, \qquad H_0^{\mathrm{MVW}}(z)\big|_{\mathrm{HWW}} = H_0^{\mathrm{HWW}}\,\mathrm{e}^{M_2 z}. \tag{4.38}$$

Namely, a particular dependence of the instanton–vortex–vortex moduli matrix $H_0^{\mathrm{IVV}}(z, w)$ on w provides the monopole–vortex–wall moduli matrix H_0^{MVW}, and a similar particular dependence of the monopole–vortex–wall moduli matrix $H_0^{\mathrm{MVW}}(z)$ on z gives the Hitchin

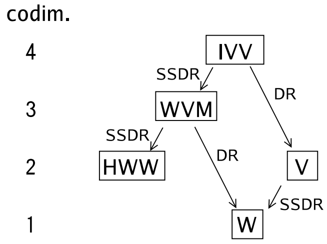

Figure 10. 'SSDR' and 'DR' denote the Scherk–Schwarz and ordinary dimensional reductions, respectively. Systems and their equations and charges are related by the SS and/or ordinary dimensional reductions.

vortex–wall–wall moduli matrix H_0^{HWW}. Also 1/2 BPS systems of vortices and domain walls can be obtained by ordinary dimensional reduction with respect to $z, \bar{z}$ (or $w, \bar{w}$) from the instanton–vortex system and the monopole–vortex–wall system, respectively. In this case, the moduli matrices are obtained by just throwing away the dependence to z or w:

$$H_0^{\mathrm{IVV}}(z, w)\big|_{\mathrm{V}} = H_0^{\mathrm{V}}(z), \qquad H_0^{\mathrm{MVW}}(z)\big|_{\mathrm{W}} = H_0^{\mathrm{W}}. \tag{4.39}$$

We summarize the relations with all 1/2 and 1/4 BPS systems in figure 10. One can easily recognizes that understanding the moduli matrix $H_0^{\mathrm{IVV}}(z, w)$ of the instanton–vortex–vortex system contains understanding all the systems.

4.2. Wall junctions

We will investigate the 1/4 BPS state of the domain walls and their junctions which are solutions of the 1/4 BPS equations (4.26)–(4.28). To simplify notation in this section, we choose the x^3 and x^4 directions in performing the SS reduction, that is, we exchange the x^3 direction with the x^2 direction in section 4.1.3. We work in the supersymmetric $U(N_{\mathrm{C}})$ gauge theory with N_{F} ($>N_{\mathrm{C}}$) hypermultiplets in this section. We turn on fully non-degenerate complex masses $M = M_3 + \mathrm{i}M_4\, \mathrm{diag}\big(m_1 + \mathrm{i}n_1, \ldots, m_{N_{\mathrm{F}}} + \mathrm{i}n_{N_{\mathrm{F}}}\big)$ for the hypermultiplets, and the FI parameter c (>0) in the third direction of the $SU(2)_R$ triplet. Most of the arguments here will follow along the lines of the 1/2 BPS domain walls in section 3.1. For instance, the total moduli space of webs of walls turns out to be identical to the total moduli space of walls: $G_{N_{\mathrm{F}},N_{\mathrm{C}}} = SU(N_{\mathrm{F}})/[SU(N_{\mathrm{C}}) \times SU(N_{\mathrm{F}} - N_{\mathrm{C}}) \times U(1)]$. However, we will find that decomposition of the total moduli space into various topological sectors exhibits interesting differences.

4.2.1. Webs of walls in the Abelian gauge theory. Let us first explain the webs of walls in the Abelian gauge theory ($N_{\mathrm{C}} = 1$) here leaving the non-Abelian gauge theory in the next subsection. As explained in section 2, there exist N_{F} discrete vacua which are labelled by an integer $\langle A \rangle$ with $A \in \{1, 2, \ldots, N_{\mathrm{F}}\}$. In section 3.1, we have found solutions of the 1/2 BPS equation (3.2) that interpolate between these discrete vacua and form stable 1/2 BPS domain walls. Recall that all the domain walls contained in the 1/2 BPS solutions are parallel and are associated with the relatively real masses for the hypermultiplet scalars. Suppose that a mass difference between non-vanishing hypermultiplet scalars in two vacua becomes complex. Even in such a situation, a 1/2 BPS wall can be formed interpolating between these two vacua. The tension of the domain wall is determined by the magnitude of the mass difference. However, the normal vector of the wall is no longer along the real axis, and the wall preserves a different half of supercharges. In the case of complex masses, we can obtain walls whose normal vectors are in different directions in a two-dimensional plane. Such a configuration preserves a quarter of supercharges. Consequently, domain walls can develop webs of domain walls as $1/4$ BPS states. Therefore the $1/2$ BPS equations (3.2) are naturally extended to the $1/4$ BPS equations (4.26)–(4.28), once we turn on the complex masses.

Solutions of the $1/4$ BPS equations (4.26)–(4.28) are given in terms of the moduli matrix H_0 which is a complex $1 \times N_{\rm F}$ matrix given in equation (4.31) in the case of the Abelian gauge theory. The configurations of the webs of walls are made from three building blocks; the vacua, the domain walls and the junctions. Let us first explain how to understand these building blocks via the moduli matrix H_0. The moduli matrix is represented as

$$H_0 = (\tau^{\langle 1\rangle}, \tau^{\langle 2\rangle}, \ldots, \tau^{\langle N_{\rm F}\rangle}), \tag{4.40}$$

with $\tau^{\langle A\rangle} \in \mathbf{C}$. This can be regarded as the homogeneous coordinate of the total moduli space $\mathbf{C}P^{N_{\rm F}-1}$ given in equation (4.33) by taking the V-equivalence relation (4.32) into account. Similarly to equation (3.20) for domain walls, we can define a weight $\exp(\mathcal{W}^{\langle A\rangle})$ of a vacuum $\langle A\rangle$ with a linear function $\mathcal{W}^{\langle A\rangle}(x^1, x^2)$ as

$$\exp(2\mathcal{W}^{\langle A\rangle}(x^1, x^2)) \equiv \exp 2(m_A x^1 + n_A x^2 + a^{\langle A\rangle}), \tag{4.41}$$

$$a^{\langle A\rangle} \equiv \mathrm{Re}(\log \tau^{\langle A\rangle}). \tag{4.42}$$

As in the case of the parallel walls given in equation (3.22), the energy density of the webs of walls can, then, be nicely estimated in terms of the weights of vacua in equation (4.41) as

$$\begin{aligned}\mathcal{E} &\simeq \frac{c}{2}\left(\partial_1^2 + \partial_2^2\right) \log\left(H_0\, \mathrm{e}^{M_1 x^1 + M_2 x^2} H_0^\dagger\right)\\ &= \frac{c}{2}\left(\partial_1^2 + \partial_2^2\right) \log\left[\sum_{\langle A\rangle} \mathrm{e}^{2\mathcal{W}^{\langle A\rangle}(x^1,x^2)}\right].\end{aligned} \tag{4.43}$$

This approximation gives sufficiently accurate profiles away from the cores, although this is not good near the core of the domain walls. Furthermore this expression becomes exact at the strong gauge coupling limit. The function $\log\left[\sum_{\langle A\rangle} \mathrm{e}^{2\mathcal{W}^{\langle A\rangle}}\right]$ to be differentiated in equation (4.43) is an almost piecewise linear function which is well approximated by smoothly connecting linear functions $2\mathcal{W}^{\langle A\rangle}(x^1, x^2)$. Therefore, the energy density (4.43) vanishes in almost all region except near the transition points between $2\mathcal{W}^{\langle A\rangle}$ and $2\mathcal{W}^{\langle B\rangle}$. The regions where the energy density vanishes are nothing but the SUSY vacua and the transition lines which now spread on the x^1–x^2 plane correspond to the domain walls dividing such vacuum domains.

We are now ready to understand the three building blocks via the moduli matrix H_0. Let us first note that the $1/4$ BPS equations (4.26)–(4.28) admit solutions of $1/2$ BPS equations. Then both the SUSY vacua and the single domain walls arise as solutions of the $1/4$ BPS equations in terms of the moduli matrices with the same characteristic properties as in the case of the $1/2$ BPS equation (3.2). Recall that the vacuum state $\langle A\rangle$ corresponds to the moduli matrix like equation (3.24)

$$H_0 = (\ldots, \tau^{\langle A\rangle}, \ldots) \sim (0, \ldots, 0, 1, 0, \ldots, 0), \tag{4.44}$$

and the $1/2$ BPS domain wall interpolating two vacua $\langle A\rangle$ and $\langle B\rangle$ corresponds to the moduli matrix

$$H_0 = (0, \ldots, 0, \tau^{\langle A\rangle}, 0, \ldots, 0, \tau^{\langle B\rangle}, 0, \ldots, 0), \tag{4.45}$$

where there are only two non-vanishing weights of the vacua $\exp(\mathcal{W}^{\langle A\rangle})$ and $\exp(\mathcal{W}^{\langle B\rangle})$ defined in equation (4.41). Similarly to the $1/2$ BPS case in equation (3.27) for the domain wall positions, the position of the domain wall can be estimated as the transition line on which the two weights become equal $\mathcal{W}^{\langle A\rangle} = \mathcal{W}^{\langle B\rangle}$:

$$(m_A - m_B)x^1 + (n_A - n_B)x^2 + a^{\langle A\rangle} - a^{\langle B\rangle} = 0. \tag{4.46}$$

When we turn off the imaginary part of the masses, this reduces to equation (3.27) of the 1/2 BPS single wall. The complex masses of the hypermultiplets determine the angle of the domain wall in the x^1–x^2 plane and its position is given by difference of the parameters $a^{\langle A\rangle} - a^{\langle B\rangle}$. Note that it was important to keep track of the ordering of the real masses in the case of parallel walls in section 3.1. Due to the ordering of the real masses, the single walls are classified into two types: elementary and non-elementary. However, the ordering is now meaningless in the space of the complex masses. Consequently, all the single walls become elementary walls in the case of the fully non-degenerate complex masses. The following tension vector is parallel to the domain wall and its magnitude gives the tension (per unit length) of the domain wall[9]

$$\vec{T}^{\langle A\rangle\langle B\rangle} = c(n_B - n_A, m_A - m_B). \tag{4.47}$$

Note that the first component of the tension is related to the central charge Z_1 and Z_2 given in equation (4.29).

The difference between the 1/2 BPS solution (4.31) and the 1/4 BPS solutions (4.31) first occurs when we consider the moduli matrix with three nonzero elements

$$H_0 = (0, \dots, 0, \tau^{\langle A\rangle}, 0, \dots, 0, \tau^{\langle B\rangle}, 0, \dots, 0, \tau^{\langle C\rangle}, 0, \dots, 0). \tag{4.48}$$

As already mentioned in section 3.1, this moduli matrix with the real masses describes the two parallel walls which divides three vacuum domains $\langle A\rangle$, $\langle B\rangle$ and $\langle C\rangle$. However, equation (4.46) shows that the complex masses change the angle of the walls. Therefore, the three walls $\langle A\rangle\langle B\rangle$, $\langle B\rangle\langle C\rangle$ and $\langle C\rangle\langle A\rangle$ should meet at a point to form a 3-pronged junction. Positions of component walls of the 3-pronged junction can be identified by the equal weight condition of two vacua as given in equation (4.46). Furthermore, the position of the domain wall junction is identified as a point where all the three weights become equal

$$\mathcal{W}^{\langle A\rangle}(x^1, x^2) = \mathcal{W}^{\langle B\rangle}(x^1, x^2) = \mathcal{W}^{\langle C\rangle}(x^1, x^2). \tag{4.49}$$

One can easily show that the tension vectors of the domain walls given in equation (4.47) are balanced each other, so that the junction is stable:

$$\vec{T}^{\langle A\rangle\langle B\rangle} + \vec{T}^{\langle B\rangle\langle C\rangle} + \vec{T}^{\langle C\rangle\langle A\rangle} = \vec{0}. \tag{4.50}$$

This condition of the balance of forces is assured by the fact that the central charges (Z_1, Z_2) of three constituent walls meeting at the junction sum up to zero. Besides the central charges (Z_1, Z_2) associated with the constituent walls, the junction has another characteristic central charge Y in equation (4.29). The Y-charge can be exactly calculated as

$$Y_{\text{Abelian}} = -\frac{2}{g^2}|(\vec{\mu}_A - \vec{\mu}_C) \times (\vec{\mu}_B - \vec{\mu}_C)|, \tag{4.51}$$

where the cross means the exterior product of 2-vector $\mu_A = (m_A, n_A)$ giving a scalar. Note that the Y-charge of the junction in the Abelian gauge theory always gives negative contribution to the total energy, which is understood as the binding energy of the domain walls meeting at the junction point.

The set of variables $\{\tau^{\langle A\rangle}, \tau^{\langle B\rangle}, \tau^{\langle C\rangle}\}$ in equation (4.48) describes the moduli space of three pronged junctions. It is just a homogeneous coordinate of $\mathbf{C}P^2$ submanifold of the total moduli space $\mathbf{C}P^{N_\text{F}-1}$. Let us illustrate how this $\mathbf{C}P^2$ manifold is decomposed into several

[9] Here the sign of the tension vector is merely a convention.

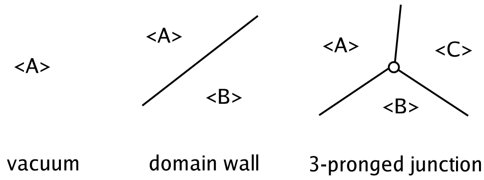

Figure 11. Building blocks of the webs of walls in the Abelian gauge theory.

topological sectors. To obtain the moduli space of a genuine 3-pronged junction, we have to remove the following subspaces: $\tau^{\langle A\rangle} = 0$, $\tau^{\langle B\rangle} = 0$ and $\tau^{\langle C\rangle} = 0$ from $\mathbf{C}P^2$, because such subspaces result from different boundary conditions due to the limits where one or two of three domain walls are taken to spatial infinity. Namely, $\mathbf{C}P^2$ has three $\mathbf{C}P^1$ submanifolds parametrized by $\mathbf{C}P^1_{\langle \not{C}\rangle} = \{\tau^{\langle A\rangle}, \tau^{\langle B\rangle}, 0\}$, $\mathbf{C}P^1_{\langle \not{A}\rangle} = \{0, \tau^{\langle B\rangle}, \tau^{\langle C\rangle}\}$ and $\mathbf{C}P^1_{\langle \not{B}\rangle} = \{\tau^{\langle A\rangle}, 0, \tau^{\langle C\rangle}\}$, respectively. Moreover, these submanifolds share the three points $\{1, 0, 0\}$, $\{0, 1, 0\}$ and $\{0, 0, 1\}$ corresponding to three vacua. Then the moduli space of the genuine 3-pronged junction is the open space which is given by subtracting three $\mathbf{C}P^1$ subspaces from $\mathbf{C}P^2$ as

$$\mathcal{M}^{\text{junction}} = \mathbf{C}P^2 - \bigcup_{A=1}^{3} \mathbf{C}P^1_{\langle \not{A}\rangle}. \tag{4.52}$$

Each $\mathbf{C}P^1$ subspace consists of two points corresponding to the vacuum states and an open space $\mathbf{C}^* \simeq \mathbf{R} \times S^1 \simeq \mathbf{C}P^1 - 2 \times \mathbf{C}P^0$ corresponding to the moduli space of the single domain wall, as was mentioned above. These are summarized in the following flow diagram in which the arrow $\rightarrow$ means $\tau^{\langle A\rangle} \rightarrow 0$, the arrow $\nearrow$ means $\tau^{\langle C\rangle} \rightarrow 0$ and the arrow $\searrow$ means $\tau^{\langle B\rangle} \rightarrow 0$.

3-Pronged junction		Single wall		Vacuum
		$\{\tau^{\langle A\rangle}, \tau^{\langle B\rangle}, 0\}$	$\rightarrow$	$\{0, 1, 0\}$
	$\nearrow$		$\nearrow\!\!\!\!\searrow$	
$\{\tau^{\langle A\rangle}, \tau^{\langle B\rangle}, \tau^{\langle C\rangle}\}$	$\rightarrow$	$\{0, \tau^{\langle B\rangle}, \tau^{\langle C\rangle}\}$		$\{1, 0, 0\}$
	$\searrow$		$\nearrow\!\!\!\!\searrow$	
		$\{\tau^{\langle A\rangle}, 0, \tau^{\langle C\rangle}\}$	$\rightarrow$	$\{0, 0, 1\}$
$\mathbf{C}P^2$		$\mathbf{C}P^1$		$\mathbf{CP}^0$

So far, we examined the three building blocks of the webs of walls: the vacua, the domain walls and the 3-pronged junctions, as shown in figure 11. The webs of walls are constructed by putting these building blocks together. In general, the Abelian gauge theory with N_{F} flavours admits webs of domain walls which divide N_{F} domains of vacua. The moduli matrix for the general configuration can be parametrized by the homogeneous coordinate of the total moduli space $\mathbf{C}P^{N_{\mathrm{F}}-1}$ as given in equation (4.40)

$$\{\tau^{\langle 1\rangle}, \tau^{\langle 2\rangle}, \ldots, \tau^{\langle N_{\mathrm{F}}\rangle}\}. \tag{4.53}$$

The area of each vacuum domain is proportional to the weight of that vacuum in equation (4.41). The boundary between two adjacent vacuum domains becomes a domain wall whose position is determined by equating the weights of the two vacua as in equation (4.46). Furthermore, a junction is formed at the point where the vacuum weights for three vacua become equal as in equation (4.49). When we let one of the vacuum weights, for instance $\exp 2\mathcal{W}^{\langle A\rangle}(x^1, x^2)$, to vanish (by taking the limit where $\tau^{\langle A\rangle} \rightarrow 0$), the corresponding vacuum domain $\langle A\rangle$ disappears

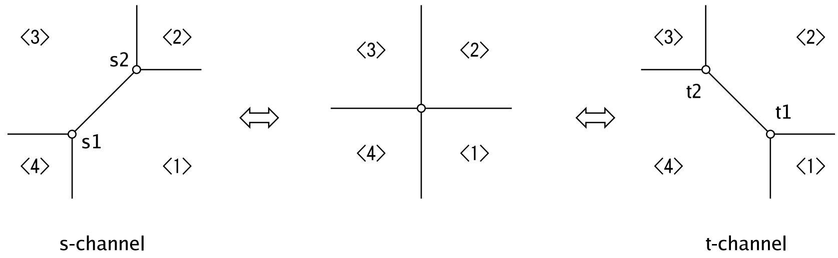

Figure 12. The s-channel and the t-channel of webs of walls. The s-channel appears when $a^{\langle 1\rangle} + a^{\langle 3\rangle} > a^{\langle 2\rangle} + a^{\langle 4\rangle}$ while the t-channel appears when $a^{\langle 1\rangle} + a^{\langle 3\rangle} < a^{\langle 2\rangle} + a^{\langle 4\rangle}$.

in the web configuration. As a result, we have a smaller web configuration which divides $N_{\mathrm{F}} - 1$ vacua and is described by the moduli matrix for $\mathbf{C}P^{N_{\mathrm{F}}-2}$:

$$\{\tau^{\langle 1\rangle}, \ldots, \tau^{\langle A-1\rangle}, 0, \tau^{\langle A+1\rangle}, \ldots, \tau^{\langle N_{\mathrm{F}}\rangle}\}. \tag{4.54}$$

Since there are N_{F} submanifolds $\mathbf{C}P^{N_{\mathrm{F}}-2}$ in the total moduli space $\mathbf{C}P^{N_{\mathrm{F}}-1}$, the moduli space of the maximal webs of walls is given by

$$\mathcal{M}^{\max} = \mathbf{C}P^{N_{\mathrm{F}}-1} - \bigcup_{A=1}^{N_{\mathrm{F}}} \mathbf{C}P^{N_{\mathrm{F}}-2}_{\langle \not{A}\rangle} \tag{4.55}$$

where $\mathbf{C}P^{N_{\mathrm{F}}-2}_{\langle \not{A}\rangle}$ is a submanifold parametrized by the homogeneous coordinate (4.54).

Let us give an example of webs of walls in $N_{\mathrm{F}} = 4$ model with masses $(m_A, n_A) = \{(1,0), (1,1), (0,1), (0,0)\}$. Then we have four linear functions $\mathcal{W}^{\langle 1\rangle} = x^1 + a^{\langle 1\rangle}$, $\mathcal{W}^{\langle 2\rangle} = x^1 + x^2 + a^{\langle 2\rangle}$, $\mathcal{W}^{\langle 3\rangle} = x^2 + a^{\langle 3\rangle}$ and $\mathcal{W}^{\langle 4\rangle} = a^{\langle 4\rangle}$. The shape of the web varies as we change the moduli parameters $a^{\langle A\rangle}$ $(A = 1, 2, 3, 4)$. The configuration has two branches which we called s-channel and t-channel in [8]. The s-channel has an internal wall dividing the vacua $\langle 1\rangle$ and $\langle 3\rangle$ while the t-channel has the other internal wall which divides the vacua $\langle 2\rangle$ and $\langle 4\rangle$, as shown in figure 12. The s-channel has two junctions, denoted as s1 and s2. The s1 separates three vacua $\langle 1\rangle$, $\langle 3\rangle$ and $\langle 4\rangle$ at $(x^1, x^2) = (a^{\langle 4\rangle} - a^{\langle 1\rangle}, a^{\langle 4\rangle} - a^{\langle 3\rangle})$. The s2 separates three vacua $\langle 1\rangle$, $\langle 2\rangle$ and $\langle 3\rangle$ at $(x^1, x^2) = (a^{\langle 3\rangle} - a^{\langle 2\rangle}, a^{\langle 1\rangle} - a^{\langle 2\rangle})$. These junctions consistently appear in the parameter region where $a^{\langle 1\rangle} + a^{\langle 3\rangle} > a^{\langle 2\rangle} + a^{\langle 4\rangle}$. The two junctions s1 and s2 approach each other when we let $(a^{\langle 1\rangle} + a^{\langle 3\rangle}) - (a^{\langle 2\rangle} + a^{\langle 4\rangle}) \to 0$ as shown in the middle of figure 12. When $a^{\langle 2\rangle} + a^{\langle 4\rangle}$ grows over $a^{\langle 1\rangle} + a^{\langle 3\rangle}$, the configuration makes a transition from the s-channel to the t-channel which has another two junctions t1 and t2. The t1 separates three vacua $\langle 1\rangle$, $\langle 2\rangle$ and $\langle 4\rangle$ at $(x^1, x^2) = (a^{\langle 4\rangle} - a^{\langle 1\rangle}, a^{\langle 1\rangle} - a^{\langle 2\rangle})$. The t2 separates three vacua $\langle 2\rangle$, $\langle 3\rangle$ and $\langle 4\rangle$ at $(x^1, x^2) = (a^{\langle 3\rangle} - a^{\langle 2\rangle}, a^{\langle 4\rangle} - a^{\langle 3\rangle})$. Other examples of the webs of walls are shown in [8].

4.2.2. Webs of walls in the non-Abelian gauge theory. In this subsection, we will study the webs of domain walls in the non-Abelian gauge theory ($N_{\mathrm{C}} > 1$), which has ${}_{N_{\mathrm{F}}}C_{N_{\mathrm{C}}}$ discrete vacua labelled by a set of N_{C} different integers $\langle A_1 \cdots A_r \cdots A_{N_{\mathrm{C}}}\rangle$, as given in section 2.2. Similarly to the Abelian case, all the 1/4 BPS solutions are given by the moduli matrix H_0 which is, now, a complex $N_{\mathrm{C}} \times N_{\mathrm{F}}$ matrix given in equation (4.31). We have found the total moduli space parametrized by H_0 to be the complex Grassmaniann $G_{N_{\mathrm{F}},N_{\mathrm{C}}} \simeq \{H_0 \sim V H_0\}$ with $V \in GL(N_{\mathrm{C}}, \mathbf{C})$ in equation (4.32). In section 3.1 we have seen that it is also useful to introduce the Plücker coordinate instead of the moduli matrix H_0 itself:

$$\tau^{\langle \{A_r\}\rangle} \equiv \det H_0^{\langle \{A_r\}\rangle}. \tag{4.56}$$

Here $\langle A_1 \cdots A_r \cdots A_{N_C}\rangle$ is abbreviated as $\langle\{A_r\}\rangle$, and the minor matrix $H_0^{\langle\{A_r\}\rangle}$ is constructed by picking up the $\{A_r\}$th row from the moduli matrix H_0. Since the number of determinants $\tau^{\langle\{A_r\}\rangle}$ is ${}_{N_F}C_{N_C}$, which is the same as the number of SUSY vacua, we assemble the Plücker coordinate in a ${}_{N_F}C_{N_C}$ component vector:

$$\{\ldots, \tau^{\langle\{A_r\}\rangle}, \ldots, \tau^{\langle\{B_r\}\rangle}, \ldots\}. \tag{4.57}$$

Similarly to the weight of the vacuum (4.40) in the Abelian gauge theory, we can define the weight of the vacuum in the non-Abelian gauge theory by

$$\exp 2\mathcal{W}^{\langle\{A_r\}\rangle} \equiv \exp 2\left(\sum_{r=1}^{N_C}\left(m_{A_r}x^1 + n_{A_r}x^2\right) + a^{\langle\{A_r\}\rangle}\right), \tag{4.58}$$

$$a^{\langle\{A_r\}\rangle} + ib^{\langle\{A_r\}\rangle} \equiv \log \tau^{\langle\{A_r\}\rangle}, \tag{4.59}$$

which is a natural extension from equation (3.20) for the case of parallel walls. The energy density of the webs of walls can be estimated in terms of these weights of vacua as

$$\begin{aligned}\mathcal{E} &\simeq \frac{c}{2}\left(\partial_1^2 + \partial_2^2\right)\log\det\left(H_0\,\mathrm{e}^{M_1x^1+M_2x^2}H_0^\dagger\right)\\ &= \frac{c}{2}\left(\partial_1^2 + \partial_2^2\right)\log\sum_{\langle\{A_r\}\rangle}\mathrm{e}^{2\mathcal{W}^{\langle\{A_r\}\rangle}}.\end{aligned} \tag{4.60}$$

We can now find out the structure of the webs in the non-Abelian gauge theory similarly to the Abelian gauge theory. The webs are also made of the three building blocks: vacua, single domain walls and their junctions. Similarly to the Abelian case in equation (4.44), vacua are represented by a single non-vanishing component $\tau^{\langle\{A_r\}\rangle}$ in the Plücker coordinate (4.57): $\{0, \ldots, 0, \tau^{\langle\{A_r\}\rangle}, 0, \ldots, 0\} \sim \{0, \ldots, 0, 1, 0, \ldots, 0\}$. The domain walls are described by equation (4.45) in the Abelian gauge theory, whereas the domain walls in the non-Abelian gauge theory are represented by only two non-vanishing components in the Plücker coordinate. Namely, the domain wall interpolating the vacua $\langle\{A_r\}\rangle$ and $\langle\{B_r\}\rangle$ is given by $\{0, \ldots, 0, \tau^{\langle\{A_r\}\rangle}, 0, \ldots, 0, \tau^{\langle\{B_r\}\rangle}, 0, \ldots, 0\}$. However, not all the Plücker coordinates are independent as we have already seen in section 3.1. The Plücker coordinates are constrained by the Plücker relations (3.33) in order for them to describe the Grassmaniann. For instance, the Plücker relations does not allow moduli matrix with only two non-vanishing components $\tau^{\langle A_r\rangle}$ whose labels differ in only one element such as $\langle\underline{\cdots}A\rangle$ and $\langle\underline{\cdots}B\rangle$. It follows that no single domain wall exists interpolating two such vacua.

Locations of domain walls are estimated by comparing weights of the two adjacent vacua as in equation (4.46): $\mathcal{W}^{\langle\underline{\cdots}A\rangle} = \mathcal{W}^{\langle\underline{\cdots}B\rangle}$ gives the domain wall interpolating $\langle\underline{\cdots}A\rangle$ and $\langle\underline{\cdots}B\rangle$ to lie

$$(m_A - m_B)x^1 + (n_A - n_B)x^2 + a^{\langle\underline{\cdots}A\rangle} - a^{\langle\underline{\cdots}B\rangle} = 0. \tag{4.61}$$

The 3-pronged junctions of the domain walls in the non-Abelian gauge theory are described by the Plücker coordinate which has only three non-vanishing components:

$$\{0, \ldots, 0, \tau^{\langle\{A_r\}\rangle}, 0, \ldots, 0, \tau^{\langle\{B_r\}\rangle}, 0, \ldots, 0, \tau^{\langle\{C_r\}\rangle}0, \ldots, 0\}. \tag{4.62}$$

The position of the 3-pronged junction can be estimated by equating the three vacuum weights $\mathcal{W}^{\langle\{A_r\}\rangle} = \mathcal{W}^{\langle\{B_r\}\rangle} = \mathcal{W}^{\langle\{C_r\}\rangle}$ as equation (4.49). In the previous subsection, we have found that junctions in the Abelian gauge theory dividing vacua $\langle A\rangle$, $\langle B\rangle$ and $\langle C\rangle$ are always characterized by the negative contribution to the energy from the topological charge Y (4.51). On the other hand, there are two kinds of domain wall junctions in the non-Abelian gauge theory. Junctions of walls are specified by choosing three different vacua $\langle\{A_r\}\rangle$, $\langle\{B_r\}\rangle$ and $\langle\{C_r\}\rangle$. In the

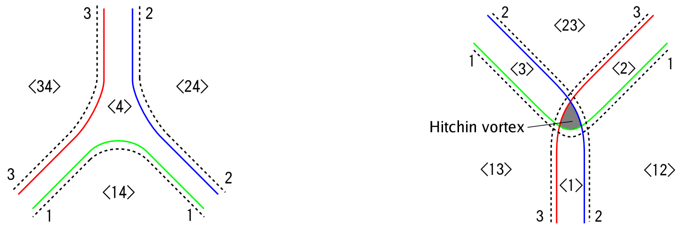

Figure 13. Internal structures of the junctions with $g\sqrt{c} \ll |\Delta m + \mathrm{i}\Delta n|$.

non-Abelian gauge theory, the Plücker relation (3.33) requires any pairs of those three vacua to have flavour labels which are different only in one colour component. Then there are two possibilities of choosing three different vacua. One possibility is the junction which separates three vacua with the same flavours except one colour component: $\langle \underline{\cdots} A\rangle$, $\langle \underline{\cdots} B\rangle$ and $\langle \underline{\cdots} C\rangle$. The other is that dividing a set of vacua with the same flavour labels except two colour component: $\langle \underline{\cdots} AB\rangle$, $\langle \underline{\cdots} BC\rangle$ and $\langle \underline{\cdots} CA\rangle$. The former (latter) is called the Abelian (non-Abelian) junction. The Abelian junction dividing the vacua $\langle \underline{\cdots} A\rangle$, $\langle \underline{\cdots} B\rangle$ and $\langle \underline{\cdots} C\rangle$ is essentially the same as the junction in the Abelian gauge theory dividing the vacua $\langle A\rangle$, $\langle B\rangle$ and $\langle C\rangle$. Actually the topological charge is the same as that given in equation (4.51), namely it is negative and should be interpreted as the binding energy of the domain walls. In contrast, the non-Abelian junction separating the three vacuum domains $\langle \underline{\cdots} AB\rangle$, $\langle \underline{\cdots} BC\rangle$ and $\langle \underline{\cdots} CA\rangle$ is essentially the same as the junction dividing three vacua $\langle AB\rangle$, $\langle BC\rangle$ and $\langle CA\rangle$ in the $U(2)$ gauge theory. Note that the non-Abelian junctions do not exist in the Abelian gauge theory. The remarkable property of the non-Abelian junction is that the topological Y-charge given in equation (4.29) always contribute positively to the energy density, so that it cannot be regarded as the binding energy, in contrast to the Abelian Y-charge

$$Y_{\text{non-Abelian}} = \frac{2}{g^2}|(\vec{\mu}_A - \vec{\mu}_C) \times (\vec{\mu}_B - \vec{\mu}_C)| > 0. \tag{4.63}$$

In order to understand the origin of negative and positive Y-charges, we find it useful to pay attention to the internal structures of the junction points of the domain walls. To this end, let us consider the model with $N_\mathrm{F} = 4$ and $N_\mathrm{C} = 2$ which has ${}_4C_2 = 6$ discrete vacua $\langle 12\rangle$, $\langle 23\rangle$, $\langle 13\rangle$, $\langle 14\rangle$, $\langle 24\rangle$ and $\langle 34\rangle$. The 1/4 BPS wall junction interpolating the three vacua $\langle 14\rangle$, $\langle 24\rangle$ and $\langle 34\rangle$ is the Abelian junction while that interpolating $\langle 12\rangle$, $\langle 23\rangle$ and $\langle 13\rangle$ is the non-Abelian junction. Internal structures of these junctions are schematically shown in figure 13. The left of figure 13 shows the Abelian junction and the right shows the non-Abelian junction. As explained in section 3.1, each component domain wall of the junction has three-layer structure in the weak gauge coupling region ($g\sqrt{c} \ll |\Delta m + \mathrm{i}\Delta n|$); see figure 1. The same $U(1)$ subgroup is recovered in all three middle layers of the Abelian junction, as denoted by $\langle 4\rangle$. They are connected at the junction point so that the middle layer of the wall junction is also in the same phase $\langle 4\rangle$ as can be seen in the left of figure 13. On the other hand, the non-Abelian junction has a complicated internal structure as shown in the right of figure 13. Although it also separates three different vacua $\langle 12\rangle$, $\langle 23\rangle$ and $\langle 13\rangle$, their middle layers preserve different $U(1)$ subgroups, $\langle 1\rangle$, $\langle 2\rangle$ and $\langle 3\rangle$ as in the right of figure 13. However, all the hypermultiplet scalars H vanish when all three middle layers overlap near the junction point, so that only the $U(2)$ vector multiplet scalar Σ is active there. The key observation is that the 1/4 BPS equations given in equations (4.26)–(4.28) reduce to the 1/2 BPS Hitchin equations

$$F_{12} = \mathrm{i}[\Sigma_3, \Sigma_4], \qquad \mathcal{D}_1\Sigma_4 - \mathcal{D}_2\Sigma_3 = 0, \qquad \mathcal{D}_1\Sigma_3 + \mathcal{D}_2\Sigma_4 = 0, \tag{4.64}$$

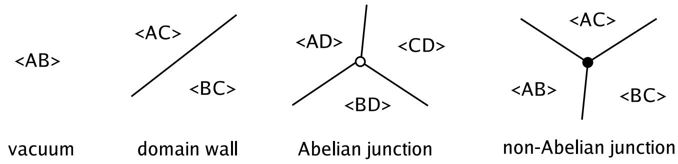

Figure 14. Building blocks of the webs of walls in the non-Abelian gauge theory.

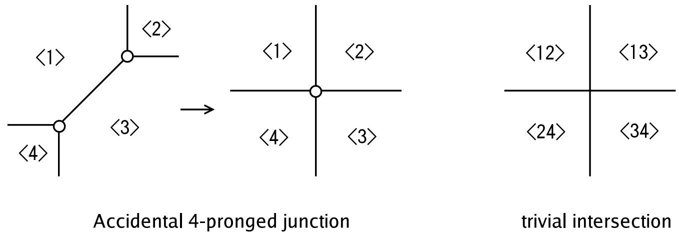

Figure 15. Accidental 4-pronged junction and a trivial intersection of walls.

if we pick up the traceless part of equations (4.26)–(4.28) and discard the hypermultiplet scalars H. This reduction occurs at the core of the non-Abelian junction, since hypermultiplet scalars vanish as we mentioned above. Therefore the system reduces to the Hitchin system of $SU(2)$ subgroup in the middle of the non-Abelian junction. Furthermore, the charge of the non-Abelian junction given in equation (4.29) completely agrees with the charge of the Hitchin system [15]. Thus we conclude that the positive Y-charges of the non-Abelian junctions given in equation (4.63) are the charges of the Hitchin system.

Now, we have found four kinds of building blocks for the webs of walls in the non-Abelian gauge theory. We have the SUSY vacua, the domain walls interpolating these discrete vacua and the Abelian and the non-Abelian junctions. These are shown in figure 14. There is one more fundamental object in the non-Abelian gauge theory. It is the trivial intersection, namely the 4-pronged junction without a junction charge, of the domain walls. Such a 4-pronged junction accidentally, of course, appears in the Abelian gauge theory as a special configuration in which two different 3-pronged junctions get together. However, these are decomposed to two 3-pronged junctions by varying moduli parameters, so we should not regard it as the building block of the webs in the Abelian gauge theory. We have already met an example in figure 12. There the s-channel and t-channel are interchanged when the moduli parameters accidentally satisfy $a^{\langle 1\rangle}+a^{\langle 3\rangle} = a^{\langle 2\rangle}+a^{\langle 4\rangle}$. On the other hand, the configuration dividing a set of four vacua, for instance $\langle 12\rangle$, $\langle 34\rangle$, $\langle 13\rangle$ and $\langle 24\rangle$, has to obey the Plücker relation (3.33). The Plücker relation restricts the moduli parameters under the condition $a^{\langle 12\rangle}+a^{\langle 34\rangle} = a^{\langle 13\rangle}+a^{\langle 24\rangle}$. So all the domain walls of the configuration certainly get together at a point, as shown in the right of figure 15. One can easily show that the Y-charge in equation (4.29) around this 4-pronged junction always vanishes, so this is the trivial intersection of the two domain walls without any kinds of additional junction charge apart from the wall tension.

4.2.3. Rules of construction. Now we are ready to construct the webs of walls both in the Abelian and the non-Abelian gauge theories. As is clear from equations (4.46) and (4.61), slopes of walls are determined by the mass parameters (m_A, n_A) for the hypermultiplet scalars. In general great pains are needed to clarify shapes of the webs corresponding to every points on the moduli space $G_{N_\mathrm{F},N_\mathrm{C}}$ as the number of flavours N_F increases. A nice tool to overcome

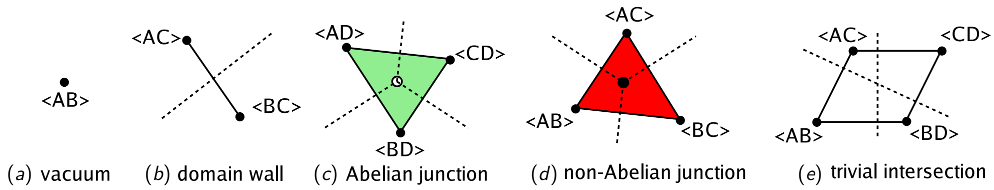

Figure 16. Building blocks of the grid diagrams.

this complication is provided by the grid diagram [8, 9], where informations are discarded about actual positions of each walls and their junctions. Namely, we try to capture the webs in the complex $\mathrm{Tr}\,\Sigma = \mathrm{Tr}(\Sigma_3 + \mathrm{i}\Sigma_4)$ plane, instead of considering them in the real space. Let us start with the SUSY vacua. The VEV of the adjoint scalar in the $\langle\{A_r\}\rangle$ vacuum is given by $\Sigma = \mathrm{diag}\big(m_{A_1} + \mathrm{i}n_{A_1}, m_{A_2} + \mathrm{i}n_{A_2}, \ldots, m_{A_{N_C}} + \mathrm{i}n_{A_{N_C}}\big)$. Hence the vacuum $\langle\{A_r\}\rangle$ is located at the point $\sum_{r=1}^{N_C}(m_{A_r} + \mathrm{i}n_{A_r})$ in the $\mathrm{Tr}\,\Sigma$ plane, as shown in figure 16(*a*). Next, domain walls can be regarded as segments between possible pairs of these points (labelled by $\langle\underline{\cdots}A\rangle$ and $\langle\underline{\cdots}B\rangle$) in the $\mathrm{Tr}\,\Sigma$ plane. A nice feature of this representation of walls is that the magnitude of the tension given in equation (4.47) is proportional to the length of the segment. Moreover, the dual line which is the vector normal to the segment is parallel to the corresponding domain wall in the real space and to the tension vector for the wall in equation (4.47). In figure 16(*b*) we denote a solid line for a segment connecting two vacua, and denote a broken line for its dual line parallel to the domain wall in the real space. The Abelian 3-pronged junctions of domain walls are realized as triangles whose vertices are labelled by $\langle\underline{\cdots}A\rangle$, $\langle\underline{\cdots}B\rangle$ and $\langle\underline{\cdots}C\rangle$ in the $\mathrm{Tr}\,\Sigma$ plane as shown in figure 16(*c*). The non-Abelian 3-pronged junctions are similarly realized as triangles whose vertices are labelled by $\langle\underline{\cdots}AB\rangle$, $\langle\underline{\cdots}BC\rangle$ and $\langle\underline{\cdots}CA\rangle$ as shown in figure 16(*d*). Their topological Y-charges given in equations (4.51) and (4.63) are proportional to areas of the triangles. Furthermore, the equilibrium condition of the tension vectors of the three components walls given in equation (4.50) is obvious because the tension vector of the wall connecting two vacua is dual ($\pi/2$ rotation) to the vector connecting these two vacua which forms a closed triangle. Lastly we identify the trivial intersection dividing the vacua $\langle\underline{\cdots}AB\rangle$, $\langle\underline{\cdots}CD\rangle$, $\langle\underline{\cdots}AC\rangle$ and $\langle\underline{\cdots}BD\rangle$ as a parallelogram like in figure 16(*e*). All together they constitute the building blocks for the webs of walls.

The followings are the rules to construct grid diagrams for the webs of walls to assemble the building blocks:

(i) Determine mass arrangement $m_A + \mathrm{i}n_A$ and plot ${}_{N_F}C_{N_C}$ vacuum points $\langle A_r\rangle$ at $\sum_{r=1}^{N_C}(m_{A_r} + \mathrm{i}n_{A_r})$ in the complex $\mathrm{Tr}\,\Sigma$ plane.
(ii) Draw a convex polygon by choosing a set of vacuum points, which determines the boundary condition of a BPS solution. Here each edge of the convex polygon must be a 1/2 BPS single wall between pairs of the vacuum points $\langle\underline{\cdots}A\rangle$ and $\langle\underline{\cdots}B\rangle$.
(iii) Draw all possible internal segments within the convex polygon describing 1/2 BPS single walls forbidding any segments to cross.
(iv) Identify Abelian triangles with vertices $\langle\underline{\cdots}A\rangle, \langle\underline{\cdots}B\rangle$ and $\langle\underline{\cdots}C\rangle$ to Abelian 3-pronged junctions. Identify non-Abelian triangles with vertices $\langle\underline{\cdots}AB\rangle, \langle\underline{\cdots}BC\rangle$ and $\langle\underline{\cdots}CA\rangle$ to non-Abelian 3-pronged junctions. Identify parallelograms with vertices $\langle\underline{\cdots}AB\rangle, \langle\underline{\cdots}CD\rangle, \langle\underline{\cdots}AC\rangle$ and $\langle\underline{\cdots}BD\rangle$ to intersections with vanishing Y-charges.

Shapes of the web diagrams in the configuration space can be obtained by drawing a dual diagram by exchanging points and faces of the grid diagram [8].

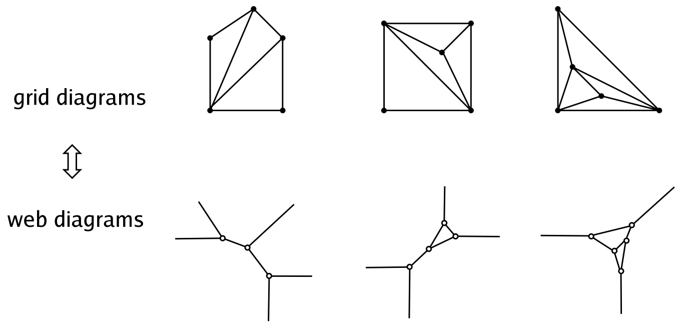

Figure 17. Examples of the grid and the web diagrams for the Abelian webs in the model with five flavours.

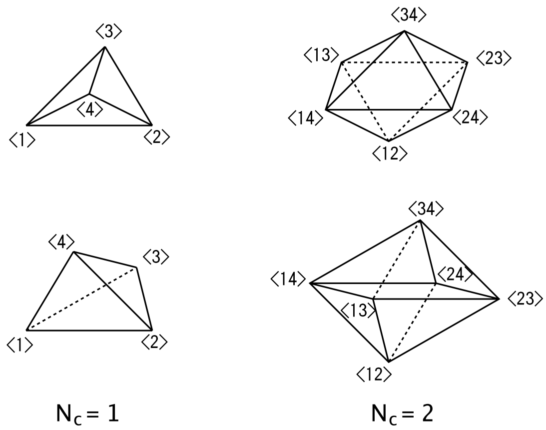

Figure 18. Examples of the grid diagrams in the model with four flavours. Each row uses the same hypermultiplet mass arrangement which is shown in the $N_C = 1$ case.

In figure 17, we show several examples of the webs in the Abelian gauge theory with $N_F = 5$ flavours. In general, the grid diagrams have $N_F = 5$ vertices. Some of these are the vertices of the convex polygon and the others are the internal points inside the polygon. The shape of the grid diagram is determined by the mass arrangement and there are $N_F - 2\ (=3)$ kinds of the convex polygons according to the number of the internal points inside the convex polygons; see figure 17. The number of the internal points of the grid diagram is the same as the number of the loops of the web diagrams in the real space. Then one can easily read the graphical relation of the configuration as

$$\dim_{\mathbf{C}} \mathcal{M} = N_F = E + L, \tag{4.65}$$

where E is the number of the external legs and L is the number of the loops in the web diagram.

The webs of walls develop richer species of configurations in the non-Abelian gauge theories. The number of different kinds of webs is the same as that in the Abelian gauge theories, namely there are N_F–2 kinds of the webs. We show several examples of the grid diagrams for the model with $N_F = 4$ flavours and various numbers of colours $N_C = 1, 2, 3$ in figure 18. The vacuum points of the grid diagrams of the $N_C = 1$ case shows the values of hypermultiplet masses directly: the upper one has an internal point, whereas the lower one does not. The same mass arrangement for each flavour of hypermultiplets is used to draw the

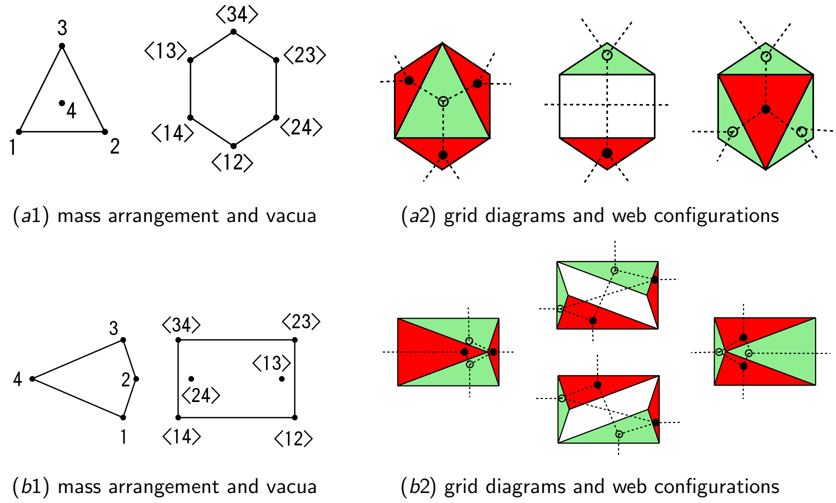

Figure 19. (a1) and (a2) for the hexagon-type and (b1) and (b2) for the parallelogram-type web.

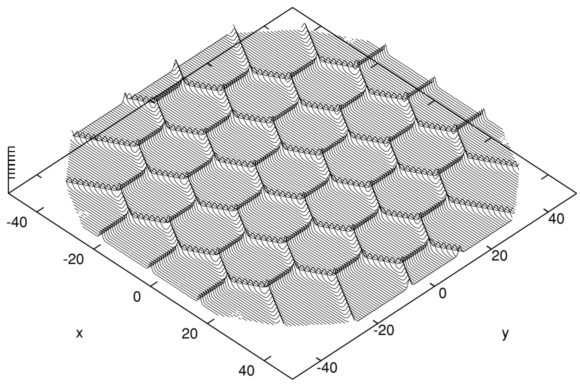

Figure 20. Honeycomb lattice of webs of walls.

grid diagrams of $N_C = 2, 3$ cases in the same row of figure 18. Let us finally illustrate an interesting phenomenon of a transition between webs with different types of junctions such as Abelian and non-Abelian by changing moduli parameters. We draw two grid diagrams in the model with $N_C = 2$ and $N_F = 4$ corresponding to two different mass arrangements in figure 19. One is the hexagon type with no internal points, which is a tree type web diagram. The other is the parallelogram-type diagram with two internal points, which has a loop. By varying the moduli parameters of the grid diagrams, we find that the internal structure of web diagrams changes as shown in figure 19(a2) and (b2): webs with Abelian junctions make a transition to webs with non-Abelian junctions and vice versa. The changes of the shape of the webs have been explicitly worked out in terms of the Plücker coordinates $\tau^{\langle\{A_r\}\rangle}$ in equation (4.57) [9]. At the end of this subsection, we give an exact solution in the strong gauge coupling limit $g^2 \to \infty$. As explained in section 4.1, the master equation reduces to just an algebraic equation. Then we can exactly solve them. In figure 20 we give a complicated configuration of webs of walls.

Interestingly, solutions of the KP and coupled KP equations were found to contain a very similar web structure to our solutions of webs of walls [127].

4.3. Composite of walls, vortices and monopoles

We will focus on another 1/4 BPS composite state of monopoles, vortices and domain walls in this subsection. The 1/4 BPS equations of this system have already been derived in equations (4.15)–(4.17). This 1/4 BPS system was studied qualitatively in [12] and lots of interesting features were found. We found that solutions of them can be described by the moduli matrix $H_0(z)$ which is an $N_\mathrm{C} \times N_\mathrm{F}$ holomorphic matrix with respect to $z = x^1 + ix^2$. Similarly to the webs of walls dealt with in the previous subsection, the moduli matrix is also a powerful tool to clarify properties of this 1/4 BPS system [11].

First of all, it should be stressed that the 1/4 BPS equations (4.15)–(4.17) are composite of the three types of 1/2 BPS solitons: $B_i = \mathcal{D}_i\Sigma$ for monopoles, $(\mathcal{D}_1 + \mathrm{i}\mathcal{D}_2)H = 0$, $B_3 + \frac{g^2}{2}\left(c\mathbf{1}_{N_\mathrm{C}} - HH^\dagger\right) = 0$ for vortices and $\mathcal{D}_3 H + \Sigma H - HM = 0$, $\mathcal{D}_3\Sigma - \frac{g^2}{2}\left(c\mathbf{1}_{N_\mathrm{C}} - HH^\dagger\right) = 0$ for domain walls. In this section we omit the subscript '4' of Σ_4 and M_4. Solutions of these 1/2 BPS equations, of course, are also solutions of the 1/4 BPS equations (4.15)–(4.17). When different types of 1/2 BPS solitons coexist, the configuration becomes a 1/4 BPS state as we will show. There are two kinds of solutions of the 1/4 BPS equations. One is a junction of two vortices living in the same Higgs vacuum, but with different orientations in the internal symmetry. This kind of composite soliton does not exist in Abelian gauge theory and is intrinsically non-Abelian. Since there is a unique vacuum in this case, domain walls do not appear. So the topological charges characterizing this system are the vortex charge and the monopole charge

$$\mathcal{E} = -c\,\mathrm{Tr}\,B_3 + \frac{2}{g^2}\,\mathrm{Tr}\,\partial_m(B_m\Sigma), \tag{4.66}$$

where the first one is the charge of the non-Abelian vortex and the second one is that of the ordinary t' Hooft–Polyakov-type monopole in the $SU(N_C)$ gauge theory. The monopole appears at the junction point of two vortices. This configuration is called the monopole in the Higgs phase which was found in [103]. The other 1/4 BPS state is also a composite state of vortices, but is now the junction of vortices living in different vacua. So the domain wall interpolating these vacua is formed. This kind of 1/4 BPS state can exist in Abelian gauge theory with $N_\mathrm{F} \geqslant 2$ flavours and is essentially a composite soliton in Abelian gauge theory. The topological charges characterizing this type of soliton in Abelian gauge theory is given by

$$\mathcal{E} = c\partial_3\Sigma - cB_3 + \frac{2}{g^2}\partial_m(B_m\Sigma), \tag{4.67}$$

where the first one is the charge of the domain wall, the second one is the charge of the ANO vortex and the third one is a somewhat strange charge which has a form very similar to the monopole charge in the $SU(N_\mathrm{C})$ gauge theory. This monopole-like charge gives a negative contribution to the energy density and will be understood as the binding energy (boojum) of the domain wall and the ANO vortex [11, 12].

4.3.1. Vortices in the massive theories. In this subsection, vortices will play a prominent role. We have clarified 1/2 BPS vortices in the massless theory in section 3.2. Here we deal with 1/2 BPS vortices in the massive theory with $M = \mathrm{diag}\left(m_1, m_2, \ldots, m_{N_\mathrm{F}}\right)$, $(m_A > m_{A+1})$. Let us start with the vortices in the $N \equiv N_\mathrm{C} = N_\mathrm{F}$ model. First recall that the massless (fully degenerate masses) model has the unique colour–flavour locking vacuum given by the condition

$$HH^\dagger = c\mathbf{1}_N, \qquad \Sigma H = 0. \tag{4.68}$$

The vacuum has the diagonal $SU(N)_{\mathrm{G+F}}$ symmetry as explained in section 2. This system admits the 1/2 BPS vortices which are solutions of the 1/2 BPS equations (3.44) and (3.45).

Solutions of the $1/2$ BPS equations are described by the moduli matrix $H_0(z)$ which is an N by N matrix holomorphic with respect to z as shown in equation (3.49). Note that we need to keep the additional condition $\Sigma H = 0$ to get regular solutions in the massless theory, although this condition is trivially satisfied by setting $\Sigma = 0$.

Roughly speaking, the vortex solutions in the non-Abelian gauge theory are obtained by embedding the Abelian ANO vortex solutions to the moduli matrices in the non-Abelian case. Then a single vortex solution breaks the $SU(N)_{\mathrm{G+F}}$ vacuum symmetry into $U(1) \times SU(N-1)$, so that the Nambu–Goldstone modes taking values on $\mathbf{C}P^{N-1} \simeq SU(N)_{\mathrm{G+F}}/[U(1) \times SU(N-1)]$ arise as orientational moduli. In terms of the $N \times N$ moduli matrix $H_0(z)$ given in equation (3.49), k-vortex solutions are generated by the matrix whose determinant is of order z^k as

$$\tau \equiv \det H_0(z) = \prod_{i=1}^{k}(z - z_i) \tag{4.69}$$

and their orientational moduli, which are the homogeneous coordinate of $\mathbf{C}P^{N-1}$, are defined by $H_0(z_i)\vec{\phi}_i = \vec{0}$:

$$\vec{\phi}_i{}^T = \left(\phi_i^1, \phi_i^2, \ldots, \phi_i^N\right) \in \mathbf{C}P^{N-1}. \tag{4.70}$$

When we turn on the non-degenerate masses M for the hypermultiplet scalars, the vacuum is still unique but the vacuum condition (4.68) is changed to

$$HH^\dagger = c\mathbf{1}_N, \qquad \Sigma H - HM = 0. \tag{4.71}$$

The second equation requires $\Sigma = \mathrm{diag}(m_1, m_2, \ldots, m_N)$, so that the flavour symmetry reduces from $SU(N)$ to $U(1)^{N-1}$. Furthermore $U(N)$ gauge symmetry also reduces to $U(1)^N$ by the VEV of the adjoint scalar (of course, these gauge symmetries are completely broken in the true vacuum by the VEV of hypermultiplet scalars). This means that there no longer exist the orientational moduli for the non-Abelian vortices and the system reduces to just N vortices of the ANO type. In other words, the non-degenerate masses M lift almost all the points of the massless orientational moduli space $\mathbf{C}P^{N-1}$ except for N fixed points of the $U(1)^{N-1}$ isometry which remain as solutions of the massive theory. Actually, the $1/2$ BPS equations are not changed from the massless one given in equations (3.44) and (3.45), and their solutions are also given by the same form as equation (3.49). However, we have to impose the additional condition $\Sigma H - HM = 0$ instead of $\Sigma H = 0$, then the moduli matrix can have non-trivial elements only in their diagonal elements. As a result, the N different ANO vortices live in the diagonal elements of the moduli matrix as $H_0(z) = \mathrm{diag}\big(H_{0\star}^1(z), H_{0\star}^2(z), \ldots, H_{0\star}^N(z)\big)$ with $H_{0\star}^A(z) = a_A \prod_{i=1}^{k_A}(z - z_i)$, $(A = 1, 2, \ldots, N)$. The orientational moduli in the massive theory reduce to just N different vectors as

$$\vec{\phi}_i{}^T = \left(\phi_i^1, \phi_i^2, \ldots, \phi_i^N\right) \rightarrow \begin{cases} (1, 0, 0, \ldots, 0, 0) : [1] - \text{vortex}, \\ (0, 1, 0, \ldots, 0, 0) : [2] - \text{vortex}, \\ \vdots \\ (0, 0, 0, \ldots, 0, 1) : [N] - \text{vortex}. \end{cases} \tag{4.72}$$

Thus we find that N different species of vortices, which we call $[A]$-vortex, can live in the unique vacuum of the massive $N = N_{\mathrm{C}} = N_{\mathrm{F}}$ system. The $[A]$-vortex is associated with the $U(1)$ phase of the Ath flavour element $H_{0\star}^A(z)$. In figure 21 we show an example of $N = 2$ model. The massless moduli space is $\mathbf{C}P^1 \simeq S^2$. Almost all of them are lifted by the non-degenerate masses except for the north and the south poles ([1]- and [2]-vortex) which remain as solutions of the massive $1/2$ BPS equation.

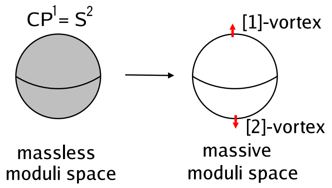

Figure 21. Orientation of non-Abelian vortices.

Let us next consider the non-Abelian semi-local vortices which arise in the massive theory with the N_F flavours being greater than the N_C colours. We have investigated the semi-local vortices in the massless theory in section 3.2.4 and found that they have additional moduli parameters (size moduli) compared to the ANO vortices in the model with $N_C = N_F$ theory. These additional moduli parameters are lifted and only several different species of ANO vortices remain, because of the same reason as the $N_F = N_C$ case mentioned above. In fact, the massless vacuum manifold Gr_{N_F,N_C} shrinks to the ${}_{N_F}C_{N_C}$ discrete vacua labelled by $\langle A_1 A_2 \cdots A_{N_C}\rangle = \langle\{A_r\}\rangle$ by the non-degenerate masses, as explained in section 3.1. The N_C different species of vortices, namely $[A_r]$-vortex ($r = 1, 2, \ldots, N_C$), can live in each vacuum. To clear matters, let us consider the semi-local vortex in the Abelian gauge theory. In the case of the massless theory the moduli matrix for the semi-local vortices are written as $H_0(z) = \left(H_{0\star}^1(z), \ldots, H_{0\star}^{N_F}(z)\right)$ with $H_{0\star}^A(z) \equiv a_A \prod_{i=1}^{k_A}(z - z_i)$ and the moduli parameters z_i and a_A can be understood as positions and sizes of the vortices, respectively. Additionally there exist non-normalizable moduli parameters which specify the position in the vacuum manifold as the boundary condition; see section 3.2.4. When we turn on the non-degenerate masses, the connection between different flavours is turned off: the size moduli and the non-normalizable moduli are frozen in solutions of the 1/2 BPS semi-local vortices in the massive theory. Therefore, the allowed moduli matrix is just N_F species of the ANO vortices labelled as $[A]$-vortex ($A = 1, 2, \ldots, N_F$):

$$H_0(z) = \left(H_{0\star}^1(z), \ldots, H_{0\star}^{N_F}(z)\right) \to \begin{cases} \left(H_{0\star}^1(z), 0, 0, \ldots, 0, 0\right), \\ \left(0, H_{0\star}^2(z), 0, \ldots, 0, 0\right), \\ \vdots \\ \left(0, 0, 0, \ldots, 0, H_{0\star}^{N_F}(z)\right). \end{cases} \tag{4.73}$$

For example, the massless vacuum manifold of $N_C = 1$ and $N_F = 2$ model is $\mathbf{C}P^1 \simeq S^2$ and we can choose each point on the $\mathbf{C}P^1$ as the boundary condition of the semi-local vortex. However, when the masses are turned on, there are only two choice for the boundary condition, either the north pole or the south pole, as illustrated in figure 22. Figure 21 for the vortices in the theory with $N_C = 2$ and $N_F = 2$ appears similar to figure 22 for vortices in the theory with $N_C = 1$ and $N_F = 2$. However, their properties are very different. The former has the unique vacuum $\langle 12\rangle$ and there exist [1]-vortices and [2]-vortices simultaneously in the vacuum. In contrast, the latter has two discrete vacua $\langle 1\rangle$ and $\langle 2\rangle$, and the [1]-vortices can live only in the vacuum $\langle 1\rangle$ while the [2]-vortices can in the vacuum $\langle 2\rangle$.

In the case of the massive model with $N_F > N_C$, there are ${}_{N_F}C_{N_C}$ discrete vacua. Although there exist N_F species of ANO vortices labelled by $[A]$-vortex ($A = 1, 2, \ldots, N_F$), only N_C of them can live in each vacuum. The vacuum $\langle A_1 A_2 \cdots A_{N_C}\rangle$ allows the $[A_r]$-vortex ($r = 1, 2, \ldots, N_C$) to live therein. With respect to the moduli matrix, the determinants of the minor matrices $H_0^{\langle\{A_r\}\rangle}$ characterize the configuration. Namely, k_{A_r} $[A_r]$-vortices in the $\langle\{A_r\}\rangle$

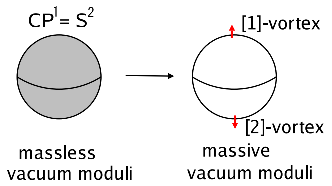

Figure 22. Semi-local vortices in the massive Abelian gauge theory.

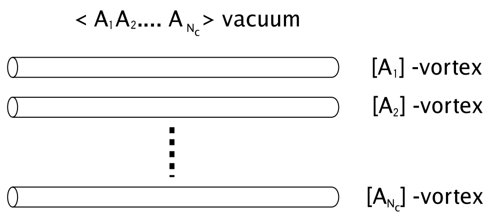

Figure 23. Orientation of a non-Abelian vortex.

vacuum is generated by the determinant of the moduli matrix

$$\tau^{\langle\{A_r\}\rangle} = \det H_0^{\langle\{A_r\}\rangle} = \prod_{i=1}^{k_{A_r}} (z - z_i), \qquad \text{others} = 0, \tag{4.74}$$

like the case of $N = N_C = N_F$ given in equation (4.69). These variables provide convenient coordinates of the moduli space and are called the Plücker coordinates as given in equation (3.19) in section 3.1. Thus we conclude that N_C different species of ANO vortices can exist in every one of the ${}_{N_F}C_{N_C}$ vacua in the $U(N_C)$ gauge theory with the massive N_F flavours.

4.3.2. Monopoles in the Higgs phase. We begin with the 1/4 BPS states of vortex junctions in a single vacuum which accompany monopoles as given in equation (4.66). We shall work in $U(2)$ gauge theory with $N_F = 2$ massive flavours with $M = \mathrm{diag}(m_1, m_2)$, $(m_1 > m_2)$. As we saw above, [1]- and [2]-vortices with orientations $\vec{\phi}^T = (1, 0)$ and $(0, 1)$ can exist in the vacuum $\langle 12\rangle$. The 1/2 BPS vortices containing k_1 [1]-vortices and k_2 [2]-vortices are given by the diagonal moduli matrix $H_0(z)\,\mathrm{e}^{Mx^3}$ in the 1/4 BPS solution (4.21) as

$$H_0(z)\,\mathrm{e}^{Mx^3} = \mathrm{diag}\big(H_{0\star}^1(z), H_{0\star}^2(z)\big)\,\mathrm{e}^{Mx^3}, \tag{4.75}$$

$$S(x^1, x^2, x^3) = \mathrm{diag}(S_\star^1(x^1, x^2), S_\star^2(x^1, x^2))\,\mathrm{e}^{Mx^3}, \tag{4.76}$$

with $H_{0\star}^A = \prod_{i=1}^{k_A}(z - z_i)$. In fact, plugging this solution into the 1/4 BPS equations (4.15)–(4.17), we find that the equations reduce to the 1/2 BPS equations for the ANO vortices: $\partial_z\bar{\partial}_z \log\Omega_\star^A = g^2\big(c - (\Omega_\star^A)^{-1}\big|H_{0\star}^A\big|^2\big)$ with $\Omega_\star^A \equiv |S_\star^A|^2$. Furthermore, the solutions given in equation (4.21) reduce to the 1/2 BPS solutions given in equation (3.49). Especially the additional condition $\Sigma H - HM = 0$ is automatically satisfied as

$$W_3 - \mathrm{i}\Sigma = -\mathrm{i}\,\mathrm{diag}(m_1, m_2). \tag{4.77}$$

When we turn on the off-diagonal elements of the moduli matrix $H_0(z)\,\mathrm{e}^{Mx^3}$ given in equation (4.75), the moduli matrix does not give a 1/2 BPS solution because $\Sigma H - HM = 0$

is no longer satisfied. Instead, it gives a 1/4 BPS solution satisfying $\mathcal{D}_3 H + \Sigma H - HM = 0$, which is one of the 1/4 BPS equations (4.15).

To clear matters, let us consider a single vortex configuration $k = k_1 + k_2 = 1$. The general moduli matrix with a unit vorticity $k = 1$ ($\det H_0(z) = \mathcal{O}(z)$) is of the form

$$H_0(z)\,\mathrm{e}^{Mx^3} = \begin{pmatrix} 1 & b \\ 0 & z - z_1 \end{pmatrix} \mathrm{e}^{Mx^3} \sim \begin{pmatrix} z - z_1 & 0 \\ b' & 1 \end{pmatrix} \mathrm{e}^{Mx^3}, \tag{4.78}$$

where $b, b' \in \mathbf{C}$ and they are related by $b = 1/b'$ except for $b = 0$ or $b' = 0$. Note that this moduli matrix is quite similar to that for the single non-Abelian vortex given in equation (3.68) in the massless theory where the moduli parameter $b \in \mathbf{C}P^1$ is the orientational moduli of the vortex. In the massive theory as mentioned above, the parameter b is no longer an orientational moduli (only $b = 0$ and $b = \infty$ give the ANO vortex solution). Nevertheless, treating b as the orientation in analogy with the massless model gives us a powerful insight in understanding the 1/4 BPS solution. To this end, it is useful to rewrite the above moduli matrix (4.78) as

$$H_0(z)\,\mathrm{e}^{Mx^3} = \mathrm{e}^{Mx^3} \begin{pmatrix} 1 & \tilde{b}(x^3) \\ 0 & z - z_1 \end{pmatrix} \sim \mathrm{e}^{Mx^3} \begin{pmatrix} z - z_1 & 0 \\ \tilde{b}'(x^3) & 1 \end{pmatrix}, \tag{4.79}$$

with $\tilde{b}(x^3) \equiv b\,\mathrm{e}^{-(m_1-m_2)x^3}$ and $\tilde{b}'(x^3) \equiv b'\,\mathrm{e}^{(m_1-m_2)x^3}$. By absorbing the prefactor e^{Mx^3} by the V-equivalence relation (4.22) at every slice at $x^3 = \text{const}$, we can regard this moduli matrix as the moduli matrix of 1/2 BPS vortices given in equation (3.49). Then the orientational moduli $\vec{\phi}^T = (\tilde{b}(x^3), 1) = (1, \tilde{b}'(x^3))$ depends on the x^3 coordinate. This means that the orientation of the vortex changes along the x^3-axis. Since we have chosen $m_1 - m_2 > 0$, $\tilde{b}(x^3) \to 0$ as $x^3 \to +\infty$ and $\tilde{b}'(x^3) \to 0$ as $x^3 \to -\infty$. Therefore, we find that the moduli matrix (4.78) gives a composite soliton which reduces to [2]-vortex ($\vec{\phi}^T = (0, 1)$) at $x^3 = +\infty$ and [1]-vortex ($\vec{\phi}^T = (1, 0)$) at $x^3 = -\infty$. Let us next focus on the transition between the [1]-vortex and [2]-vortex. As we mentioned above, the transition is accompanied by the monopole charge; see equation (4.66). We can directly calculate the monopole charge by taking account of limits where $B_3 = \mathrm{diag}(B_{3\star}, 0)$ at $x^3 \to -\infty$ and $B_3 = \mathrm{diag}(0, B_{3\star})$ at $x^3 \to +\infty$ while $B_1 = B_2 = 0$ and $\Sigma = \mathrm{diag}(m_1, m_2)$ both at $x^3 = \pm\infty$. Here $B_{3\star}$ is the flux of the single ANO vortex defined by $B_{3\star} = -\frac{1}{2}\left(\partial_1^2 + \partial_2^2\right)\Omega_\star$ and it satisfies $\int B_{3\star}\,\mathrm{d}x^1\,\mathrm{d}x^2 = -2\pi$. Then the monopole charge M_+ is calculated as

$$\begin{aligned} M_+ &= \frac{2}{g^2} \int \mathrm{d}^3x\, \partial_m \,\mathrm{Tr}(B_m \Sigma) \\ &= \frac{2}{g^2}\,\mathrm{Tr}\left[\left\{\int_{\mathbf{R}^2_+} \mathrm{d}^2x \begin{pmatrix} 0 & 0 \\ 0 & B_{3\star} \end{pmatrix} - \int_{\mathbf{R}^2_-} \mathrm{d}^2x \begin{pmatrix} B_{3\star} & 0 \\ 0 & 0 \end{pmatrix}\right\} \begin{pmatrix} m_1 & 0 \\ 0 & m_2 \end{pmatrix}\right] \\ &= \frac{4\pi}{g^2}(m_1 - m_2) > 0 \end{aligned} \tag{4.80}$$

where $\mathbf{R}^2_\pm$ are the boundary surface at $x^3 = \pm\infty$; see figure 24. Note that the ordering of the mass parameters $m_1 > m_2$ is not important here. In fact, if we reconsider this system with the opposite ordering $m_2 > m_1$, we again obtain the monopole with positive definite mass $\frac{4\pi}{g^2}(m_2 - m_1) > 0$ since the orientation also changes as $\vec{\phi}^T \to (1, 0)$ at $x^3 \to +\infty$ and $(0, 1)$ at $x^3 \to -\infty$.

Let us next consider the physical meaning of the moduli parameter b in the moduli matrix (4.78) in the massive theory. At this stage, $\tilde{b}(x^3) = b\,\mathrm{e}^{-(m_1-m_2)x^3}$ can be thought of a quantity representing how close to the [1]- or [2]-vortex the configuration is. Especially, we found that $\tilde{b} = 0, \infty$ correspond to [1]-vortex and [2]-vortex, respectively. The transition point $\tilde{b} = 1$,

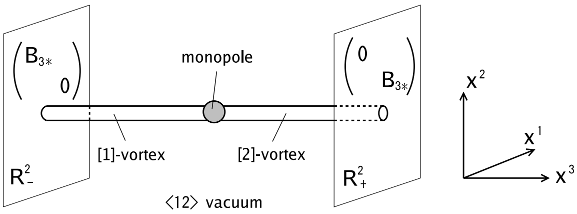

Figure 24. Monopole in the Higgs phase.

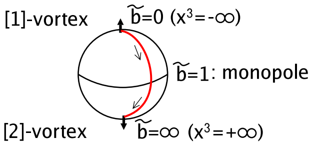

Figure 25. Orientation of the vortex and position of the monopole.

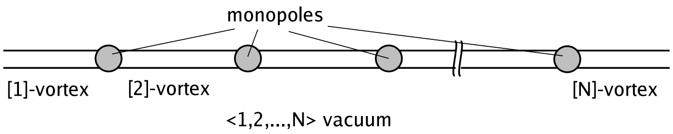

Figure 26. Beads of monopoles.

which is the middle point between the north pole and the south pole of $\mathbf{C}P^1$, can be regarded as the monopole from the view point both of the moduli space and the real space; see figure 25. So we conclude that b is related to the position of the monopole in the real space as

$$|\tilde{b}(x^3)| \approx 1 \quad \Leftrightarrow \quad x^3 \approx \frac{1}{m_1 - m_2} \log|b|. \tag{4.81}$$

Note that the monopole goes away to the spatial infinity when we take the limit of $b \to 0, \infty$. This observation agrees with the previous argument that the moduli matrix (4.78) reduces to those for the 1/2 BPS vortex given in equation (4.75).

A natural extension of this is multiple monopoles in the Higgs phase which is sometimes called beads of monopoles. To get such a configuration, we need to consider $U(N)$ gauge theory with N massive flavours. The vortices in the massless theory have orientational moduli $\vec{\phi}^T = (\vec{b}^T, 1) \in \mathbf{C}P^{N-1}$, which reduce to N fixed points when we turn on the nondegenerate masses. Similarly to the case of $N = 2$, the orientational moduli $\vec{b}$ can be understood as the positions of $N - 1$ monopoles connecting N different species of the ANO vortices. The moduli matrix describing the beads of monopoles penetrated by vortices are of the form

$$H_0\, \mathrm{e}^{Mx^3} = \begin{pmatrix} \mathbf{1}_{N-1} & \vec{b} \\ 0 & z - z_1 \end{pmatrix} \mathrm{e}^{Mx^3} = \mathrm{e}^{Mx^3} \begin{pmatrix} \mathbf{1}_{N-1} & \vec{\tilde{b}}(x^3) \\ 0 & z - z_1 \end{pmatrix}, \tag{4.82}$$

where we have defined the orientational vector $\vec{\phi}^T = (\vec{\tilde{b}}(x^3)^T, 1)$ with $\vec{\tilde{b}}(x^3)^T \equiv (b_1\, \mathrm{e}^{-(m_1 - m_N)x^3}, \ldots, b_{N-1}\, \mathrm{e}^{-(m_{N-1} - m_N)x^3})$. Positions of the monopoles are estimated by $|b_A|\, \mathrm{e}^{-(m_A - m_N)x^3} \approx |b_{A+1}|\, \mathrm{e}^{-(m_{A+1} - m_N)x^3}$:

$$x^3 \approx \frac{1}{m_A - m_{A+1}} \log\left|\frac{b_A}{b_{A+1}}\right|, \tag{4.83}$$

where $A = 1, 2, \ldots, N - 1 (b_N = 1)$.

4.3.3. Boojums: junctions of walls and vortices. Let us next investigate the other composite 1/4 BPS state made of the ANO vortices and the domain walls whose topological charges are given in equation (4.67). As already mentioned above, this composite soliton is essentially a 1/4 BPS state in the Abelian gauge theory. The moduli matrix is just an $N_{\rm F}$ component complex vector in the Abelian gauge theory. Although the moduli matrix is completely the same as that for the 1/2 BPS semi-local vortex, it is very important to realize that the moduli matrix is accompanied by the factor e^{Mx^3} as given in equation (4.15). The 1/4 BPS equations (4.15)–(4.17) admit the 1/2 BPS solutions also. Namely, the 1/2 BPS vortices in the massive theory dealt in section 4.3.1 are solutions of the 1/4 BPS equations. As already explained, a part of moduli of the semi-local vortices in the massless theory are lost when they are put into the massive theory. Then the moduli spaces of semi-local vortices are split into those of the ANO vortices in the massive theory. Indeed, the moduli matrix for the 1/2 BPS solutions turns into that for the $N_{\rm F}$ ANO vortices as given in equation (4.73). However, due to the additional factor e^{Mx^3}, the general moduli matrix which has two or more nonzero components can give solutions of the BPS equations. But it no longer gives 1/2 BPS solutions but 1/4 BPS solutions:

$$H_0\,e^{Mx^3} = \left(H_{0\star}^{1}(z)\,e^{m_1x^3}, H_{0\star}^{2}(z)\,e^{m_2x^3}, \ldots, H_{0\star}^{N_{\rm F}}(z)\,e^{m_{N_{\rm F}}x^3}\right) \tag{4.84}$$

where $H_{0\star}^{A}(z)$ is again the moduli matrix for the ANO vortices defined by $H_{0\star}^{A}(z) \equiv a_A \prod_{i_A=1}^{k_A}(z - z_{i_A})$. We will show that the moduli parameters contained in the general moduli matrix in equation (4.84) can be reinterpreted as the moduli of the ANO vortices and the domain walls in the massive theory instead of those of the semi-local vortices in the massless theory. Note that the set of $H_0(z)\,e^{Mx^3}$ can be thought of as the moduli matrix for the domain walls if we fix the coordinate z, whereas it can be regarded as that for the semi-local vortices if we fix the coordinate x^3. Thus, the moduli parameters in the moduli matrix (4.84) will be reinterpreted in terms of both the semi-local vortices and the domain walls in the following.

Let us first consider the simplest example of a junction of a vortex and a domain wall in the $N_{\rm F} = 2$ theory with the nondegenerate mass $M = {\rm diag}(m_1, m_2)$ ordered as $m_1 > m_2$. We focus on a single semi-local vortex given by the moduli matrix $H_0(z) = (a_1(z-z_1), a_2(z-z_2))$ where the moduli parameters z_1, z_2 are the positions and the size of the semi-local vortex, and the ratio $a \equiv a_1/a_2 \in \mathbf{C}P^1$ corresponds to the position of the wall. In the massive theory this moduli matrix is multiplied by the additional factor e^{Mx^3} and can be reinterpreted as follows,

$$\begin{aligned} H_0(z)\,e^{Mx^3} &\sim e^{m_2x^3}(\tilde{a}(x^3)(z - z_1), z - z_2) \\ &\sim e^{m_1x^3}(z - z_1, \tilde{a}'(x^3)(z - z_2)) \end{aligned} \tag{4.85}$$

with $\tilde{a}(x^3) \equiv e^{(m_1-m_2)x^3}a_1/a_2$ and $\tilde{a}'(x^3) \equiv \tilde{a}(x^3)^{-1}$. The new parameter $\tilde{a}(x^3)$ again gives us the boundary condition at the spatial infinity $|z| \to \infty$ but now it varies along the x^3-axis in the massless vacuum manifold $\mathbf{C}P^1$. Since $\tilde{a} \to 0$ at $x^3 \to -\infty$, the moduli matrix (4.85) reduces to that for the 1/2 BPS [2]-vortex sitting on $z = z_2$ at $x^3 = -\infty$. On the other hand, $\tilde{a}' \to 0$ at $x^3 \to +\infty$, then the moduli matrix (4.85) reduces that for the 1/2 BPS [1]-vortex sitting on $z = z_1$ at $x^3 = +\infty$. Thus the parameter $\tilde{a}(x^3)$ gives the flow connecting [1]-vortex and [2]-vortex. One can easily recognize a similarity between the monopoles in the Higgs phase in the previous section and this system: the orientational modulus b of the non-Abelian vortex is promoted to a function $\tilde{b} = b\,e^{-(m_1-m_2)x^3}$ which is reinterpreted as the flow in the massless moduli space $\mathbf{C}P^1$ while the boundary modulus a of the semi-local vortex is also promoted to a function $\tilde{a} = a^{(m_1-m_2)x^3}$ which is reinterpreted as the anti-flow of the massless vacuum manifold $\mathbf{C}P^1$; see figure 27.

As studied in section 4.3.1, the $[A]$-vortex can live only in the vacuum $\langle A\rangle$. So the transition between [1]-vortex and [2]-vortex necessarily accompanies a transition between $\langle 1\rangle$

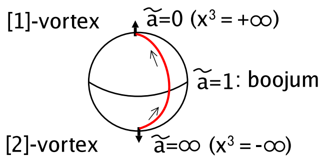

Figure 27. Boundary condition of the vortex and position of the domain wall.

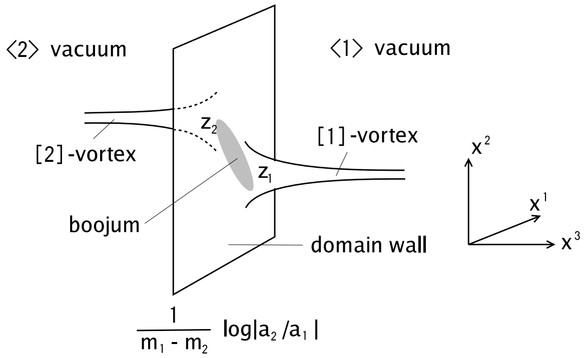

Figure 28. Two vortices ending on the domain wall from both sides.

and $\langle 2\rangle$ vacua, namely a domain wall. The position of the domain wall can be estimated by comparing the weights of vacua $|\mathcal{W}^{\langle 1\rangle}(z)| \approx |\mathcal{W}^{\langle 2\rangle}(z)|$ with $\mathcal{W}^{\langle A\rangle}(z) \equiv a_A(z - z_A)\,\mathrm{e}^{m_A x^3}$ as we explained in section 3.1. Then we get the position of the domain wall by

$$x^3(z) \approx \frac{1}{m_1 - m_2} \log \left| \frac{a_2(z - z_2)}{a_1(z - z_1)} \right| \rightarrow \frac{1}{m_1 - m_2} \log \left| \frac{a_2}{a_1} \right| \tag{4.86}$$

as $|z| \rightarrow \infty$. Thus, the moduli parameters z_1, z_2 for the positions of the semi-local vortices are reinterpreted as the positions of the ANO vortices ending on both sides of domain walls, whereas the size of the semi-local vortex $a = a_1/a_2$ is reinterpreted as the position of the domain wall. We give a schematic figure of this system in figure 28.

Let us next study the junction charge given in the last term of equation (4.67). Note that we now consider the Abelian gauge theory and then the charge is not the usual monopole charge in the non-Abelian gauge theories. It is called the boojum; see [12]. We can explicitly calculate the boojum charge M_- similarly to the monopole charge in equation (4.80). The domain wall sits on $x^3 = \frac{1}{m_1 - m_2} \log |a_2/a_1|$ and the vortex in the left vacuum $\langle 2\rangle$ resides at $z = z_2$, and the vortex in the right vacuum $\langle 1\rangle$ at $z = z_1$. At the both infinities $x^3 = \pm\infty$ the magnetic flux reduces to that of the ANO vortex $\vec{B} = (0, 0, B_{3\star})$. On the other hand, the VEV of the scalar Σ in the vector multiplet approaches $\Sigma = m_1$ at $x^3 \rightarrow +\infty$ and $\Sigma = m_2$ at $x^3 \rightarrow -\infty$. Then we obtain

$$\begin{aligned} M_- &= \frac{2}{g^2} \int \mathrm{d}^3x\, \partial_m (B_m \Sigma) \\ &= \frac{2}{g^2} \left(\int_{\mathbf{R}^2_+} \mathrm{d}^2x\, B_{3\star} m_1 - \int_{\mathbf{R}^2_-} \mathrm{d}^2x\, B_{3\star} m_2 \right) \\ &= -\frac{4\pi}{g^2}(m_1 - m_2) < 0 \end{aligned} \tag{4.87}$$

where we have used $\int \mathrm{d}^2x\, B_{3\star} = -2\pi$. Here the ordering of mass parameters $m_1 > m_2$ is not essential because the opposite ordering $m_2 > m_1$ requires us to set $\Sigma = m_2$ at $x^3 \to +\infty$ and $\Sigma = m_1$ at $x^3 \to -\infty$ to get a consistent domain wall configuration; see section 3.1. So the boojum charge always gives a negative contribution to the energy although their magnitude is the same as the monopole charge given in equation (4.80). This negative charge of the boojum is understood as the binding energy of the domain wall and the ANO vortex [12]. The sign difference between the monopole energy in equation (4.80) and the boojum energy in equation (4.87) comes from a different mechanisms of picking up the mass difference at the boundary. Different orientations of left and right vortices gives the mass difference for the monopole, whereas different VEV of Σ of left and right vacua provides it for the boojum. This distinction is also reflected in the opposite direction of the flows $\tilde{b}(x^3) = b\,\mathrm{e}^{-(m_1-m_2)x^3}$ for the monopole and $\tilde{a}(x^3) = a\,\mathrm{e}^{(m_1-m_2)x^3}$ for the boojum in the $\mathbf{C}P^1$ manifold of the vortex orientation, as shown in figures 25 and 27. Note that the position of the boojum can be estimated similarly to the position of the monopole in the previous section: the north pole ($\tilde{a} = 0$) corresponds to the [1]-vortex while the south pole ($\tilde{a} = \infty$) to the [2]-vortex. Then the middle point of $\mathbf{C}P^1$, namely $|\tilde{a}(x^3)| = 1$ can be regarded as the position of the boojum

$$|\tilde{a}(x^3)| = 1 \quad \Rightarrow \quad x^3 = \frac{1}{m_1 - m_2}\log\left|\frac{a_2}{a_1}\right|. \tag{4.88}$$

Note that the position of the boojum given above agrees with the position of the domain wall in equation (4.86). The boojum energy is spread inside the domain wall on which the two vortices end from both sides, as shown in figure 28.

Let us consider more general configurations with multiple domain walls and multiple vortices ending on the domain walls. In Abelian gauge theory, the moduli matrix has been given in equation (4.84). From the view point of the domain wall, we can regard $\mathcal{W}^{\langle A\rangle}(z) = H_{0\star}^A(z)\,\mathrm{e}^{m_A x^3}$ as the weight of the $\langle A\rangle$ vacuum. Then the position of the domain wall interpolating two vacua $\langle A\rangle$ and $\langle A+1\rangle$ can be estimated by equating weights of the adjacent vacua $\left|H_{0\star}^A(z)\,\mathrm{e}^{m_A x^3}\right| \approx \left|H_{0\star}^{A+1}(z)\,\mathrm{e}^{m_{A+1}x^3}\right|$:

$$x^3(z) \approx \frac{1}{m_A - m_{A+1}}\log\left|\frac{H_{0\star}^{A+1}(z)}{H_{0\star}^A(z)}\right|. \tag{4.89}$$

Let us next change the view from the domain wall to the vortex. Each component $H_{0\star}^A(z)$ of the moduli matrix (4.84) is then thought of as the moduli matrix for the $[A]$-vortex in the $\langle A\rangle$ vacuum. Therefore, $H_{0\star}^A(z) = a_A\prod_{i_A=1}^{k_A}\left(z - z_{i_A}\right)$ gives the k_A vortices sitting on $z = z_{i_A}$ in vacuum $\langle A\rangle$. Thus we conclude that the moduli matrix (4.84) gives us the domain walls interpolating N_F vacua as $\langle N_\mathrm{F}\rangle \leftrightarrow \langle N_\mathrm{F}-1\rangle \leftrightarrow \cdots \leftrightarrow \langle 2\rangle \leftrightarrow \langle 1\rangle$ and each vacuum holds the k_A ANO vortices at z_{i_A} which end on the domain walls sandwiching the vacuum $\langle A\rangle$. A generic configuration of the vortices ending on domain walls is depicted in figure 29.

It is worth commenting on the expression of wall positions given in equation (4.89). When the number k_{A+1} of the vortices ending on the wall from the left ($\langle A+1\rangle$ vacuum) and the number k_A of that ending on the wall from the right ($\langle A\rangle$ vacuum) is different from each other, the domain wall bends logarithmically. This is because the vortices pull the domain wall and the domain wall needs to pull the vortices back to keep themselves static and stable. The logarithmic bending always appears when p-brane ends on $(p+2)$-brane at a point like D-branes in the string theory. Note that completely the same result as equation (4.89) has been obtained from the view point of the low energy effective theory on the world volume of

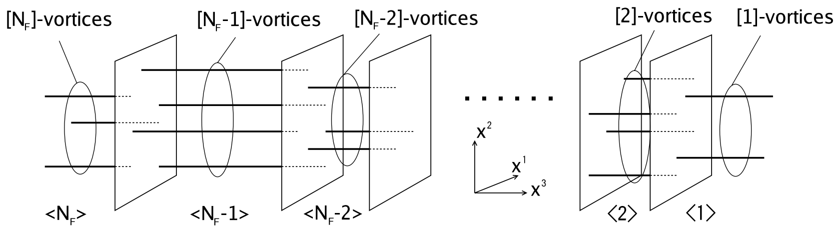

Figure 29. A generic configuration of the ANO vortices ending on domain walls.

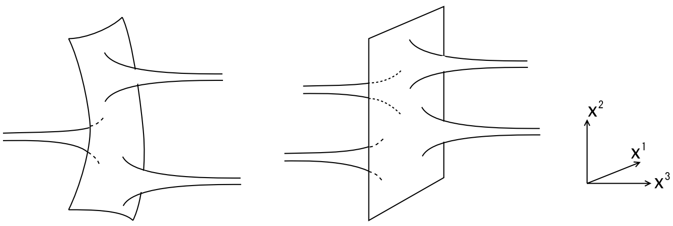

Figure 30. Logarithmic bending and flat domain walls.

the domain wall in [12]. When $k_A = k_{A+1}$, the ratio $\frac{H_{0\star}^{A+1}(z)}{H_{0\star}^{A}(z)}$ becomes constant at the spatial infinity on the z plane ($|z| \to \infty$)

$$x^3(z) \to \frac{1}{m_A - m_{A+1}} \log \left| \frac{a_{A+1}}{a_A} \right| \tag{4.90}$$

as $|z| \to \infty$. So the domain wall with the same number of vortices at left and right vacua becomes asymptotically flat; see figure 30.

4.3.4. General configurations. So far we have dealt with the minimal models: one is the $N_{\rm C} = N_{\rm F} = 2$ for the monopoles in the Higgs phase and the other is the $N_{\rm C} = 1$, $N_{\rm F} \geqslant 2$ for the composite of vortices and domain walls (the boojums). Let us next investigate a more general configuration which includes both the monopole and the boojum as the junction charges of vortices and domain walls. For that purpose, we shall consider $U(2)$ gauge theory with $N_{\rm F} = 3$ flavours with $M = {\rm diag}(m_1, m_2, m_3)$ ordered as $m_1 > m_2 > m_3$. This model has three discrete vacua $\langle 12\rangle$, $\langle 23\rangle$ and $\langle 13\rangle$. Let us focus on the configuration which has the single domain wall interpolating the $\langle 13\rangle$ vacuum at $x^3 = +\infty$ and the $\langle 23\rangle$ vacuum at $x^3 = -\infty$. Furthermore, we put a vortex in both sides of the domain wall. In terms of the Plücker coordinates in equation (4.74), this configuration is represented by $\tau^{\langle 12\rangle} = 0$, $\tau^{\langle 13\rangle} = \mathcal{O}(z)$ and $\tau^{\langle 23\rangle} = \mathcal{O}(z)$. Exploiting the V-equivalence relation (4.22), we can reduce all possible moduli matrix satisfying these conditions to either one of the following three different kinds of the moduli matrices $H_0\, {\rm e}^{Mx^3}$:

$$\begin{pmatrix} 1 & a_1 & b \\ 0 & 0 & z - z_1 \end{pmatrix} {\rm e}^{Mx^3} \sim \begin{pmatrix} \frac{1}{a_1}(z - z_1) & z - z_1 & 0 \\ \frac{1}{b} & \frac{a_1}{b} & 1 \end{pmatrix} {\rm e}^{Mx^3}, \tag{4.91}$$

$$\begin{pmatrix} z - z_2 & a_2(z - z_3) & 0 \\ 0 & 0 & 1 \end{pmatrix} {\rm e}^{Mx^3}, \tag{4.92}$$

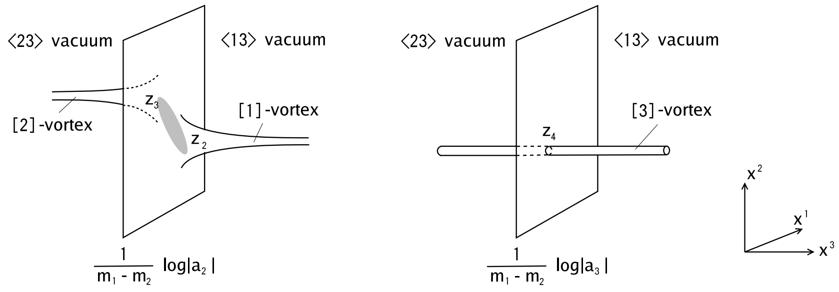

Figure 31. The junction and intersection between the vortices and the domain wall.

$$\begin{pmatrix} 1 & a_3 & 0 \\ 0 & 0 & z - z_4 \end{pmatrix} e^{Mx^3}, \tag{4.93}$$

with $z_1, z_2, z_3, z_4 \in \mathbf{C}$ and $a_1, a_2, a_3, b \in \mathbf{C}^*$.

Let us begin by investigating the moduli matrices (4.92) and (4.93). These are simple in the sense that the moduli matrices do not have off-diagonal elements which mix the first colour and the second colour components. In fact, $\Omega_0 = H_0(z)\, e^{2Mx^3} H_0^\dagger$ which is the source of the master equation (4.25) becomes diagonal. Then we can deal with the first row and the second row independently. In the case of the moduli matrix (4.92) the second row gives no physical effects, so the moduli matrix is essentially that for the Abelian gauge theory. In fact, the first row $((z - z_2)\, e^{m_1 x^3}, a_2(z - z_3)\, e^{m_2 x^3}, 0)$ is nothing but the moduli matrix for the vortices ending on the domain wall with boojum studied in section 4.3.3. Then the position of the domain wall interpolating $\langle 13 \rangle$ vacuum and $\langle 23 \rangle$ vacuum can be estimated by equation (4.86), so we have $x^3 \approx \frac{1}{m_1 - m_2} \log|a_2|$. A [1]-vortex ends on the domain wall from the right (vacuum $\langle 13 \rangle$) at $z = z_2$ while a [2]-vortex ends on from the left (vacuum $\langle 23 \rangle$) at $z = z_3$. They accompany the boojum whose x^3 position is the same as that of the domain wall; see equation (4.88). The configuration is depicted in the left of figure 31. On the other hand, the moduli matrix (4.93) has the domain wall in the first row $(e^{m_1 x^3}, a_3\, e^{m_2 x^3}, 0)$ and the [3]-vortex $(0, 0, (z - z_4)\, e^{m_3 x^3})$ in the second row. Since these two rows contribute to Ω_0 as an incoherent sum, the moduli matrix (4.93) can be regarded as that for the direct product of two decoupled $U(1)$ gauge theories rather than the $U(2)$ gauge theory. The first row gives the domain wall interpolating $\langle 13 \rangle$ and $\langle 23 \rangle$ vacua and the second row gives the [3]-vortex. The domain wall and the vortex do not interact, so the composite soliton represents just an intersection without the monopole and/or the boojum. The position of the domain wall is $x^3 \approx \frac{1}{m_1 - m_2} \log|a_3|$ and that of the [3]-vortex is z_4. This situation is depicted in the right of figure 31.

Let us next investigate a more interesting moduli matrix (4.91) which has an off-diagonal element b and is intrinsically non-Abelian. It turns out that the configuration has the domain wall, the vortices, the monopoles and the boojum. We have $\tau^{\langle 12 \rangle}(z) = 0$, $\tau^{\langle 23 \rangle}(z) = a_1(z - z_1)$ and $\tau^{\langle 13 \rangle}(z) = z - z_1$ and the weights of vacua $\mathcal{W}^{\langle AB \rangle}(z) = \tau^{\langle AB \rangle}(z)\, e^{(m_A + m_B)x^3}$:

$$\mathcal{W}^{\langle 12 \rangle}(z) = 0, \tag{4.94}$$

$$\mathcal{W}^{\langle 23 \rangle}(z) = a_1(z - z_1)\, e^{(m_2 + m_3)x^3}, \tag{4.95}$$

$$\mathcal{W}^{\langle 13 \rangle}(z) = (z - z_1)\, e^{(m_1 + m_3)x^3}. \tag{4.96}$$

The position of the domain wall dividing those two vacua can be estimated by the same method as equation (4.89):

$$x^3|_{\rm wall} \approx \frac{1}{(m_1+m_3)-(m_2+m_3)}\log\left|\frac{\tau^{\langle 23\rangle}}{\tau^{\langle 13\rangle}}\right| = \frac{1}{m_1-m_2}\log|a_1|. \tag{4.97}$$

The $z-z_1$ in $\tau^{\langle 23\rangle}$ and $\tau^{\langle 13\rangle}$ gives us the single ANO vortex both in the vacua $\langle 23\rangle$ and $\langle 13\rangle$ sit on $z=z_1$. As shown previously, $\tau^{\langle 23\rangle}\propto z-z_1$ means a [2]- or [3]-vortex in the vacuum $\langle 23\rangle$ while $\tau^{\langle 13\rangle}\propto z-z_1$ means a [1]- or [3]-vortex in the vacuum $\langle 13\rangle$. In order to identify which vortex arises in the vacua, we rewrite the moduli matrix (4.91) in the following form and understand it from the view point of the vortex moduli matrix

$$\mathrm{e}^{M^{\langle 13\rangle}x^3}\begin{pmatrix}1 & \tilde a_1(x^3) & \tilde b(x^3)\\ 0 & 0 & z-z_1\end{pmatrix} \sim \mathrm{e}^{M^{\langle 23\rangle}x^3}\begin{pmatrix}\frac{z-z_1}{\tilde a_1(x^3)} & z-z_1 & 0\\ \frac{1}{\tilde b(x^3)} & \frac{\tilde a_1(x^3)}{\tilde b(x^3)} & 1\end{pmatrix} \tag{4.98}$$

with $M^{\langle AB\rangle}\equiv \mathrm{diag}(m_A,m_B)$, $\tilde a_1(x^3)\equiv \mathrm{e}^{-(m_1-m_2)x^3}a_1$ and $\tilde b(x^3)\equiv \mathrm{e}^{-(m_1-m_3)x^3}b$. Taking the mass ordering $m_1>m_2>m_3$ into account, we easily find that the configuration at both the boundary $x^3\to\pm\infty$ from this expression:

$$\begin{pmatrix}1 & \tilde a_1(x^3) & \tilde b(x^3)\\ 0 & 0 & z-z_1\end{pmatrix} \to \begin{pmatrix}1 & 0 & 0\\ 0 & 0 & z-z_1\end{pmatrix} \tag{4.99}$$

as $x^3\to\infty$ and

$$\begin{pmatrix}\frac{z-z_1}{\tilde a_1(x^3)} & z-z_1 & 0\\ \frac{1}{\tilde b(x^3)} & \frac{\tilde a_1(x^3)}{\tilde b(x^3)} & 1\end{pmatrix} \to \begin{pmatrix}0 & z-z_1 & 0\\ 0 & 0 & 1\end{pmatrix} \tag{4.100}$$

as $x^3\to-\infty$. Then the moduli matrix (4.91) has the [3]-vortex in the $\langle 13\rangle$ vacuum at $x^3\to+\infty$ and the [2]-vortex in the $\langle 23\rangle$ vacuum at $x^3\to-\infty$. When going along the x^3-axis, the [2]-vortex makes a transition to the [3]-vortex with the monopole and/or the boojum charge.

Let us first consider a parameter region where $|b|\gg|a_1|, 1$. Then there exists a region where $|\tilde a_1(x^3)|\ll|\tilde b(x^3)|\ll 1$ and the moduli matrix reduces to

$$\mathrm{e}^{M^{\langle 13\rangle}x^3}\begin{pmatrix}1 & 0 & \tilde b(x^3)\\ 0 & 0 & z-z_1\end{pmatrix}. \tag{4.101}$$

Since the second column has no contribution, this moduli matrix has the same form as the middle moduli matrix in equation (4.78) and gives the monopole attached by the [1]-vortex from the left and the [3]-vortex from the right in the vacuum $\langle 13\rangle$. The mass of the [13]-monopole is given by $M_+^{[13]}=\frac{4\pi}{g^2}(m_1-m_3)$, and its position is given by the condition $|\tilde b(x^3)|\approx 1$ as $x^3|_{[13]\text{-monopole}}\approx\frac{1}{m_1-m_3}\log|b|$. There is another region where $\left|\frac{1}{\tilde b(x^3)}\right|, \left|\frac{\tilde a_1(x^3)}{\tilde b(x^3)}\right|\ll 1$ and there the moduli matrix reduces to the following form:

$$\mathrm{e}^{M^{\langle 23\rangle}x^3}\begin{pmatrix}\frac{z-z_1}{\tilde a_1(x^3)} & z-z_1 & 0\\ 0 & 0 & 1\end{pmatrix}. \tag{4.102}$$

This is nothing but the moduli matrix for the domain wall interpolating $\langle 13\rangle$ and $\langle 23\rangle$ vacua on which the [1]-vortex ends from the right and the [2]-vortex from the left with the boojum. The mass of the boojum is given by $M_-^{[12]}=-\frac{4\pi}{g^2}(m_1-m_2)$, and its position is the same as that of the domain wall given by equation (4.97). The configuration is depicted in the right of figure 32.

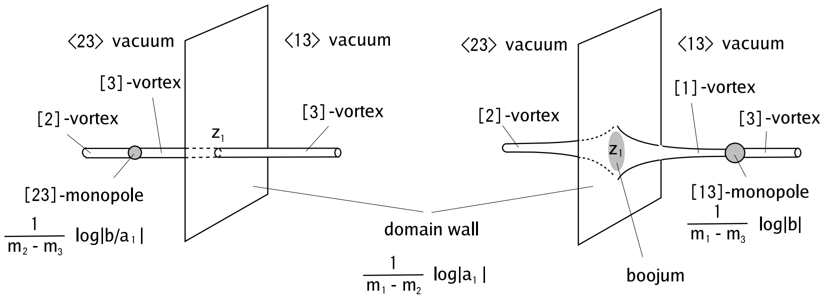

Figure 32. The composite states of the vortices, the domain wall, the monopoles and the boojum. The left figure is for the parameter region $|a_1| \gg |b|$ while the right is for $|a_1| \ll |b|$.

Let us next consider the parameter region where $|b| \ll |a_1|$. Then the moduli matrix reduces to the following form in the region where $1, |\tilde{a}_1(x^3)| \gg |\tilde{b}(x^3)|$:

$$e^{M^{\langle 13\rangle}x^3}\begin{pmatrix}1 & \tilde{a}_1(x^3) & 0\\ 0 & 0 & z-z_1\end{pmatrix}. \tag{4.103}$$

This moduli matrix gives us the trivial intersection of the domain wall and the [3]-vortex as explained for the moduli matrix (4.93). There also exists a region where $1, \left|\frac{1}{\tilde{b}(x^3)}\right| \ll \left|\frac{\tilde{a}_1(x^3)}{\tilde{b}(x^3)}\right|$. There the moduli matrix reduces to

$$e^{M^{\langle 23\rangle}x^3}\begin{pmatrix}0 & z-z_1 & 0\\ 0 & \frac{\tilde{a}_1(x^3)}{\tilde{b}(x^3)} & 1\end{pmatrix}. \tag{4.104}$$

Since the first column has no contribution, this moduli matrix has the same form as the right-hand side of equation (4.78) and gives the [23]-monopole sandwiched by [2]-vortex from the left and [3]-vortex from the right. The mass of the monopole is given by $M_+^{[23]} = \frac{4\pi}{g^2}(m_2 - m_3)$, and its position is given by $\left|\frac{\tilde{a}_1(x^3)}{\tilde{b}(x^3)}\right| \approx 1$: $x^3|_{[23]\text{-monopole}} \approx \frac{1}{m_2-m_3}\log\left|\frac{b}{a_1}\right|$. The configuration is depicted in the left of figure 32.

Let us summarize the configuration given by the moduli matrix (4.91). There are two types of infinitely heavy objects: one is the domain wall sitting at $x^3 = \frac{1}{m_1-m_2}\log|a_1|$, and the other type is the ([1]-, [2]- and [3]-)vortices penetrating the domain wall at $z = z_1$. For the time being, let us fix the parameters z_1 and a_1. Then only parameter b remains as a free parameter corresponding to the position of the monopole which has a finite mass. When $|b| \ll |a_1|$, the [23]-monopole sandwiched by the [2]-vortex from the left and [3]-vortex from the right in the vacuum $\langle 23\rangle$, namely in the left of the domain wall. As parameter b grows, the monopole moves to the left along the x^3-axis. Around the region where $|b| \sim |a_1|$, the monopole, the vortices and the domain wall merge. After the [23]-monopole passes through the domain wall, namely the region where $|b| \gg |a_1|$, the [2]-vortex ends on the domain wall from the left and the [1]-vortex appears from the domain wall with the [13]-boojum left in the wall. Furthermore, the [1]-vortex makes a transition to the [3]-vortex at the [13]-monopole. Of course, the masses of the monopole and the boojum are preserved before and after the monopole passes the domain wall: $M_+^{[13]} + M_-^{[12]} = M_+^{[23]}$. Interestingly, the centre of mass of the [13]-monopole and the [12]-boojum for $|b| \gg |a_1|$ becomes the position of the [23]-monopole for $|b| \ll |a_1|$.

Before closing this section, we give a comment on the relation between the three moduli matrices (4.91)–(4.93). When we take $b \to 0$ in the moduli matrix (4.91), it reduces to

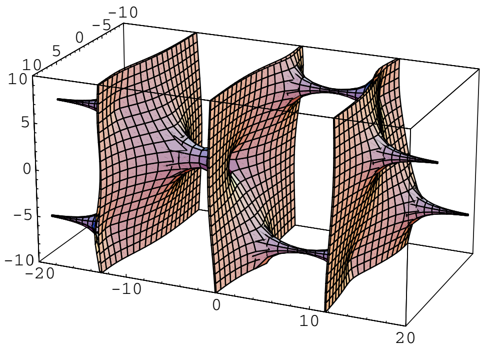

Figure 33. Composite soliton of vortices (lumps) and domain walls.

the same form as matrix (4.93). This fact implies that the [23]-monopole can be sent to the minus infinity of the x^3-axis, so that the only trivial intersection between the domain wall and the [3]-vortex remains. On the other hand, when we take $b \to \infty$ in the moduli matrix (4.91), namely the [13]-monopole is sent to the plus infinity of the x^3-axis, the moduli matrix reduces to almost the same form as matrix (4.92). However, there is a small but crucial difference between them: the positions of two vortices can take different values ($z_2 \neq z_3$) in the matrix (4.92) while they must coincide in the limit ($b \to \infty$) of the moduli matrix (4.91). Therefore, we conclude that the positions of the vortices have to coincide when monopoles attach anywhere on the vortices. Only after removing the monopoles by sending them to the spatial infinity, the vortex in the left of the domain wall and that in the right can separate on the domain wall. At the end of this subsection, we give an exact solution in the strong gauge coupling limit $g^2 \to \infty$. As explained in equation (4.36), the master equation reduces to just an algebraic equation. Then we can exactly solve them. In figure 33 we give a configuration which is composite of vortices (lumps) and domain walls.

4.4. Composite of vortices and instantons

Although the total moduli space $\mathcal{M}^{\text{total}}_{\text{IVV}}$ in equation (4.14) of the 1/4 BPS composite system of instantons and vortices is a parent of other 1/4 BPS composite solitons, we leave its full analysis to future works. Instead we will here restrict ourselves to two cases of physical interest: one is 1/4 BPS solutions interpretable as 1/2 BPS lumps on the world volume of 1/2 BPS vortices in the 1–3 plane, and the other is the intersection of two vortices. We wish to stress, however, that these solutions are genuine solutions of the 1/4 BPS equations, rather than the solutions of the effective theory on host vortices.

4.4.1. Instantons as lumps on vortices. We first consider 1/2 BPS lumps in the effective theory on the world volume of a vortex (3.135) before constructing a genuine solution of the 1/4 BPS equations. For simplicity, let us take the $N_{\text{C}} = N_{\text{F}} \equiv N = 2$ case. Defining $z = x^1 + \mathrm{i}x^2$, the BPS equations (3.44) and (3.45) for vortices give a solution (3.49). For a single vortex the moduli matrix in a patch $\mathcal{U}^{(1,0)}$ (3.66) is given by

$$H^{\text{single}}_{\text{v0}}(z; z_0, b) \equiv \begin{pmatrix} z - z_0 & 0 \\ b & 1 \end{pmatrix}, \tag{4.105}$$

where $b \in \mathbf{C}$ is an orientational modulus of a vortex and an inhomogeneous coordinate of $\mathbf{C}P^1$ as we explained. By promoting the moduli parameter b to a field on the world volume of the vortex, we obtain the effective Lagrangian on the vortex (3.132). By an almost identical argument to obtain (3.44) and (3.45) in section 3.2, we obtain a 1/2 BPS equation for lumps [75] on the vortex

$$\bar{\partial}_w b(w, \bar{w}) = 0, \qquad w \equiv x^3 + \mathrm{i}x^4. \tag{4.106}$$

This equation gives a k-lump solution which can be expressed in terms of rational functions of degree k [72, 75]

$$b(w) = \frac{P_k(w)}{\alpha P_k(w) + a Q_{k-1}(w)}, \tag{4.107}$$

$$P_k(w) \equiv \prod_{i=1}^{k}(w - p_i), \qquad Q_{k-1}(w) \equiv \prod_{j=1}^{k-1}(w - q_j). \tag{4.108}$$

Among the moduli parameters, $\{p_1, p_2, \ldots, p_k\}$ correspond to the positions of the k-lumps on the host vortex, and a to the total size of the configurations, and $\{q_1, q_2, \ldots, q_{k-1}\}$ to the relative sizes of the k-lumps. The remaining modulus α specifies the boundary condition at $|w| \to \infty$ and parametrizes a point in the vacuum manifold $\mathbf{C}P^1$, since $b(w) \to 1/\alpha$ as $|w| \to \infty$. When $\alpha = 0$, $\{p_i, a, q_j\}$ can be identified with positions and sizes of k-lumps precisely. The zeros of the denominator in equation (4.107) are mere coordinate singularities caused by the use of an inhomogeneous coordinate b of the $\mathbf{C}P^1$ manifold. The configurations are smooth and continuous at these coordinate singularities. However, the point $a = 0$ and the points $p_i = q_j$ are true singularities of the moduli space of the lumps and are called small lump singularities.

For a more general case of $N = N_{\mathrm{F}} = N$, the orientational moduli space for the non-Abelian vortex is $SU(N)/[SU(N-1) \times U(1)] \simeq \mathbf{C}P^{N-1}$ [76, 77, 79]. The multi-lump solutions on the vortex in this case are obtained as lump solutions for the $\mathbf{C}P^{N-1}$ nonlinear sigma model, which are also known [73].

4.4.2. 1/4 BPS solutions of the instantons in the Higgs phase. With the aid of the lump solution in the effective theory on the world volume of vortex, we can now obtain the genuine solutions of the 1/4 BPS equations (4.2)–(4.4) for instantons in the Higgs phase. Our idea is to start replacing the moduli parameter b in the moduli matrix $H_{\mathrm{v}0}^{\mathrm{single}}(z; z_0, b)$ in equation (4.105) for a single vortex by the lump solution $b(w)$ in equation (4.107)

$$H_0(z, w) \sim H_{\mathrm{v}0}^{\mathrm{single}}(z; z_0, b(w)) = \begin{pmatrix} z - z_0 & 0 \\ \frac{P_k}{\alpha P_k + a Q_{k-1}} & 1 \end{pmatrix}. \tag{4.109}$$

This moduli matrix is very close to the solution, except for the following deficiency: $b(w) = \frac{P_k}{\alpha P_k + a Q_{k-1}}$ is not holomorphic at some points in w where $b(w)$ diverges. As stated in equation (4.14), all components in the moduli matrix $H_0(z, w)$ should be holomorphic with respect to both z and w at any point $(z, w) \in \mathbf{C}^2$. We can overcome this problem by noting that the lump solution $b(w)$ is given in terms of an inhomogeneous coordinate b on $\mathbf{C}P^1$. We now transform the moduli matrix $H_{\mathrm{v}0}^{\mathrm{single}}(z; z_0, b(w))$ written in the inhomogeneous coordinate b into that in homogeneous coordinates. The correct moduli matrix should then be

$$H_0(z, w) = \begin{pmatrix} (z - z_0)A_{k-1}(w) & (z - z_0)(\alpha A_{k-1}(w) + a B_{k-2}(w)) \\ P_k(w) & \alpha P_k(w) + a Q_{k-1}(w) \end{pmatrix}, \tag{4.110}$$

with A_{k-1} and B_{k-2} as polynomial functions of order $k-1$ and $k-2$ in w, given by

$$A_{k-1}(w) = \sum_{i=1}^{k} \frac{1}{Q_{k-1}(p_i)} \prod_{i'(\neq i)=1}^{k} \left(\frac{w - p_{i'}}{p_i - p_{i'}} \right), \tag{4.111}$$

$$B_{k-2}(w) = \sum_{j=1}^{k-1} \frac{-1}{P_k(q_j)} \prod_{j'(\neq j)=1}^{k-1} \left(\frac{w - q_{j'}}{q_j - q_{j'}} \right). \tag{4.112}$$

We can determine these $A_{k-1}(w)$ and $B_{k-2}(w)$ uniquely by the following condition,

$$A_{k-1}Q_{k-1} - B_{k-2}P_k = 1, \tag{4.113}$$

which requires the vorticity of the solution to agree with that in equation (4.109): the solution should have a single vortex in the 1–3 plane and no vortices in the 2–4 plane. We see that the right-hand side of equations (4.109) and (4.110) are related by

$$H_0(z, w) = V(P_k(w), Q_{k-1}(w)) H_{\mathrm{v0}}^{\mathrm{single}}(z; z_0, b(w)), \tag{4.114}$$

with the matrix $V(P_k, Q_{k-1})$ defined by

$$V(P_k, Q_{k-1}) \equiv \begin{pmatrix} \frac{a}{\alpha P_k + a Q_{k-1}} & (z - z_0)(\alpha A_{k-1} + a B_{k-2}) \\ 0 & \alpha P_k + a Q_{k-1} \end{pmatrix}. \tag{4.115}$$

In a particular region of w with non-vanishing $\alpha P_k + a Q_{k-1}$, this matrix $V(P_k, Q_{k-1})$ is a V-equivalence transformation (4.13). However, it cannot be a legitimate V-equivalence transformation, since it has a singularity in w. Although $V(P_k, Q_{k-1})$ is not a valid V-equivalence transformation because of these singularities in w, it is needed precisely to compensate singularities of $H_{\mathrm{v0}}^{\mathrm{single}}(z; z_0, b(w))$ in equation (4.109), if we wish to obtain the regular moduli matrix (4.110).

We now examine the moduli parameters of the k-instantons in the Higgs phase in detail. Since no new parameters appear in A_{k-1} and B_{k-2}, the configuration of k-instantons in the Higgs phase has the $2k+2$ complex moduli parameters $(z_0, \{p_i\}, \{q_j\}, a, \alpha)$. The position of the single vortex on the 1–3 plane is given by the moduli parameter z_0, which decouples from other moduli parameters and has a flat metric. This decoupling of z_0 can be recognized also from the Kähler potential (3.135). Therefore the moduli space of instantons in the Higgs phase can be written as

$$\mathcal{M}^{k\text{-instantons}} \simeq \mathbf{C} \times \mathcal{M}^{k\text{-lumps}} \simeq \mathbf{C} \times \{\varphi | \mathbf{C} \to \hat{\mathcal{M}}^{1\text{-vortex}}, \bar{\partial}_w \varphi = 0\}. \tag{4.116}$$

We easily realize that $\{p_i\}$ correspond to the positions of k-instantons inside the vortex, a to the total size and the orientation of the configurations and $\{q_j\}$ to the relative sizes and the orientations of the instantons. In the limit of vanishing a, the rank of the moduli matrix (4.110) reduces by 1 and its determinant vanishes. Then the point $a \to 0$ is singular in the moduli space. On the other hand, the small lump singularities coming from $p_i = q_j$ in equation (4.107) arise as divergences of $1/P_k$ and $1/Q_{k-1}$ in A_{k-1} and B_{k-2} in equations (4.111) and (4.112). Therefore we observe that the small lump singularities with $a = 0$ or $p_i = q_j$ in equation (4.107) are now interpreted as the small instanton singularities in the Higgs phase. We can easily confirm that the points $p_i = p_{i'}$ for $i \neq i'$ and $q_j = q_{j'}$ for $j \neq j'$, respectively, are not singularities of equations (4.111) and (4.112). The remaining parameter α parametrizes $\mathbf{C}P^1$ similarly to the lump solutions. In the case of 1/2 BPS vortex, this $\alpha \in \mathbf{C}P^1$ is a normalizable moduli, whereas it becomes a nonnormalizable moduli in the case of the 1/4 BPS lumps. This sort of phenomenon occurs often: normalizable moduli of the host soliton can become a non-normalizable moduli of a soliton on the host soliton. In summary we find $z_0 \in \mathbf{C}$, $p_i \in \mathbf{C}$, $a \in \mathbf{C}^* \equiv \mathbf{C} - \{0\} \simeq \mathbf{R} \times S^1$, $q_j \in \mathbf{C} - \{p_1, p_2, \ldots, p_k\}$ and $\alpha \in \mathbf{C}P^1$.

Let us consider the simplest case of a single instanton ($k = 1$) with $A_0 = 1$ and $B_{-1} = 0$ in some detail. The lump solution $b(w) = \frac{w - p_1}{\alpha(w - p_1) + a}$ in the effective theory on a vortex suggests a solution of the 1/4 BPS equations with the moduli matrix

$$H_0^{\text{1-instanton}} = \begin{pmatrix} z - z_0 & \alpha(z - z_0) \\ w - p_1 & \alpha(w - p_1) + a \end{pmatrix}. \tag{4.117}$$

We can clarify the physical significance of these four complex moduli parameters z_0, p_1, a, α, by transforming the moduli matrix in equation (4.117) into that with $\alpha = 0$ by an $SU(2)_\mathrm{F}$ rotation U combined with a V-equivalence transformation:

$$H_{\mathrm{v}0}^{\text{1-instanton}}(z; a, p_1, \alpha) \sim H_{\mathrm{v}0}^{\text{1-instanton}}(z; a_0, p_0, \alpha = 0)U. \tag{4.118}$$

Then we obtain the physical position p_0 and the size $|a_0|$ of the instanton in the vortex as

$$p_0 = p_1 - \frac{\alpha^*}{1 + |\alpha|^2} a, \qquad |a_0| = \frac{|a|}{1 + |\alpha|^2}, \tag{4.119}$$

which are invariant under the $SU(2)_\mathrm{F}$ rotation.

Let us now consider the topology of the moduli space of one instanton in the Higgs phase. The moduli matrix $H_0^{\text{1-instanton}}$ can be transformed into $H_0^{\prime\,\text{1-instanton}}$ in another patch of the moduli space by a V-equivalence transformation in (4.13)

$$H_0^{\prime\,\text{1-instanton}} \equiv \begin{pmatrix} \alpha'(w - p_1') + a' & w - p_1' \\ \alpha'(z - z_0) & z - z_0 \end{pmatrix} \sim H_0^{\text{1-instanton}}, \tag{4.120}$$

with the following relation between coordinates in two patches

$$\alpha' = \frac{1}{\alpha}, \qquad a' = -\frac{a}{\alpha^2}, \qquad p_1' = p_1 - \frac{a}{\alpha}. \tag{4.121}$$

Both α and α' are the standard inhomogeneous coordinates of the $\mathbf{C}P^1$ in different patches, which are enough to cover the whole manifold. Since we find that a requires a nontrivial transition function $-1/\alpha^2$ between two patches, it is a tangent vector as a fibre on the $\mathbf{C}P^1$. On the other hand, we can use an invariant global coordinate for two patches, p_0, instead of p_1. This implies that the space $\mathbf{C}$ parametrized by p_0 is a direct product to the $\mathbf{C}P^1$. Therefore the topology of the moduli space of one $U(2)$ instanton in the Higgs phase is given by

$$(z_0, p_0, a, \alpha) \in \mathbf{C} \times \mathbf{C} \times (\mathbf{C}^* \times^* \mathbf{C}P^1) \simeq \mathcal{M}^{\text{1-instanton}}, \tag{4.122}$$

where $(\mathbf{C}^* \times^* \mathbf{C}P^1)$ is the tangent bundle with a base space $\mathbf{C}P^1$ and a fibre $\mathbf{C}^*$.

For $N > 2$, we can specify the moduli matrix $H_0(z, w)$ for a particular class of 1/4 BPS solutions which can be interpreted as 1/2 BPS states in the vortex theory, similarly to the case of $N = 2$. Thus we can obtain the 1/4 BPS states corresponding to the $U(N)$ instantons in the Higgs phase by repeating the same discussion.

4.4.3. Intersection of vortices. We can obtain more varieties of solutions, if we do not restrict ourselves to solutions interpretable as solitons in the effective theory on a host vortex. For instance, the intersection of two or more vortices cannot be understood as solitons on vortices, since the energy of such composite solitons diverges in the effective theory. The moduli matrix approach allows us to construct such solitons of intersecting vortices directly.

In the theory with $N_\mathrm{C} = N_\mathrm{F} \equiv N = 2$, the following two moduli matrices give configurations with $\nu_\mathrm{v} = k_z$ ($\geqslant 0$) vortices in the 1–3 plane and $\nu_{\mathrm{v}'} = k_w$ ($\geqslant 0$) vortices in the 2–4 plane

$$H_0 = \begin{pmatrix} z^{k_z} & 0 \\ 0 & w^{k_w} \end{pmatrix}, \tag{4.123}$$

$$H_0 = \begin{pmatrix} z^{k_z} w^{k_w} & 0 \\ 0 & 1 \end{pmatrix}. \tag{4.124}$$

The two vortices intersect at a point $z = w = 0$ in both cases. The moduli matrix in equation (4.123) gives a trivial intersection carrying no instanton charge. On the other hand, the moduli matrix in equation (4.124) gives two vortices with a nontrivial intersection carrying the instanton charge $\nu_{\mathrm{i}} = -k_z k_w$ at the intersection point. In this case the instanton charge contributes negatively to the energy of the composite soliton. This negative contribution can be interpreted as a binding energy of two vortices at the intersection, similarly to the case of an Abelian junction of domain walls in equation (4.51). The (infinitely) large energy coming from vortices is slightly cancelled by the negative contribution from the intersection giving a positive energy as a whole. We can call this composite soliton as an 'intersecton', since the instanton charge is stuck at the intersecting point of vortices. It cannot move once the vortices are fixed.

Let us consider the case of $N_{\mathrm{C}} < N_{\mathrm{F}}$ theory where semi-local vortices are available. In this case, we can take a strong coupling limit $g^2 \to \infty$ to obtain an exact solution. In this strong coupling limit, we obtain a nonlinear sigma model whose target space is the cotangent bundle over the complex Grassmann manifold, $T^*(G_{N_{\mathrm{F}},N_{\mathrm{C}}})$, as explained in section 2.3. Then the master equation (4.12) can be solved algebraically as $\Omega^{g^2\to\infty} = \Omega_0 = c^{-1} H_0 H_0^{\dagger}$. For simplicity we take the $U(1)$ gauge theory with four flavours: $N_{\mathrm{C}} = 1$, $N_{\mathrm{F}} = 4$. We obtain non-trivially intersecting vortices with $\nu_{\mathrm{v}} = k_z$, $\nu_{\mathrm{v}'} = k_w$ by considering the following moduli matrix,

$$H_0 = (z^{k_z} w^{k_w}, z^{k_z}, w^{k_w}, 1). \tag{4.125}$$

We find the exact solution $H = (1/\sqrt{\Omega^{g\to\infty}})H_0$ with

$$\Omega^{g\to\infty} = \Omega_0 = (|z|^2 + 1)^{k_z} (|w|^2 + 1)^{k_w}. \tag{4.126}$$

The instanton charge is found to be the product of vorticities, namely $\nu_{\mathrm{i}} = -k_z k_w$. This solution explicitly shows that the $U(1)$ instantons are stuck at the intersection of vortices. This instanton charge also contributes negatively to energy, in agreement with our observation that the instanton charge in Abelian gauge theories can be interpreted as a binding energy of vortices. However, we have observed that the instanton charge ν_{i} changes its sign under the duality transformation $N_{\mathrm{C}} \leftrightarrow N_{\mathrm{F}} - N_{\mathrm{C}}$ (with fixed N_{F}) of nonlinear sigma models in equation (2.23). By using this duality transformation, we can also obtain intersections of vortices in nonlinear sigma models coming from non-Abelian gauge theories. As a result, we find intersections of vortices that contribute positively to energy of the composite soliton, similarly to the non-Abelian junction contributing positively to the energy.

Let us summarize this section by observing that there exist three types of instantons. The first type is interpretable as lumps living inside a vortex. The second type is an instanton stuck at the intersection point of vortices. The third type is the intersection of vortices without any interaction. This last type has been observed in equation (4.123). We expect that the most general solution is given by the mixture of these configurations, similarly to the webs of walls in section 4.2.

4.5. Solitons in world volume of solitons

In this section we have discussed 1/4 BPS states of composite solitons. To do that we have worked out the moduli parameters in the moduli matrix for 1/4 BPS systems. If we could solve the master equations analytically or numerically we would obtain the full solutions.

As discussed below one big advantage of this method is that the moduli matrix contains non-normalizable modes also.

In order to discuss the composite solitons there exists another method, the moduli approximation. In this method one first constructs the effective action of a host 1/2 BPS soliton by using the Manton's method [29] as discussed in section 3.3. Then one constructs 1/2 BPS solitons in this effective theory. At the end, one has to check matching of topological charges in the original theory and in the effective theory.

It was this method to find a confined monopole in the Higgs phase [103]. Namely one constructs effective theory on a single non-Abelian vortex in the model with $N_{\rm F} = N_{\rm C} = 2$ with massive hypermultiplets. It is the $\mathbf{C}P^1$ model with a potential, which contains two vacua. Its Kähler potential is given in equation (3.135). Here note that the coefficient in the second term (the Kähler class of $\mathbf{C}P^1$) is given by $4\pi/g^2$. Then one constructs a kink interpolating between these two vacua. The energy of the kink can be calculated from equation (3.3) as the product of the Kähler class $4\pi/g^2$ and the mass difference Δm, to give $4\pi\Delta m/g^2$. This coincides with the energy (4.80) of a monopole, and the topological charges match in the original theory and in the effective theory. Therefore the kink in the vortex can be interpreted as a monopole in the original (bulk) theory. In fact it was this argument for the authors in [105] to determine the Kähler class from only symmetry argument, while we have derived it in equation (3.135) from direct calculation.

In the same way, one can construct instantons. First one constructs a single vortex in the model with $N_{\rm F} = N_{\rm C} = 2$ with massless hypermultiplets. The effective action on it is the $\mathbf{C}P^1$ model without potential. Then one can construct the $\mathbf{C}P^1$-lumps. The energy of lumps can be calculated by the product of the Kähler class $4\pi/g^2$ and the lump number $n \in \mathbf{Z} \simeq \pi_2(\mathbf{C}P^1)$, to give $4\pi n/g^2$. This coincides with the instanton number, and so lumps in the vortex can be regarded as instantons in the original theory [13].

The wall–vortex system can be constructed from the wall point of view. When a vortex ends on a domain wall, it can be understood as a BIon in the effective theory on the wall [109]. The negative energy of the boojum can also be obtained from the effective theory on a double wall [14].

These configurations can be classified into two cases. The first is the case that the soliton is made of the internal (orientational) moduli of the host soliton. The second is the case that it is made of spacetime moduli. The first case contains monopoles (instantons) on a vortex while the second case contains vortices ending on a domain wall.

Clearly this moduli approximation has limitations. First the slow movement approximation is used to construct effective action. Therefore this method cannot be applied to a region with rapidly varying fields. For instance, the centre of the vortex of wall–vortex composite system cannot be described accurately by the wall effective action. Second it cannot be applied to non-normalizable modes because one cannot construct an effective action for those modes. Our method of the moduli matrix overcomes both of these problems. We do not use the slow movement approximation at all. Moreover the moduli matrix contains non-normalizable modes also. When we wish to view 1/4 BPS system of monopole, vortex and walls from the vortex point of view, for instance, the incorporation of non-normalizable modes provides the following advantage. Semi-local vortices (lumps) have non-normalizable modes as well as normalizable modes, as seen in section 3.2. If a modus corresponding to normalizable mode in the moduli matrix for 1/2 BPS vortex is promoted to a 'field' depending on the vortex world volume in the sense of (4.82), it can produce a kink inside the vortex, namely a confined monopole attached by vortices. On the other hand, if non-normalizable mode depends on the coordinates corresponding to the vortex world volume, domain walls appear in the bulk instead of inside the vortex. This is because non-normalizable moduli of a vortex are bulk modes living at spatial infinities of the vortex. This point of view is missing in the moduli approximation.

However the moduli approximation is powerful for non-BPS composite solitons, for which the method of the moduli matrix cannot be used. For instance, domain walls and instantons cannot coexist as a BPS state [15]. If we consider them together, the configuration breaks all SUSY and therefore it is non-BPS. Nevertheless we can construct the effective action on walls as usual, and can construct a soliton on it. We have found in [16] that effective action on walls is precisely the Skyrme model including the four derivative term. Skyrmions are non-BPS and so we cannot compare energy in effective theory and the original theory. Instead we should calculate topological charges directly. Since we can show that the baryon (Skyrmion) number in the effective theory coincides with the instanton number, the Skyrmions in the effective theory can be regarded as instantons in the original theory.

5. Discussion

We have seen that the SDYM-Higgs equation describing the instanton–vortex system is the most general in the sense that it gives all other equations by dimensional reductions. Accordingly, the moduli matrix $H_0(z, w)$ of this system contains the moduli matrices of all other systems as special cases. However a complete understanding of $H_0(z, w)$ is still missing at present while the moduli matrices have been more thoroughly studied in this review for walls, vortices, domain wall webs and wall–vortex–monopole systems.

In this review, we have considered only static solutions. Time-dependent stationary solitons, such as Q-kinks [48] and Q-lumps [74], are also BPS states. Some of these dyonic objects have been discussed in [15, 119]. These solitons are worth studying in more detail.

We have considered effective Lagrangian on only elementary solitons, namely vortices and walls. Construction of effective Lagrangian of composite solitons is also possible, if they have normalizable modes. For instance, effective Lagrangian of monopoles (instantons) in a vortex may be obtainable, but essentially the same dynamics should already be contained in the kink (lump) solutions using the effective Lagrangian on vortex. Some nontrivial examples of effective Lagrangian on composite solitons are

- loops in domain wall webs,
- vortices stretched between domain walls in the wall–vortex–monopole system.

We know from the discussion of conserved SUSY [15] that they are described by a $(2, 0)$ sigma model in $d = 1 + 1$ dimensions or its dimensional reduction. Construction of these effective Lagrangians is very interesting because they resemble the (p, q) 5-brane webs [100] and the Hanany–Witten brane configuration [111], respectively.

We should note that another set of $1/4$ BPS equations and the unique set of $1/8$ BPS equations have also been found [15, 119]. Let us list their co-dimensions in $d = 5 + 1$ dimensions [15]. Another set of $1/4$ BPS equations contains triply intersecting vortices [128] whose co-dimensions are listed by × (world volume is denoted by ◯) as

1/4 VVV	0	1	2	3	4	5
Vortex	◯	◯	×	×	◯	◯
Vortex	◯	×	◯	×	◯	◯
Vortex	◯	×	×	◯	◯	◯

The unique set of $1/8$ BPS equations can contain various solitons with co-dimensions denoted by × (world volume is denoted by ◯) as

$1/8\ \mathrm{IV}^6$	0	1	2	3	4	5
Instanton	○	×	×	×	×	○
Vortex	○	○	×	×	○	○
Vortex	○	×	○	×	○	○
Vortex	○	×	×	○	○	○
Vortex	○	×	○	○	×	○
Vortex	○	○	×	○	×	○
Vortex	○	○	○	×	×	○

Systematically solving these equations is much more difficult than so far studied and remains as a future problem.

Let us finally list some of other interesting future directions: quantum effects of solitons, non-perturbative dynamics of field theories as well as string theory, and applications to particle physics, cosmology, condensed matter physics and nuclear physics. We hope this review article to be useful to explore these and other problems.

Acknowledgments

We would like to thank Masato Arai, Toshiaki Fujimori, Kazuya Kakimoto, Nobuhito Maru, Masashi Naganuma, Kazutoshi Ohta, Yuji Tachikawa, David Tong and Yisong Yang for collaborations in various stages. We also thank Joao Baptista, Jarah Evslin, Koji Hashimoto, Kimyeong Lee, Nick Manton and Ho-Ung Yee for a useful discussion. This work is supported in part by grant-in-aid for Scientific Research from the Ministry of Education, Culture, Sports, Science and Technology, Japan No. 17540237 (NS) and 16028203 for the priority area 'origin of mass' (NS). The work of MN and KO (ME and YI) is supported by Japan Society for the Promotion of Science under the Post-doctoral (Pre-doctoral) Research Programme.

References

[1] Isozumi Y, Nitta M, Ohashi K and Sakai N 2004 Construction of non-Abelian walls and their complete moduli space *Phys. Rev. Lett.* **93** 161601 (*Preprint* hep-th/0404198)

[2] Isozumi Y, Nitta M, Ohashi K and Sakai N 2004 Non-Abelian walls in supersymmetric gauge theories *Phys. Rev.* D **70** 125014 (*Preprint* hep-th/0405194)

[3] Eto M, Isozumi Y, Nitta M, Ohashi K, Ohta K and Sakai N 2005 D-brane construction for non-Abelian walls *Phys. Rev.* D **71** 125006 (*Preprint* hep-th/0412024)

[4] Eto M, Isozumi Y, Nitta M, Ohashi K, Ohta K, Sakai N and Tachikawa Y 2005 Global structure of moduli space for BPS walls *Phys. Rev.* D **71** 105009 (*Preprint* hep-th/0503033)

[5] Sakai N and Yang Y 2005 Moduli space of BPS walls in supersymmetric gauge theories *Comm. Math. Phys.* (in press) (*Preprint* hep-th/0505136)

[6] Eto M, Isozumi Y, Nitta M, Ohashi K and Sakai N 2006 Moduli space of non-Abelian vortices *Phys. Rev. Lett.* **96** 161601 (*Preprint* hep-th/0511088)

[7] Eto M, Fujimori T, Isozumi Y, Nitta M, Ohashi K, Ohta K and Sakai N 2006 Non-Abelian vortices on cylinder: duality between vortices and walls *Phys. Rev.* D **73** 085008 (*Preprint* hep-th/0601181)

[8] Eto M, Isozumi Y, Nitta M, Ohashi K and Sakai N 2005 Webs of walls *Phys. Rev.* D **72** 085004 (*Preprint* hep-th/0506135)

[9] Eto M, Isozumi Y, Nitta M, Ohashi K and Sakai N 2006 Non-Abelian webs of walls *Phys. Lett.* B **632** 384 (*Preprint* hep-th/0508241)

[10] Eto M, Isozumi Y, Nitta M, Ohashi K, Ohta K and Sakai N 2005 D-brane configurations for domain walls and their webs *AIP Conf. Proc.* **805** 354 (*Preprint* hep-th/0509127)

[11] Isozumi Y, Nitta M, Ohashi K and Sakai N 2005 All exact solutions of a 1/4 Bogomol'nyi–Prasad–Sommerfield equation *Phys. Rev.* D **71** 065018 (*Preprint* hep-th/0405129)

[12] Sakai N and Tong D 2005 Monopoles, vortices, domain walls and D-branes: the rules of interaction *J. High Energy Phys.* JHEP03(2005)019 (*Preprint* hep-th/0501207)

[13] Eto M, Isozumi Y, Nitta M, Ohashi K and Sakai N 2005 Instantons in the Higgs phase *Phys. Rev.* D **72** 025011 (*Preprint* hep-th/0412048)

[14] Eto M, Isozumi Y, Nitta M, Ohashi K and Sakai N 2006 Manifestly supersymmetric effective Lagrangians on BPS Solitons *Phys. Rev.* D (in press) (*Preprint* hep-th/0602289)

[15] Eto M, Isozumi Y, Nitta M and Ohashi K 2005 1/2, 1/4 and 1/8 BPS equations in SUSY Yang–Mills–Higgs systems: field theoretical brane configurations *Preprint* hep-th/0506257

[16] Eto M, Nitta M, Ohashi K and Tong D 2005 Skyrmions from instantons inside domain walls *Phys. Rev. Lett.* **95** 252003 (*Preprint* hep-th/0508130)

[17] Isozumi Y, Nitta M, Ohashi K and Sakai N 2004 *Proc. 'NathFest' at PASCOS Conf. (Northeastern University, Boston, MA)* (*Preprint* hep-th/0410150) at press

Isozumi Y, Nitta M, Ohashi K and Sakai N 2005 Walls and vortices in supersymmetric non-Abelian gauge theories *Themes in Unification; the Pran Nath Festschrift* (Singapore: World Scientific) pp 229–38 (*Preprint* hep-th/0410150)

Eto M, Isozumi Y, Nitta M, Ohashi K and Sakai N 2005 *AIP Conf. Proc.* **805** 266 (*Preprint* hep-th/0508017)

[18] Manton N S and Sutcliffe P 2004 *Topological Solitons* (Cambridge, UK: Cambridge University Press)

[19] Vilenkin A and Shellard E 1994 *Cosmic Strings and Other Topological Defects* (Cambridge: Cambridge University Press)

[20] Mermin N D 1979 The topological theory of defects in ordered media *Rev. Mod. Phys.* **51** 591

[21] Rajaraman R 1982 *Solitons and Instantons* (Amsterdam: Elsevier)

[22] Tong D 2005 TASI lectures on solitons *Preprint* hep-th/0509216

[23] Horava P and Witten E 1996 Eleven-dimensional supergravity on a manifold with boundary *Nucl. Phys.* B **475** 94 (*Preprint* hep-th/9603142)

[24] Arkani-Hamed N, Dimopoulos S and Dvali G R 1998 The hierarchy problem and new dimensions at a millimeter *Phys. Lett.* B **429** 263 (*Preprint* hep-ph/9803315)

Antoniadis I, Arkani-Hamed N, Dimopoulos S and Dvali G R 1998 New dimensions at a millimeter to a Fermi and superstrings at a TeV *Phys. Lett.* B **436** 257 (*Preprint* hep-ph/9804398)

[25] Randall L and Sundrum R 1999 A large mass hierarchy from a small extra dimension *Phys. Rev. Lett.* **83** 3370 (*Preprint* hep-ph/9905221)

Randall L and Sundrum R 1999 An alternative to compactification *Phys. Rev. Lett.* **83** 4690 (*Preprint* hep-th/9906064)

[26] Bogomolny E B 1976 Stability of classical solutions *Sov. J. Nucl. Phys.* **24** 449

Bogomolny E B 1976 *Yad. Fiz.* **24** 861

Prasad M K and Sommerfield C M 1975 An exact classical solution for the 'T Hooft monopole and the Julia-Zee Dyon *Phys. Rev. Lett.* **35** 760

[27] Witten E and Olive D I 1978 Supersymmetry algebras that include topological charges *Phys. Lett.* B **78** 97

[28] Seiberg N and Witten E 1994 Electric–magnetic duality, monopole condensation, and confinement in $N = 2$ supersymmetric Yang–Mills theory *Nucl. Phys.* B **426** 19

Seiberg N and Witten E 1994 *Nucl. Phys.* B **430** 485 (*Preprint* hep-th/9407087) (erratum)

Seiberg N and Witten E 1994 Monopoles, duality and chiral symmetry breaking in $N = 2$ supersymmetric QCD *Nucl. Phys.* B **431** 484 (*Preprint* hep-th/9408099)

[29] Manton N S 1982 A remark on the scattering of bps monopoles *Phys. Lett.* B **110** 54

[30] Dorey N, Hollowood T J, Khoze V V and Mattis M P 2002 The calculus of many instantons *Phys. Rep.* **371** 231 (*Preprint* hep-th/0206063)

[31] Townsend P K 2000 Brane theory solitons *NATO Advanced Study Institute: TMR Summer School on Progress in String Theory and M-Theory (Cargese 1999)* ed L Baulieu, M Green, M Picco and P Windey (Dordrecht: Kluwer) pp 265–96 (*Preprint* hep-th/0004039)

[32] Callan C G and Maldacena J M 1998 Brane dynamics from the Born–Infeld action *Nucl. Phys.* B **513** 198 (*Preprint* hep-th/9708147)

Gibbons G W 1998 Born–Infeld particles and Dirichlet p-branes *Nucl. Phys.* B **514** 603 (*Preprint* hep-th/9709027)

[33] Atiyah M F, Hitchin N J, Drinfeld V G and Manin Y I 1978 Construction of instantons *Phys. Lett.* A **65** 185

[34] Corrigan E and Goddard P 1984 Construction of instanton and monopole solutions and reciprocity *Ann. Phys.* **154** 253

[35] Nahm W 1980 A simple formalism for the Bps monopole *Phys. Lett.* B **90** 413

Nahm W 1980 On Abelian selfdual multi-monopoles *Phys. Lett.* B **93** 42

Nahm W 1983 Selfdual monopoles and calorons BONN-HE-83-16, Presented at *12th Colloq. on Group Theoretical Methods in Physics (Trieste, Italy, 5–10 Sep)*

[36] Alvarez-Gaume L and Freedman D Z 1981 Geometrical structure and ultraviolet finiteness in the supersymmetric sigma model *Commun. Math. Phys.* **80** 443

[37] Zumino B 1979 Supersymmetry and Kahler manifolds *Phys. Lett.* B **87** 203

[38] Lindström U and Roček M 1983 Scalar tensor duality and $n = 1$, $n = 2$ nonlinear sigma models *Nucl. Phys.* B **222** 285

[39] Hitchin N J, Karlhede A, Lindström U and Roček M 1987 Hyperkahler metrics and supersymmetry *Commun. Math. Phys.* **108** 535

[40] Alvarez-Gaume L and Freedman D Z 1983 Potentials for the supersymmetric nonlinear sigma model *Commun. Math. Phys.* **91** 87

[41] Arai M, Nitta M and Sakai N 2005 Vacua of massive hyper-Kaehler sigma models of non-Abelian quotient *Prog. Theor. Phys.* **113** 657 (*Preprint* hep-th/0307274)
Arai M, Nitta M and Sakai N 2005 Massive hyper-Kaehler sigma models and BPS domain walls *Phys. At. Nucl.* **68** 1634
Arai M, Nitta M and Sakai N 2005 *Yad. Fiz.* **68** 1698 (*Preprint* hep-th/0401102)

[42] Argyres P C, Plesser M R and Seiberg N 1996 The moduli space of $N = 2$ SUSY QCD and duality in $N = 1$ SUSY QCD *Nucl. Phys.* B **471** 159 (*Preprint* hep-th/9603042)

[43] Antoniadis I and Pioline B 1997 Higgs branch, hyperKaehler quotient and duality in SUSY $N = 2$ Yang–Mills theories *Int. J. Mod. Phys.* A **12** 4907 (*Preprint* hep-th/9607058)

[44] Higashijima K and Nitta M 2000 Supersymmetric nonlinear sigma models as gauge theories *Prog. Theor. Phys.* **103** 635 (*Preprint* hep-th/9911139)

[45] Curtright T L and Freedman D Z 1980 Nonlinear sigma models with extended supersymmetry in four-dimensions *Phys. Lett.* B **90** 71
Curtright T L and Freedman D Z 1980 *Phys. Lett.* B **91** 487 (erratum)
Alvarez-Gaume L and Freedman D Z 1980 Ricci flat Kahler manifolds and supersymmetry *Phys. Lett.* B **94** 171
Rocek M and Townsend P K 1980 Three loop finiteness of the $n = 4$ supersymmetric nonlinear sigma model *Phys. Lett.* B **96** 72

[46] Eguchi T and Hanson A J 1978 Asymptotically flat selfdual solutions to Euclidean gravity *Phys. Lett.* B **74** 249
Eguchi T and Hanson A J 1979 Selfdual solutions to Euclidean gravity *Ann. Phys.* **120** 82

[47] Fayet P and Iliopoulos J 1974 Spontaneously broken supergauge symmetries and Goldstone spinors *Phys. Lett.* B **51** 461

[48] Abraham E R C and Townsend P K 1992 Q kinks *Phys. Lett.* B **291** 85
Abraham E R C and Townsend P K 1992 More on Q kinks: a $(1 + 1)$-dimensional analog of dyons *Phys. Lett.* B **295** 225

[49] Lambert N D and Tong D 2000 Kinky D-strings *Nucl. Phys.* B **569** 606 (*Preprint* hep-th/9907098)

[50] Gauntlett J P, Tong D and Townsend P K 2001 Multi-domain walls in massive supersymmetric sigma-models *Phys. Rev.* D **64** 025010 (*Preprint* hep-th/0012178)

[51] Tong D 2002 The moduli space of BPS domain walls *Phys. Rev.* D **66** 025013 (*Preprint* hep-th/0202012)

[52] Lee K S M 2003 An index theorem for domain walls in supersymmetric gauge theories *Phys. Rev.* D **67** 045009 (*Preprint* hep-th/0211058)

[53] Gauntlett J P, Tong D and Townsend P K 2001 Supersymmetric intersecting domain walls in massive hyper-Kähler sigma models *Phys. Rev.* D **63** 085001 (*Preprint* hep-th/0007124)

[54] Arai M, Naganuma M, Nitta M and Sakai N 2003 Manifest supersymmetry for BPS walls in $N = 2$ nonlinear sigma models *Nucl. Phys.* B **652** 35 (*Preprint* hep-th/0211103)

[55] Arai M, Naganuma M, Nitta M and Sakai N 2003 BPS wall in $N = 2$ SUSY nonlinear sigma model with Eguchi–Hanson manifold *Garden of Quanta—In Honor of Hiroshi Ezawa* ed A Arai *et al* (Singapore: World Scientific) pp 299–325 (*Preprint* hep-th/0302028)

[56] Arai M, Ivanov E and Niederle J 2004 Massive nonlinear sigma models and BPS domain walls in harmonic superspace *Nucl. Phys.* B **680** 23 (*Preprint* hep-th/0312037)

[57] Arai M, Fujita S, Naganuma M and Sakai N 2003 Wall solution with weak gravity limit in five dimensional supergravity *Phys. Lett.* B **556** 192 (*Preprint* hep-th/0212175)

[58] Eto M, Fujita S, Naganuma M and Sakai N 2004 BPS multi-walls in five-dimensional supergravity *Phys. Rev.* D **69** 025007 (*Preprint* hep-th/0306198)

[59] Eto M, Maru N and Sakai N 2004 Non-BPS walls and their stability in 5D supersymmetric theory *Nucl. Phys.* B **696** 3 (*Preprint* hep-th/0404114)

[60] Isozumi Y, Ohashi K and Sakai N 2003 Massless localized vector field on a wall in $D = 5$ SQED with tensor multiplets *J. High Energy Phys.* JHEP11(2003)061 (*Preprint* hep-th/0310130)

[61] Isozumi Y, Ohashi K and Sakai N 2003 Exact wall solutions in 5-dimensional SUSY QED at finite coupling *J. High Energy Phys.* JHEP11(2003)060 (*Preprint* hep-th/0310189)

[62] Tong D 2003 Mirror on the wall: on two-dimensional black holes and Liouville theory *J. High Energy Phys.* JHEP04(2003)031 (*Preprint* hep-th/0303151)
[63] Hanany A and Tong D 2005 On monopoles and domain walls *Preprint* hep-th/0507140
[64] Shifman M and Yung A 2004 Localization of non-Abelian gauge fields on domain walls at weak coupling (D-brane prototypes II) *Phys. Rev.* D **70** 025013 (*Preprint* hep-th/0312257)
[65] Tong D 2005 D-branes in field theory *Preprint* hep-th/0512192
[66] Abrikosov A A 1957 On the magnetic properties of superconductors of the second group *Sov. Phys.—JETP* **5** 1174
Abrikosov A A 1957 *Zh. Eksp. Teor. Fiz.* **32** 1442
Nielsen H B and Olesen P 1973 Vortex-line models for dual strings *Nucl. Phys.* B **61** 45
[67] Taubes C H 1980 Arbitrary N-vortex solutions to the first order Landau–Ginzburg equations *Commun. Math. Phys.* **72** 277
[68] Samols T M 1992 Vortex scattering *Commun. Math. Phys.* **145** 149
[69] Manton N S and Speight J M 2003 Asymptotic interactions of critically coupled vortices *Commun. Math. Phys.* **236** 535 (*Preprint* hep-th/0205307)
[70] Chen H Y and Manton N S 2005 The Kaehler potential of Abelian Higgs vortices *J. Math. Phys.* **46** 052305 (*Preprint* hep-th/0407011)
[71] Vachaspati T and Achucarro A 1991 Semilocal cosmic strings *Phys. Rev.* D **44** 3067
Achucarro A and Vachaspati T 2000 Semilocal and electroweak strings *Phys. Rep.* **327** 347
Achucarro A and Vachaspati T 2000 *Phys. Rep.* **327** 427 (*Preprint* hep-ph/9904229)
[72] Ward R S 1985 Slowly moving lumps in the cp**1 model in (2 + 1)-dimensions *Phys. Lett.* B **158** 424
[73] Stokoe I and Zakrzewski W J 1987 Dynamics of solutions of the cp**1 and cp**2 models in (2 + 1)-dimensions *Z. Phys.* C **34** 491
[74] Leese R A 1991 Q lumps and their interactions *Nucl. Phys.* B **366** 283
Abraham E 1992 Nonlinear sigma models and their Q lump solutions *Phys. Lett.* B **278** 291
[75] Polyakov A M and Belavin A A 1975 Metastable states of two-dimensional isotropic ferromagnets *JETP Lett.* **22** 245
Polyakov A M and Belavin A A 1975 *Pisma Zh. Eksp. Teor. Fiz.* **22** 503
[76] Hanany A and Tong D 2003 Vortices, instantons and branes *J. High Energy Phys.* JHEP07(2003)037 (*Preprint* hep-th/0306150)
[77] Auzzi R, Bolognesi S, Evslin J, Konishi K and Yung A 2003 Nonabelian superconductors: vortices and confinement in $N = 2$ SQCD *Nucl. Phys.* B **673** 187 (*Preprint* hep-th/0307287)
[78] Kneipp M A C and Brockill P 2001 BPS string solutions in non-Abelian Yang–Mills theories *Phys. Rev.* D **64** 125012 (*Preprint* hep-th/0104171)
[79] Eto M, Nitta M and Sakai N 2004 Effective theory on non-Abelian vortices in six dimensions *Nucl. Phys.* B **701** 247 (*Preprint* hep-th/0405161)
[80] Markov V, Marshakov A and Yung A 2005 Non-Abelian vortices in $N = 1^*$ gauge theory *Nucl. Phys.* B **709** 267 (*Preprint* hep-th/0408235)
[81] Gorsky A, Shifman M and Yung A 2005 Non-Abelian Meissner effect in Yang–Mills theories at weak coupling *Phys. Rev.* D **71** 045010 (*Preprint* hep-th/0412082)
[82] Bolognesi S 2005 The holomorphic tension of nonabelian vortices and the quark = dual-quark condensate *Nucl. Phys.* B **719** 67 (*Preprint* hep-th/0412241)
[83] Shifman M and Yung A 2005 Non-Abelian flux tubes in SQCD: supersizing world-sheet supersymmetry *Phys. Rev.* D **72** 085017 (*Preprint* hep-th/0501211)
[84] Hashimoto K and Tong D 2005 Reconnection of non-Abelian cosmic strings *J. Cosmol. Astropart. Phys.* JCAP09(2005)004 (*Preprint* hep-th/0506022)
[85] Bolognesi S and Evslin J 2005 Stable vs unstable vortices in SQCD *Preprint* hep-th/0506174
[86] Bolognesi S 2005 Domain walls and flux tubes *Nucl. Phys.* B **730** 127 (*Preprint* hep-th/0507273)
[87] Auzzi R, Shifman M and Yung A 2005 Composite non-Abelian flux tubes in $N = 2$ SQCD *Preprint* hep-th/0511150
[88] Bolognesi S and Gudnason S B 2005 Multi-vortices are wall vortices: a numerical proof *Preprint* hep-th/0512132
[89] Gorsky A, Shifman M and Yung A 2006 Nonabelian strings and axion *Preprint* hep-th/0601131
[90] Krauss L and Wilczek F 1989 Discrete gauge symmetry in continuum theories *Phys. Rev. Lett.* **62** 1221
Alford M G, Benson K, Coleman S R, March-Russell J and Wilczek F 1990 The interactions and excitations of nonabelian vortices *Phys. Rev. Lett.* **64** 1632
Alford M G, Benson K, Coleman S R, March-Russell J and Wilczek F 1990 *Phys. Rev. Lett.* **65** 668 (erratum)
Alford M G, Benson K, Coleman S R, March-Russell J and Wilczek F 1991 Zero modes of nonabelian vortices *Nucl. Phys.* B **349** 414

Alford M G, Lee K-M, March-Russell J and Preskill J 1992 Quantum field theory of nonabelian strings and vortices *Nucl. Phys.* B **384** 251 (*Preprint* hep-th/9112038)

[91] Carroll S M and Trodden M 1998 Dirichlet topological defects *Phys. Rev.* D **57** 5189 (*Preprint* hep-th/9711099)

Bowick M, De Felice A and Trodden M 2003 The shapes of Dirichlet defects *J. High Energy Phys.* JHEP10(2003)067 (*Preprint* hep-th/0306224)

Dvali G and Vilenkin A 2003 Solitonic D-branes and brane annihilation *Phys. Rev.* D **67** 046002 (*Preprint* hep-th/0209217)

[92] Saffin P M 1999 Tiling with almost-BPS-invariant domain–wall junctions *Phys. Rev. Lett.* **83** 4249 (*Preprint* hep-th/9907066)

Bazeia D and Brito F A 2000 Tiling the plane without supersymmetry *Phys. Rev. Lett.* **84** 1094 (*Preprint* hep-th/9908090)

Nam S K 2000 Modeling a network of brane worlds *J. High Energy Phys.* JHEP03(2000)005 (*Preprint* hep-th/9911104)

Bazeia D and Brito F A 2000 Bags, junctions, and networks of BPS and non-BPS defects *Phys. Rev.* D **61** 105019 (*Preprint* hep-th/9912015)

Bazeia D and Brito F A 2000 Pattern formation through the entrapment of a network of domain walls *Phys. Rev.* D **62** 101701 (*Preprint* hep-th/0005045)

Brito F A and Bazeia D 2001 Network of domain walls on soliton stars *Phys. Rev.* D **64** 065022 (*Preprint* hep-th/0105296)

Sutcliffe P 2003 Domain wall networks on solitons *Phys. Rev.* D **68** 085004 (*Preprint* hep-th/0305198)

Pogosian L and Vachaspati T 2003 Domain wall lattices *Phys. Rev.* D **67** 065012

Antunes N D, Pogosian L and Vachaspati T 2004 On formation of domain wall lattices *Phys. Rev.* D **69** 043513

Antunes N D and Vachaspati T 2004 Spontaneous formation of domain wall lattices in two spatial dimensions *Phys. Rev.* D **70** 063516

[93] Matsuda T 2005 Brane necklaces and brane coils *J. High Energy Phys.* JHEP05(2005)015 (*Preprint* hep-ph/0412290)

Matsuda T 2005 Primordial black holes from monopoles connected by strings *Preprint* hep-ph/0509061

[94] Gibbons G W and Townsend P K 1999 A Bogomolnyi equation for intersecting domain walls *Phys. Rev. Lett.* **83** 1727 (*Preprint* hep-th/9905196)

Carroll S M, Hellerman S and Trodden M 2000 Domain wall junctions are 1/4-BPS states *Phys. Rev.* D **61** 065001 (*Preprint* hep-th/9905217)

[95] Oda H, Ito K, Naganuma M and Sakai N 1999 An exact solution of BPS domain wall junction *Phys. Lett.* B **471** 140 (*Preprint* hep-th/9910095)

[96] Ito K, Naganuma M, Oda H and Sakai N 2000 Nonnormalizable zero modes on BPS junctions *Nucl. Phys.* B **586** 231 (*Preprint* hep-th/0004188)

Ito K, Naganuma M, Oda H and Sakai N 2001 An exact solution of BPS junctions and its properties *Nucl. Phys. Proc. Suppl.* **101** 304 (*Preprint* hep-th/0012182)

[97] Naganuma M, Nitta M and Sakai N 2002 BPS walls and junctions in SUSY nonlinear sigma models *Phys. Rev.* D **65** 045016 (*Preprint* hep-th/0108179)

[98] Shifman M A and Veldhuis T ter 2000 Calculating the tension of domain wall junctions and vortices in generalized Wess–Zumino models *Phys. Rev.* D **62** 065004 (*Preprint* hep-th/9912162)

Gorsky A and Shifman M A 2000 More on the tensorial central charges in $N = 1$ supersymmetric gauge theories (BPS wall junctions and strings) *Phys. Rev.* D **61** 085001 (*Preprint* hep-th/9909015)

[99] Kakimoto K and Sakai N 2003 Domain wall junction in $N = 2$ supersymmetric QED in four dimensions *Phys. Rev.* D **68** 065005 (*Preprint* hep-th/0306077)

[100] Aharony O and Hanany A 1997 Branes, superpotentials and superconformal fixed points *Nucl. Phys.* B **504** 239 (*Preprint* hep-th/9704170)

Aharony O, Hanany A and Kol B 1998 Webs of (p, q) 5-branes, five dimensional field theories and grid diagrams *J. High Energy Phys.* JHEP01(1998)002 (*Preprint* hep-th/9710116)

Kol B and Rahmfeld J 1998 BPS spectrum of 5 dimensional field theories, (p, q) webs and curve counting *J. High Energy Phys.* JHEP08(1998)006 (*Preprint* hep-th/9801067)

[101] Hindmarsh M and Kibble T W B 1985 Beads on strings *Phys. Rev. Lett.* **55** 2398

[102] Kneipp M A C 2003 $Z(k)$ string fluxes and monopole confinement in non-Abelian theories *Phys. Rev.* D **68** 045009 (*Preprint* hep-th/0211049)

Kneipp M A C 2004 Color superconductivity, $z(N)$ flux tubes and monopole confinement in deformed $N = 2^*$ super Yang–Mills theories *Phys. Rev.* D **69** 045007 (*Preprint* hep-th/0308086)

[103] Tong D 2004 Monopoles in the Higgs phase *Phys. Rev.* D **69** 065003 (*Preprint* hep-th/0307302)

[104] Auzzi R, Bolognesi S, Evslin J and Konishi K 2004 Nonabelian monopoles and the vortices that confine them *Nucl. Phys.* B **686** 119 (*Preprint* hep-th/0312233)

[105] Shifman M and Yung A 2004 Non-Abelian string junctions as confined monopoles *Phys. Rev.* D **70** 045004 (*Preprint* hep-th/0403149)

[106] Hanany A and Tong D 2004 Vortex strings and four-dimensional gauge dynamics *J. High Energy Phys.* JHEP04(2004)066 (*Preprint* hep-th/0403158)

[107] Auzzi R, Bolognesi S and Evslin J 2005 Monopoles can be confined by 0, 1 or 2 vortices *J. High Energy Phys.* JHEP02(2005)046 (*Preprint* hep-th/0411074)

[108] Ferretti L and Konishi K 2006 Duality and confinement in $SO(N)$ gauge theories *Preprint* hep-th/0602252

[109] Gauntlett J P, Portugues R, Tong D and Townsend P K 2001 D-brane solitons in supersymmetric sigma-models *Phys. Rev.* D **63** 085002 (*Preprint* hep-th/0008221)

[110] Shifman M and Yung A 2003 Domain walls and flux tubes in $N = 2$ sQCD: D-brane prototypes *Phys. Rev.* D **67** 125007 (*Preprint* hep-th/0212293)

[111] Hanany A and Witten E 1997 Type IIB superstrings, BPS monopoles, and three-dimensional gauge dynamics *Nucl. Phys.* B **492** 152 (*Preprint* hep-th/9611230)

[112] Auzzi R, Shifman M and Yung A 2005 Studying boojums in $N = 2$ theory with walls and vortices *Phys. Rev.* D **72** 025002 (*Preprint* hep-th/0504148)

[113] Scherk J and Schwarz J H 1979 How to get masses from extra dimensions *Nucl. Phys.* B **153** 61

[114] Bradlow S B 1990 Vortices in holomorphic line bundles over closed Kahler manifolds *Commun. Math. Phys.* **135** 1

[115] Mundet i Riera I 1999 Yang–Mills–Higgs theory for symplectic fibrations *Preprint* math.sg/9912150
Hitchin-Kobayashi A 2000 Correspondence for Kahler fibrations *J. Angew. Math.* **528** 41

[116] Cieliebak K, Rita Gaio A and Salamon D A 2000 J-holomorphic curves, moment maps, and invariants of Hamiltonian group actions *Int. Math. Res. Not.* 831 (*Preprint* math.SG/9909122)

[117] Baptista J M 2006 Vortex equations in Abelian gauged sigma-models *Commun. Math. Phys.* **261** 161 (*Preprint* math.dg/0411517)

[118] Cieliebak K, Rita Gaio A, Mundet i Riera I and Salamon D A 2002 The symplectic vortex equations and invariants of Hamiltonian group actions *J. Symplectic Geom.* **1** 543 (*Preprint* math.SG/0111176)
Mundet i Riera I 2003 Hamiltonian Gromov–Witten invariants *Topology* **42** 525
Baptista J M 2005 A topological gauged sigma-model *Preprint* hep-th/0502152

[119] Lee K and Yee H U 2005 New BPS objects in $N = 2$ supersymmetric gauge theories *Phys. Rev.* D **72** 065023 (*Preprint* hep-th/0506256)

[120] Inami T, Minakami S and Nitta M 2006 Non-integrability of self-dual Yang–Mills–Higgs system *Preprint* hep-th/0605064

[121] Bando M, Kuramoto T, Maskawa T and Uehara S 1984 Structure of nonlinear realization in supersymmetric theories *Phys. Lett.* B **138** 94
Bando M, Kuramoto T, Maskawa T and Uehara S 1984 Nonlinear realization in supersymmetric theories *Prog. Theor. Phys.* **72** 313
Bando M, Kuramoto T, Maskawa T and Uehara S 1984 Nonlinear realization in supersymmetric theories. 2 *Prog. Theor. Phys.* **72** 1207
Higashijima K, Nitta M, Ohta K and Ohta N 1997 Low energy theorems in $N = 1$ supersymmetric theory *Prog. Theor. Phys.* **98** 1165 (*Preprint* hep-th/9706219)
Nitta M 1999 Moduli space of global symmetry in $N = 1$ supersymmetric theories and the quasi-Nambu–Goldstone bosons *Int. J. Mod. Phys.* A **14** 2397 (*Preprint* hep-th/9805038)
Furuta K, Inami T, Nakajima H and Nitta M 2001 Supersymmetric extension of non-Abelian scalar–tensor duality *Prog. Theor. Phys.* **106** 851 (*Preprint* hep-th/0106183)

[122] Hori K, Ooguri H and Oz Y 1998 Strong coupling dynamics of four-dimensional $N = 1$ gauge theories from M theory five brane *Adv. Theor. Math. Phys.* **1** 1 (*Preprint* hep-th/9706082)

[123] Nakajima H 1999 *Lectures on Hilbert Schemes of Points on Surfaces* (Providence, RI: American Mathematical Society)

[124] Popov A D and Szabo R J 2006 Quiver gauge theory of nonabelian vortices and noncommutative instantons in higher dimensions *J. Math. Phys.* **47** 012306 (*Preprint* hep-th/0504025)
Lechtenfeld O, Popov A D and Szabo R J 2006 Rank two quiver gauge theory, graded connections and noncommutative vortices *Preprint* hep-th/0603232

[125] Donaldson S K 1985 Anti self-dual Yang–Mills connections over complex algebraic surfaces and stable vector bundles *Proc. Lond. Math. Soc.* **50** 1
Donaldson S K 1987 Infinite determinants, stable bundles, and curvature *Duke Math. J.* **54** 231
Uhlenbeck K and Yau S T 1986 On the existence of Hermitian Yang–Mills connections in stable bundles *Commun. Pure Appl. Math.* **39** 257

[126] Yang C N 1977 Condition of selfduality for $SU(2)$ gauge fields on Euclidean four-dimensional space *Phys. Rev. Lett.* **38** 1377

[127] Isojima S, Willox R and Satsuma J 2002 On various solutions of the coupled KP equation *J. Phys. A: Math. Gen.* **35** 6893

Isojima S, Willox R and Satsuma J 2003 Spider-web solutions of the coupled KP equation *J. Phys. A: Math. Gen.* **36** 9533

Biondini G and Kodama Y 2003 On a family of solutions of the Kadomtsev–Petviashvili equation which also satisfy the Toda lattice hierarchy *J. Phys. A: Math. Gen.* **36** 10519 (*Preprint* nlin.SI/0306003)

[128] Naganuma M, Nitta M and Sakai N 2002 BPS lumps and their intersections in $N = 2$ SUSY nonlinear sigma models *Grav. Cosmol.* **8** 129 (*Preprint* hep-th/0108133)

Portugues R and Townsend P K 2002 Sigma-model soliton intersections from exceptional calibrations *J. High Energy Phys.* JHEP04(2002)039 (*Preprint* hep-th/0203181)